UNITED STATES DEPARTMENT OF THE INTERIOR
GEOLOGICAL SURVEY

DISTRIBUTION OF TRACE ELEMENTS IN BOTTOM SEDIMENT OF THE NORTHERN BERING SEA

by

BRADLEY R. LARSEN
C. HANS NELSON
CHRIS HEROPOULOS
JEFFRY J. PATRY

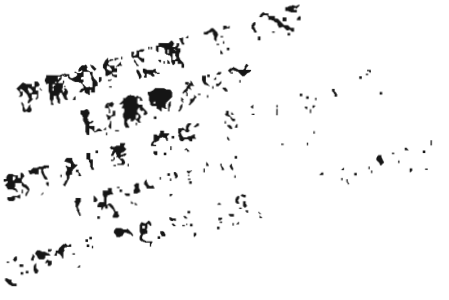

Open-File Report
80-399A

This report is preliminary and has not been edited or reviewed for conformity with Geological Survey standards or nomenclature.

TABLE OF CONTENTS

I. SUMMARY

2-dimensional contour and 3-dimensional value-surface maps of semi-quantitative emission spectographic analyses for over 50 elements in surface sediment from 180 sampling stations are presented. For purposes of discussion, certain of these elements have been grouped into the following categories: petroleum indicators, heavy metals, potentially toxic elements, chemically sensitive elements, major elements, minor elements, and a group of elements of economic interest.

Of the petroleum indicator elements, Ni and V, Ni showed only average concentrations in sediment near a gas seep 35 km south of Nome, Alaska; V showed slightly lower values in samples taken recently from the gas-seep area and relatively high values in samples collected earlier from the same area. High amounts of V and Ni were found in sediment 40 km west of the south tip of St. Lawrence Island, suggesting that potential petroleum seeps should be searched for in this area. All other anomalous values for Ni and V seem to be related to specific sediment types or to nearby onshore sources.

The elements Zr, Sn, Cr, and Ce were categorized as heavy metals. Zr is found in high amounts in sediment surrounding the Yukon Delta and in Norton Sound. It is generally low in sediment in the region of the Chirikov Basin. Very high Zr concentrations are found off NE Cape of St. Lawrence Island as well as off the western and southern portions of St. Lawrence Island. These high amounts are probably derived from zircon containing quartz-monzanite plutons widely dispersed throughout the island. Sn was detected in only 23 samples. High concentrations were found off Cape Prince of Wales, in Anadyr Strait; and in the areas of King Island, Port Clarence, Bluff, Cape Rodney, and off the north central coast of St. Lawrence Island. It is possible that the high values in Anadyr Strait, Port Clarence and King Island are

hydraulically concentrated. Values in other areas appear to be derived from immediate land sources. Cr is evenly distributed except for high concentrations close to Stuart Island, at locations south and north of St. Lawrence Island, and off Cape Prince of Wales. These high amounts appear to be closely related to the mafic rock types found on adjacent land areas. Cerium is found in few raw-bulk samples but where present it is associated with lanthanum and neodymium which suggests the presence of the heavy mineral monazite. The greatest concentrations of Zn, Cr and Ce were found in a sample taken from 30 km south of Cape Prince of Wales. Because this sample also contains the highest amounts of Ti, Mn, La, Sc, Y, Yb and Nd, it may indicate a significant placer area.

Of the potentially toxic elements, Sb, As, Cu, Pb and Zn, Sb was detected in only a few samples from the Bluff, NE Cape of St. Lawrence Island, and Stuart Island beaches. As was detected only in samples from Bluff beach where lode cinnabar deposits occur. High concentrations for Cu, Pb, and Zn occur together in the same areas off St. Lawrence Island, along the southern coast of the Seward Peninsula and in Norton Sound. These high values seem directly related to highly mineralized areas in concentrations adjacent to land areas. Cu and Zn also show the same trend as Zr, with high values off the Yukon Delta in Norton Sound and low values in the Chirikov Basin.

Value-surface maps for the chemically or environmentally sensitive elements Fe, Mn, Co and Ba all show high concentrations off the volcanogenic areas of north-central St. Lawrence Island and Stuart Island. They also exhibit high values off Yukon Delta and low values within Chirikov Basin. Ba is singled out in this group because of its use in drilling muds. It also exhibits high concentrations surrounding Yukon Delta, near Stuart Island and along the southern coast of the Seward Peninsula. Maximum values occur off the

southern edge of St. Lawrence Island and in the middle of Anadyr Strait. The elevated Ba concentrations off the Yukon Delta probably originate in sediment from the Yukon River drainage as do higher concentrations of Zr, Cu, Zn, Fe, and Mn. The anomalies near Stuart Island and Seward Peninsula appear to be derived from specific land sources.

Of the major elements, the highest amounts of Ti, as with Fe and Mn discussed above, are in sediment found close to volcanic source rocks of Stuart Island and St. Lawrence Island, although the highest value of Ti is from a sample from 30 km south of Cape Prince of Wales. Sediment containing high concentrations of Ti, Fe and Mn is typically found in regions associated with mafic rock types. Ca and Mg also exhibit elevated values in these areas but are in greatest abundance in sediment south of Port Clarence and offshore from Cape Prince of Wales where paleozoic limestone formations are found. Value-surface maps for Na, K, and Al do not show strong trends. Concentrations of K are highest off NE Cape of St. Lawrence Island, and are probably related to the granitic bodies there. Al shows highest values in the Stuart Island area and eastern Norton Sound. Mn, Fe, Ti, and to a lesser degree Ca, Mg, Na, K, and Al all have high concentrations in the region of the Yukon Delta and in Norton Sound. The highest amount of P was in a sample from an enclosed basin northeast of St. Lawrence Island.

Of the minor elements, Sr has the highest correlation coefficients with K, Na, and Ba, but the highest Sr values as depicted by value-surface maps correlate with the highest Ca values. Concentrations of Sc correlate closest to concentrations of Ti, Fe, V, La, and Mn and Sc shows the same broad high anomaly surrounding the Yukon Delta and the low anomaly in the Chirikov Basin already mentioned for Ti, Fe, and Mn. Ga has high correlation coefficients with La, Sc and Ti and high amounts of Ga are found in Anadyr Strait and the

eastern end of Norton Sound. Nb is concentrated east of Cape Darby and may be related to the high concentrations of Nb reported in stream sediments from Cape Darby peninsula. Nd correlates closely with Ce and La. Concentrations of Y follow the trend of high amounts in the Yukon Delta/Norton Sound area and lowest amounts in Chirikov Basin. Yb has the highest correlation coefficients with Mn, Zn, and Y and also is found in greater concentration in the area of the Yukon Holocene sediment distribution. Ag is found in 8 samples close to areas of St. Lawrence Island known to have silver mineralization, close to Stuart Island, the Yukon Delta, Cape Nome, and Bluff. The highest concentrations of Mo were found close to Stuart Island off Cape Prince of Wales in a sample containing a high amount of Sn, and in a Bluff beach sample.

Q-mode factor analysis showed that 4 factors were sufficient to explain 92% of the variance between samples. A map of loadings for the most significant factor (Factor III) covers an area that roughly corresponds to the area of Yukon Holocene sediment deposition and an area NW of St. Lawrence Island. Elements that are related to Factor III are La, Na, Ga, Ba, Sr, Sc, K, V and Al. A map of loadings for the next most significant factor (Factor I) corresponds approximately to the extent of relict sediment cover in Chirikov Basin. Elements related to Factor I are B, V, Yb, Ba and Al. These two factors (Factors I and II) seem to explain the trend exhibited by many of the elements of generally high concentrations in sediment surrounding the Yukon Delta and in the Norton Sound area and generally low concentrations in the Chirikov Basin. However, some of the elements that show this trend most conspicuously are not closely related to Factor III, but instead are better related to Factor II. Distribution of samples with high loadings for Factor II corresponds roughly to the highly mineralized areas along the southern Seward Peninsula. Elements related to Factor II are Y, Yb, Ti, Fe, Sc, Co, V

and Mn. Plots of Factor IV loadings indicate this factor correlates somewhat with subaqueous glacial morain deposits. The one correlative element is Nb.

II. INTRODUCTION

A. General Nature and Scope of Study

This study has been undertaken to assess the major and trace element content of bulk bottom sediment in the northern Bering Sea. The values arrived at are useful as geochemical baseline data that can be compared with similar data from bottom sediment in the same region and elsewhere. The data are also useful for monitoring possible changes in chemistry of the bottom sediments that might result from future development in the region. Present anomalously high major and trace element concentrations are mapped and related to highly mineralized sources on land so that these high values will not be mistaken at some future time as sites of contamination caused by mineral resource development.

B. Specific Objectives

More specifically, this study considers 7 groups of elements of varying environmental significance and resource potential; we map their areal distribution in surface sediments and relate these to probable sediment source. The 7 groups of elements include: (1) V and Ni as possible petroleum indicators; (2) the heavy metals Sn, Zr, Ce, and Cr as possible indicators of placer deposits (Hg and Au are considered in separate studies, see Nelson et al., 1975; and Nelson and Hopkins, 1972); (3) the potentially toxic elements Pb, Cu, Zn, As, Sb, and Cd (Hg is considered elsewhere, see above); (4) Fe, Mn, Co, and Ba as elements which are sensitive to change in the chemistry of the sedimentary environment, with Ba as a particular indicator of petroleum drilling muds; (5) a suite of major and trace elements, and (6) a miscellaneous group of economic elements.

The data are both graphically and statistically displayed. Computer maps have been generated that display both contoured and 3-dimensional value-surfaces for each element. Geometric means and deviations as well as value ranges for each element are given in Tables I and II. Results of correlation analyses are found in Tables III and IV. Maps showing the generalized geology of the area, the sampling locations and onshore mineralizaton sites, and the significant offshore anomalies are depicted in Figs. 1, 2, and 3. A map of significant Q-mode factor loadings is found in Fig. 4.

III. CURRENT STATE OF KNOWLEDGE

The toxic element Hg, has been previously studied in the sediments of this area by Nelson, et al., 1975. Gold placer deposits in the nearshore areas of Nome-Bluff and in the offshore areas of Chirikov Basin have been extensively studied by Nelson and Hopkins, 1972. Reports by McManus, et al. (1977), Venkatarathnam (1971), and Sheth, (1971), discuss in detail the related topic of heavy mineral and sediment distribution, dispersal and provenance in the northern Bering Sea shelf region. Gardner et al., (1980), have completed a study similar to this one in the central and southern Bering Sea shelf regions.

IV. STUDY AREA

The bottom surface sediment samples analyzed for this study came from 180 sampling stations spread over Norton Basin (Fig. 2). The western part of the area, Chirikov Basin, is covered with what is thought to be relict medium-fine sand (Nelson and Hopkins, 1972). The region surrounding the Yukon Delta as well as much of Norton Sound, and several depressions in an eastern corridor extending up to the Bering Strait, is generally covered with more recent sediment grading from coarse silt to fine sand. The major source of Holocene sediment in this region is the Yukon River (Nelson and Creager, 1977). There

are some areas where the relict and modern sediments intersect creating a palimpsest mixture of the two (McManus et al., 1977). Much of the sediment coming from the Yukon and deposited in Norton Sound is thought to be re-suspended periodically and then flushed through the Bering Strait and deposited in the Chukchi Sea by normal and storm tides (Nelson and Creager, 1977). This is helped by currents which trend generally northwards to the Bering Strait and have velocities as high as 190 cm/sec in the Strait itself (Coachman, et al., 1976).

Water in the region is characterized by two fairly distinct masses. Colder, more saline waters dominate the central and western parts of the region. These are surrounded by a shoreward hugging mass of Alaskan coastal water which is warmer, less dense and generally moving along the eastern coast northward to the Bering Strait.

Significant mineralized deposits are found in several areas bounding this region (Fig. 2; Cobb, 1960a,b,c, 1962, 1964, and 1970; Eberlein and Menzie, 1978; Hudson and DeYoung, 1978, Hudson, et al., 1977; Hummel, 1977, Nelson and Hopkins, 1972, Nelson, et al., 1972; Overstreet, et al., 1974, 1978; Patton and Csejtey, 1971, 1972; and Sainsbury, 1969, 1975). Of particular importance are the gold placer deposits found in the Nome Bluff area. Gold placers are also located in various relict beach ridges or reworked glacial moraines presently submerged off the coast from Nome as well as off Chutkotka Peninsula and St. Lawrence Island (Nelson, Hopkins, 1972).

Lode deposits of economic interest occur in many areas surrounding Norton Basin. They include copper, lead, zinc, silver and molybdenum deposits in western and eastern St. Lawrence Island; tin and beryllium deposits of the Lost River ining district on the western tip of Seward Peninsula which also contain high concentrations of copper, lead, zinc, antimony, gold and

molybdenum; the general area of the southern Seward Peninsula where there are numerous occurrences of gold, copper, lead, zinc, mercury, antimony, iron, and some tungsten and niobium; the lands to the east of Norton Sound where gold, tungsten, antimony, tin, copper, silver, lead, zinc, molybdenum, platinum, chromium and titanium are found; and the entire Yukon drainage basin where mineral concentrations containing high concentrations of most of the aforementioned elements are located.

All of the areas mentioned are drained by streams and rivers that have undoubtedly been contributing substantial amounts of mineralized sediment to Norton Basin for the past several thousand years.

V. SOURCES, METHODS, AND RATIONALE OF DATA COLLECTION

Two groups of samples were utilized for this study. The first group consists of samples collected on 3 different cruises during the years 1968, 1969, and 1970. These samples were originally collected to delineate sediment characteristics and faunal distributions in the region and to assess placer gold dispersal from Seward Peninsula sources (Nelson and Hopkins, 1972). They were taken using a 5 gallon galvanized steel Van Veen grab sampler which would normally penetrate the top 5-10 cm of bottom sediment. The resulting samples were given no special treatment and were stored at room temperature. The second group of samples were collected using a Soutar Van Veen grab sampler during 1976 and 1977 U.S.G.S. cruises of the U.S.G.S. R/V SEA SOUNDER. The Soutar grab sampler is teflon coated and causes minimal disturbance of surface samples. Subsamples were selected for trace element analysis from the top 1-2 cm of each sample collected using the Soutar sampler and were immediately frozen and kept frozen until analyzed in Menlo Park, California.

This sampling technique was developed by Ian Kaplan of UCLA for BLM/NOAA trace element study of sediments on the western North American outer continental shelf.

The average distance between samples is approximately 30 km. In an analysis of variance of samples from the central and southern Bering Sea, Gardner, et al., 1980, found this distance to be adequate to show statistically significant trends in sediment composition.

Samples, including pore water salts, were air dried at 110o C. Each sample was then homogenized and a one gram split of each sample was analyzed by the Analytical Laboratories Branch, U.S.G.S, for a suite of over 50 elements using semi-quantitative optical emission spectroscopy (Grimes and Marinzino, 1968).

To assess the precision and accuracy of the 6-step semi-quantitative optical emission spectrographic technique used in this study, replicate analyses were done on both U.S.G.S. rock standards and on subsamples of the sediment samples being studied. Additionally, several replicate subsamples were analyzed by neutron activation.

VI. ANALYTIC RESULTS

Semi-quantitative emission spectroscopy, although not as precise as other analytic techniques, yields values that are adequate to delineate regional trends. Care must be taken, however, to establish the limits of precision and accuracy for the technique as used with a particular type of sample to detect a particular element.

The precision of the 6-step emission spectroscopy technique is influenced by two factors: variability of the substance being analyzed and the variability introduced by the imprecision in the use of the technique or in the technique itself. To reduce errors due to sample variability, samples

were ground to 230 mesh and homogenized. Sub-splits from the sample were then used for replicate analyses. The overall precision of the 6-step emission spectrographic technique was determined by running 5 to 8 replicate analyses on each of three samples. The subsamples used for the replicate analyses were submitted in a random sequence along with the other samples analyzed. The precision was calculated by averaging the percent difference between each replicate analysis and the mean value for all of the replicate analyses. Additional replicate analyses were run on subsamples from the same set of test samples by neutron activation as a further test of both the precision and accuracy of the emission spectrographic technique. Values of replicate analyses for all elements except zinc, were within 25 percent of the mean values for the replicate analyses, and replicate values for most of the elements fall within 15 percent of their mean (Patry, et al., 1977).

The accuracy of the 6-step emission spectographic analyses was tested by analyzing four U.S.G.S. standard rock samples of known element composition. Two analyses were made on each rock sample and the average of the two values was calculated for each of 30 elements. Then the percent difference between these values and the actual values for each rock was determined. Next, the percent differences for all four rock standards were averaged to give the average percent error between values yielded by the 6-step emission spectrographic technique and the known values for the rocks. Element values for Y, Ca, Ba, K, Cr, Cu, Na, Co, Nb, Ni, V, and Zn, as determined by emission spec, were within 30 percent of the established values for the rock standards. This group of elements is almost entirely within the bounds of the 'accepted' error for this analytic technique and therefore provides baseline data for the study area that is relatively free of analytic error. Values for eleven elements including Sr, Al, Sc, Zr, Ti, Ga, Pb, Fe, Mn, and Mg, were

within 35 to 65 percent of the actual values for the rock standards and can still be considered reasonable baseline data for these elements. Two elements, Yb and B, had values varying by more than 80% from the known values. Values for these elements should be regarded as only gross estimates of their actual content in the sediment. Accuracy for the determination of eight elements, Ag, As, Bi, Mo, Nd, Sb, Sn, and Ce, could not be assessed because quantities present were too low to be detected by the analytic method. These elements were not statistically analyzed but where present above the detection limit, they were plotted as anomalous values. Si was eliminated because its values were all greater than the upper limit of detection of the analytic technique (Patry, et al., 1977).

The data was transformed into base 10 logarithms and the arithmetic means and standard deviations were determined for the log values. The arithmetic mean of the log values of a distribution is equivalent to the geometric mean of the original values and if the distribution approximates log normality, the geometric mean is the best measurement of the central tendency of the distributon (Table I; Miesch, 1967). The distributions in this study were presumed to approximate log normality. Correlation analyses relating element pairs were also run on the logs of the data values. Q-mode factor analysis was performed to examine significant relationships among samples and elements (Fig. 4, Tables VI, VII, and VIII). Most of the elements had no values less than the lower limit of detection. If an element had only one to three values above or below the upper or lower limit of detection, these indeterminate values were substituted with definite values set two class intervals above or below the value of the limit of detection. Nine elements (Ag, As, Bi, Mo, Nd, Si Sb, Sn, and Ce) had too few values for statistical treatment but enough values were obtained for Ag, Mo, and Sn to be plotted graphically.

Concentrations of twenty-six elements were all below detection limits (Table II). Two elements, Ga and P, had a considerable number of values that were less than the lower limits of detection.

Computer software developed by the Dynamic Graphics Company, Berkeley, California (Dynamic Graphics Surface Display Library) was used to display the geochemical values. For each element (Figs. 5-66) there is a two-dimensional contour map of the value-surface and a three-dimensional mesh plot of the value-surface shown at an oblique perspective to the land surface.[1] A single viewing perspective of 20° degrees to the horizontal and looking NNW was chosen for all of the three-dimensional mesh plots because the uniformity was found to enhance the ease with which one can compare plots for different elements. The value surface of each three-dimensional plot was made to decrease to zero as it impinged on a rough polygonal outline of surrounding coastlines. To further help viewer orientaion, a map view showing the coastal outline in the same perspective as the three-dimensional plot was generated above the three-dimensional plot.

The Dynamic Graphics software used to generate the plotting grids from which the two- and three-dimensional map plots are made, employs an iterative technique to solve biharmonic equations which produces a surface of least tension passing through all the data points. It is this surface which is contoured or graphically represented by a mesh pattern. Contour intervals for the two-dimensional contour plots are chosen automatically by the program which makes the selection based on the maximum, minimum and distribution of values encountered.

VII. DISCUSSION

A. Petroleum Indicators

High concentrations of V and Ni in sediments near petroleum seeps have been attributed to contamination of the sediments by high concentrations of

[1] Microfiche copy displaying lists and map-plots of element concentrations and locations is available as Open-File Report 80-399B.

these elements as chelated porphyrins in the oils and tars of the seeps (Reed and Kaplan, 1977; Yen, 1975). Therefore, relatively high concentrations of V and Ni together in a particular area might indicate the presence of thermogenic hydrocarbons.

The one known gas seep in Norton Basin is located roughly 35 km south of Nome. At this site concentrations of Ni in surface sediment are not anomalously high but concentrations of V are up to 200 ppm, more than two geometric deviations higher than the geometric mean for V in sediment of the northern Bering Sea region (Figs. 5,7,8; Table I). But the high V values in the gas-seep area may be a result of being located in the region of Yukon Holocene sedimentation because equally high values are found quite generally throughout this area. The lack of both Ni and V anomalies at the Norton Sound Seep is in keeping with the fact that it is primarily a CO_2 gas seep with only traces of low molecular weight thermogenic hydrocarbons (Kvenvolden, et al., 1979).

Additional sediment samples were collected in a grid surrounding the gas seep in order to look for possible chemical differences between sediment in the gas seep area and sediments in surrounding areas. The samples were analyzed for 54 elements including V and Ni. The average concentrations of V and Ni in these samples are 68.8 ppm and 18.8 ppm respectively, which are lower than backgound V and Ni concentrations for this region (Table I).

It is clear that the V and Ni values for the detailed sampling grid do not support thermogenic origin of the anomalous hydrocarbons found in this area. There was a seven-year difference between the collection time of the grid of samples and the first group of samples in the gas-seep area. Differences in the V and Ni content of these two sets of samples may reflect a basic change in the sediment due perhaps to the large storm surge of 1974 (Pathauer, T.F., 1975).

Sediments in an area located approximately 40 km west of the southern tip of St. Lawrence Island had V and Ni concentrations of 200 and 100 ppm (Fig. 3). Both of these values are higher than the expected ranges for V and Ni (Table I). These relatively high values coupled with the fact that the sample locations are at some distance from any possible land source could be taken as sufficient evidence to warrant a closer examination of this area for hydrocarbons.

B. Heavy Metals

General Characteristics

Sn, Cr, Zr, and Ce are treated as a group because they are found in minerals which are heavy and stable enough to be mechanically concentrated into placer deposits. Au and Hg, etc., are not considered in this report because their distribution is described in other published reports (Nelson and Hopkins, 1972; Nelson et al., 1975-1977).

Previous studies including those by Venkatarathnam, 1971; Sheth, 1971; and McManus et al., 1976, have looked at the distribution of heavy minerals in the Norton Basin region but these studies were either limited to a small area or involved only mineral concentrates from a portion of the sand-size range.

The degree to which a heavy mineral is concentrated in placers is dependent on winnowing forces and the magnitude of the density and size differences between the heavy mineral and the containing sediment. For example, if the heavy mineral particles in a sediment are relatively uniform in size, the mineral may be evenly distributed throughout hydraulically-equivalent sediment. Concentration can begin to take place only when the hydraulic balance between the particle size and density for the various mineral constituents of a sediment becomes unequal. An example would be when mechanical and chemical forces wear down heavy mineral particles in a sediment at a slower rate than the other mineral constituents of the sediment.

Once a given heavy mineral has been concentrated, the main factor influencing whether the concentration will be detected is the sampling interval. If the sampling interval was chosen primarily to detect significant areal variability in an average suite of elements, it may be too large to detect significant variability in specific heavier elements that tend to change in concentration over shorter distance. Also, the sampling interval may be entirely adequate to pick up general variability of the heavy element as it is distributed in sediments from a particular provenance but it may miss smaller scale variability caused by localized hydraulic fractionation (Flores and Shideler, 1978).

Zr

Relatively high concentrations of Zr are found in sediments surrounding the Yukon Delta, in Norton Sound, and around St. Lawrence Island (Figs. 9 and 10). This contrasts with the much lower values in Chirikov Basin. The presence of relatively higher concentrations of Zr in Yukon-derived sediment is probably because the Yukon River passes through a terrain which is composed mainly of sialic rocks, predominant contributers of zircon (Mason and Berry, 1968). A comparison of our contoured value-surface map for Zr and Venkatarathnam's percentage distribution maps (1971) of the heavy-mineral zircon in the 1-2.75 and 2.75-4.0 phi size-range show that his areas of high values generally correspond with the high value areas of our 2-dimensional map. This is particularly true off the NE Cape of St. Lawrence Island where his values as well as ours are highest. Our data also show persistently high concentrations for Zr off the western and southern parts of St. Lawrence Island. Probable sources for these high values are sediments derived from quartz-monzanite plutons which are found over much of St. Lawrence Island.

A strong Zr concentration occurs in a sample from the central part of Norton Sound, relatively far from land. Sediment analyzed at this locale was taken from a depth of about 10 meters and, according to McManus et al., 1976, in an area of generally higher sand content than the rest of Norton Sound. The lack of a nearby land source and the lack of generally high values in similar surrounding sediments might suggest that this sample may contain hydraulically concentrated zircon in a zone of coarser sediment. Strong tidal currents pass through this area (Cacchione and Drake, 1978) and may concentrate the heavier zircon grains.

Another sample with a high concentration of Zr was found 30 km south of Cape Prince of Wales (see Fig. 3; this sample is not represented on the value-surface maps). The Zr content in sediment from this location is as great as in any other sample in this study and the concentrations of Ti, Mn, Cr, La, Sc, Y, Zr, Yb, Nd, Ce, Sn and Zn are also greater than the expected ranges for these elments.

Venkatarathnam reports high concentrations of heavy minerals in the 2.75-4.0 phi size-range from this area, especially further south and east in the sand wave region west of Port Clarence. Similar concentrations are found in Anadyr and Shpanberg Straits. It is probable that the high speed currents in these areas have concentrated heavy minerals there. The high concentrations of various elements in the sample 30 km south of Cape Prince of Wales may represent a significant anomaly and may indicate deposits heretofore undetected and of considerable economic potential.

Sn

Sn concentrations in 156 of the 180 samples analyzed were below the limit of detection of 2 ppm. The highest values occurred close to Tin City on the southwest coast of Cape Prince of Wales; lesser anomalies were found in the

area of King Island, Port Clarence, Bluff, Cape Rodney, the western and north-central coast of St. Lawrence Island, half way between Cape Prince of Wales and St. Lawrence Island, and the aforementioned sample from 30 km south of Cape Prince of Wales (Figs. 11 and 12). The highest concentrations of Sn, near Tin City, are obviously derived from the same mineralized formation which gave Tin City its name. Anomalies near Bluff, north central St. Lawrence Island, and Cape Rodney-Nome areas also appear to be related to adjacent onshore mineralization. The isolated high concentrations off of the NW tip of St. Lawrence Island may have been hydraulically concentrated. High values off Pt. Clarence and in the area of King Island are in an area of high currents and sand dune fields that also may represent an area of tin concentration.

Cr

The distribution of Cr in the Norton Basin is uniform except in the areas of Stuart Island, St. Lawrence Island, and Cape Prince of Wales (Figs. 13 and 14). These locations have relatively high concentrations of Cr, some of which are greater than one geometric deviation above the geometric mean.

All of these anomalies, except the sample site 30 km south of Cape Prince of Wales discussed earlier, are located close to igneous outcrops on land. Cape Prince of Wales is the site of granitic plutons that are cut by occassional mafic dikes. Gabbro and metagabbro bodies are also found throughout the same region. Stuart Island, the adjacent peninsula and the central portion of St. Lawrence Island are composed largely of alkali olivine basalts. Because chromite ($FeCr_2O_4$), which is the principal mineral of chromium, is thought to form as a magmatic segregation in ultrabasic rocks and is usually associated with olivine, there is probably a direct connection between anomalous values of Cr offshore, and the adjacent mafic igneous outcrops on land.

Nelson and Hopkins found an abundance of harzburgite among rock fragments collected in dredge hauls in Akeftapak Bay off the NNE end of St. Lawrence Island (Patton and Csejtey, 1972). Semi-quantitative emission spectrographic analysis of some of these harzburgite samples yielded chromium values as high as 2,000 to 10,000 ppm. Patton and Csejtey also reported very high chromium values in the lower reaches of streams feeding into Akeftapak Bay. From this evidence, Patton and Csejtey infer the presence of an ultramafic body existing just below a thin veneer of sediment at this location. However, samples from the same area in our study did not have high concentrations of Cr. The distance between the dredge haul site and the nearest sampling site used in this study is 14 km. The fact that our study did not detect the dredge haul anomalies illustrates the importance of selecting the right sampling interval when attempting to delineate concentrations of heavy minerals and their associated heavy metals.

Ce (and associate Lanthanides, La and Nd)

Ce (cerium) is a heavy metal classified with a group of chemically similar elements called the lanthanides. The lanthanides usually occur together and their most common source mineral is monazite which is a fairly rare and complex phosphate occuring as an accessory mineral in granites, gneisses, aplites, and pegmatites. Monazite is resistant to chemical attack and is often concentrated in sands, particularly beach placers (Bateman, 1965; Sienko and Plane, 1961). The presence of cerium and other lanthanide elements in the same samples would be strong evidence for the presence of monazite in the samples.

La (lanthanum) and Ce anomalies on our maps (Figs. 15, 16, and 49, 50) generally coincide. The only real difference is that La has a much lower limit of detection than Ce and therefore shows much greater definition in the

lower value range. Neodymium (Nd), another lanthanide, was detected in three raw bulk samples and these three samples also had anomalously high concentrations of La and Ce. It is clear that these three elements occur together. Additional evidence that the containing mineral for these elements is monazite is the detection of Ce and Nd in analyses of mechanical concentrates of samples used in the study (not reported here). Analyses from raw bulk samples of the same sample set show either an absence of Ce or Nd or much lower values. This indicates that these elements are present in a heavy mineral like monazite that may be hydraulically concentrated.

The highest concentratios of Ce, La, and Nd are in a sample 30 km south of Cape Prince of Wales. Their presence together lends support to the probability that the sample had indeed been concentrated. Areas where monazite has been reported in this region are from Brooks Mountain, Ear Mountain, and Gold Run on the eastern Seward Peninsula (Cobb, 1970). High concentrations of Cerium in sediment west of Cape Rodney may be related to the Gold-Run location.

C. Potentially Toxic Elements

Of the potentially toxic elements considered in this report, only Cu, Pb, and Zn have sufficient numbers of values greater than their lower limits of detection to calculate meaningful statistics or to plot their value surfaces. Cd (cadmium) was not detected in any sample analyzed. Sb (antimony) was detected only in beach samples taken near Bluff, the NE Cape of St. Lawrence Island, and from Stuart Island; As (arsenic) was detected only in the beach samples from Bluff. Anomalous values are not found offshore from these beach areas. The values for Sb and As in these samples are several orders of magnitude higher than their limits of detection by the 6-step emission spectrographic technique and can therefore be considered to be

anomalous. The map depicting source areas (Fig. 2) for some of the more economically important elements of this study shows Bluff to be a known area of concentrations of As.

Distribution of Cu, Pb, and Zn surface values in shelf sediments of Norton Basin are generally similar, including anomalously high values off St. Lawrence Island, along the southern coast of the Seward Peninsula, and throughout Norton Sound. The maps for Cu and Zn show much greater similarity to each other, however, than to the map for Pb (Figs. 17, 18, 19, 20, 21, and 22). Statistically, Pb correlates better with Cu and Zn than with any other element represented in the study (Table III), but Cu and Zn have a much higher correlation between themselves (.8023) than with Pb which supports the relative visual similarity between the maps of these elements.

A significant trend that appears in value-surface maps of both Cu and Zn is the generally higher values in Norton Sound compared to Chirikov basin. High values for Cu and Zn form a halo surrounding the Yukon Delta and the western edge of the halo trends due north along a line extending from the southern edge of the Yukon Delta towards the Bering Strait. The location of this halo coincides closely with the area of maximum deposition of Yukon-derived sediment in Norton Sound (Nelson and Creager, 1977). The gradation of Cu and Zn values away from the delta and the generally higher concentrations of these elements in Norton Sound suggest a source and dispersal coincident with Yukon-derived sediment. The Yukon River flows through an area highly mineralized in these elements and thus appears to be the dominant source for minerals bearing these elements.

Another significant aspect of the distribution of Cu, Zn and Pb is the presence of localized high values generally close to certain coastal areas. All three elements have their highest concentrations in beach samples taken near

Bluff, Alaska (not completely represented on value surface maps.) Pb and Cu show a continuation of these high values up to 20 km offshore from Bluff. Unlike Cu and Zn, and except for values from the Bluff beach samples, Pb deviates little from the geometric mean throughout Norton Basin; although fairly high values can be seen adjacent to Stuart Island and the eastern tip of St. Lawrence Island. Cu is also concentrated near Stuart Island and the eastern tip of St. Lawrence Island. In addition, high concentrations are found off the southern coast of eastern St. Lawrence Island and off the north-central projection of the island as well as off Nome and in an area around King Island. High Zn concentrations occur off south-central and north-central St. Lawrence Island. Concentrations of Zn are also relatively high concentrations off Nome, in a sample taken 30 km south of Cape Prince of Wales, and along the eastern edge of Norton Sound, but are greatest (except for the Bluff beach samples) in the central part of eastern Norton Sound. This last Zn anomaly is rather puzzling and does not appear to be related to dispersal of Yukon sediment or to the nearshore high values that seem to be caused by concentration in sediment derived from immediately adjacent land areas.

In summary, the toxic elements discussed here apparently have their highest values in relatively localized beach areas close to known terrestrial sources or are clearly derived from the sediments eroding from nearshore areas close to probable higher concentrations of these elements. Other elevated concentrations offshore are probably related to general sediment dispersal within the region and the possible placer concentration of those elements aggregated in heavy minerals. An example of high values over a broad area which are probably related to sediment type/source terrains are the regionally high values of Cu and Zn over Norton Sound.

D. Chemical-Environmental Change Indicators

Though the evidence cited below indicates concentrations of Fe, Mn, and Co in Norton Basin sediments are source related, they are singled out here because they are more responsive to changing oxidation/reduction environments than most of the other elements under discussion. Ba is included because of its use as a drilling mud and the resulting potential contamination of sediment where it is used.

The value-surface maps for Fe, Mn and Co are quite similar (Figs. 23, 24, 25, 26, 27, and 28). The most obvious correlations are the high anomalous values each map shows in the areas of the volcanics of north-central St. Lawrence Island and Stuart Island. Anomalies in these volcanogenic areas have also been found for Cu, Ni, and Cr (other mafic-associated elements) as has already been pointed out. The other obvious correlation is the wide area with high values surrounding the Yukon Delta in particular and Norton Sound in general.

High values surrounding the Yukon Delta, much of Norton Sound, and northward toward the Bering Strait seem to fall mainly within the area defining the prevalence of modern Yukon sediment. The generally high values in this region probably are directly related to Yukon source sediments which are in part derived from the input of mafic volcanic terrain in the river drainage basin. Anomalous values of Fe, Mn or Co resulting from concentrated precipitates of these elements are not readily apparent. This could only be determined by taking a closer look at the exact mineral species containing Fe and Mn.

The highest Mn value was detected in a sample from 30 km south of Cape Prince of Wales that has been previously discussed. This sample is considerably removed from land and it is probable that its high Mn values are

due to mechanical concentration rather than having been directly derived from volcanic terrain.

The value surface maps for Ba show slightly anomalous values surrounding the Yukon Delta, in addition to high values near Stuart Island and at various locations along the southern coast of Seward Peninsula (Figs. 29 and 30). The highest anomalies are just off the southern edge of St. Lawrence Island and in the middle of Anadyr Strait. The general increase in concentrations of a number of elements in this area surrounding the delta has already been noted and seems to be related to the Yukon sediment source and dispersal pattern. The anomalies near Stuart Island and the southern coast of Seward Peninsula appear as lobes coming off the land and may be correlated with sediment sources from igneous rocks in those areas. The origin of the high values close to St. Lawrence Island are more obscure. None of the elements that correlate with Ba have outstanding anomalies in the Anadyr Strait and only Sr has high values off the southern edge of St. Lawrence Island. The value of 1500 ppm in Anadyr Strait is equal to .15% and could reflect a source for Ba mineralization on the point of the Chukotka Peninsula.

E. Major Elements

All samples used in this study were analyzed for all of the major elements Si, Ti, Al, Fe, Mn, Mg, Ca, Na, K, and P. Values for Si, however, were higher than the upper limit of detection (10%) in every sample analyzed and are not reported here.

Value-surface maps for major elements show some of the general element distribution patterns already discussed. Mn, Fe, and Ti have higher values surrounding the Yukon Delta and in Norton Sound relative to the Chirikov Basin (Figs. 23, 24, 25, 26, 31, and 32). Ca, Mg, Na, K, and Al show a similar trend to some degree (Figs. 33, 34, 35, 36, 37, 38, 39, 40, 41, and 42). Each

element also has anomalously high values shown as lobes that appear to be coming from nearby land sources.

Areas with higher Ti concentrations generally correspond to areas with high concentrations of Mn and Fe which have already been shown to be associated with the volcanics of Stuart Island and St. Lawrence Island. This is expected because Ti is relatively high in basaltic rock types. The highest Ti value is from the sample previously discussed that comes from a possible placer 30 km south of Cape Prince of Wales.

Concentrations of Ca and Mg are also high near the Stuart Island and St. Lawrence volcanics, but they are highest offshore from the southern coast of Cape Prince of Wales and south of Port Clarence. High concentrations of Ca and Mg in these last areas probably are related to the limestone formations found on Cape Prince of Wales and in outcrops reported on the sea floor south of Port Clarence (Nelson et al. in preparation,; Nelson and Hopkins, 1972). Sr anomalies, normally associated with limestone, exist in the same areas.

Value-surface maps for Na, K, and Al are more varied than maps of the other major elements. They consist of alternating high and low values and show only slight regional differences. The anomalies that do seem to originate from land sources appear broader in areal extent than some of the less common elements already discussed. The sample containing highest concentrations of K is off of the NE Cape of St. Lawrence Island and is probably derived from granitic bodies that are found there. Samples with highest concentrations of Al are from the areas of Stuart Island and eastern Norton Sound and are probably derived from basalts.

P (phosphorus) was detected in only 54 samples, and was not used in the correlation analysis. The lower limit of detection is .10% which is somewhat higher than concentrations found in average shales and sandstones (Mason,

1966). Elevated concentratios of P are found in the eastern portion of Norton Sound, in a few patches surrounding the Yukon Delta and in a swath running through eastern Anadyr Strait and hooking to north of St. Lawrence Island. The highest concentration of P occurs in a sample from an enclosed basin just off the northeast coast of St. Lawrence Island. This high value may be related in some way to the reducing conditons of the enclosed basin (Mason, 1966).

F. Minor Elements

The minor elements Sr, Sc, La, Ga, Nb, Nd, B, Y, Yb, and Be correlate with other elements. Sr is normally associated with limestone and, as expected, high concentrations of Sr correspond quite closely to the Ca anomalies previously mentioned. However, correlation coefficients are higher between Sr and K, Na, Ba, and Al than between Sr and Ca (see Tables III and IV). The association of Sr with Ba is common. The association of Sr with K, Na, Al, and Ca suggests a possible relationship with feldspar where Sr and Ba substitute for K.

Sc (scandium) correlates most closely with Ti, Fe, V, La and Mn and exhibits the same general distribution as these elements, with higher values grading off the Yukon to lower values in Chirikov Basin (Figs. 47 and 48). The association of Sc with La and Nd is common and the usual mineral containing them is monazite (Figs. 49 and 50). Ga (gallium) also shows some association with La, Sc, and Ti. The highest values of Ga are in Anadyr Straits and the eastern end of Norton Sound (Figs. 51 and 52).

Nb (niobium) exhibits no correlation with any other element. The highest concentrations are in samples from off Cape Darby in Norton Sound and southwest of St. Lawrence Island (Figs. 53 and 54). The anomaly off Cape Darby correlates with the highest Nb anomalies detected in western Alaska

found on the Darby Peninsula (Miller and Grybeck, 1973).

B (boron) is most closely correlated with K and Ba. High concentrations are located at the eastern end of Norton Sound, off Cape Darby, off the coast from Bluff, off Cape Rodney, and southwest of St. Lawrence Island (Figs. 55 and 56).

Y (yttrium) follows the pattern of elements with generally high concentrations in sediment surrounding the Yukon Delta and Norton Sound and low concentrations in sediment from the Chirikov Basin (Figs. 57 and 58). It correlates most closely with Mn, Fe, and Ti which also follow this pattern. Very localized high anomalies are found off Cape Prince of Wales, Nome, and Bluff.

Yb (yterbium) correlates most closely with Mn, Zn, and Y but has no pronounced trends except for the general trend of high values in Norton Sound, and low values in Chirikov Basin (Figs. 59 and 60). A few very high concentrations occur in sediment off Cape Prince of Wales, at various localized points off the southern coast of Seward Peninsula, in the general area of eastern Norton Sound, and NNE of St. Lawrence Island.

Beryllium (Be) correlates closest with La, Yb, and Sc with high concentrations in eastern Norton Sound, along the southern coast of the Seward Peninsula, and off the southwest and southeast coasts of St. Lawrence Island. Highest concentrations occur in samples from just off Tin City at Cape Prince of Wales and one close to Stuart Island. These two high values as well as other high values that appear as lobes coming off the land indicate that specific mineralized terrains are probable sources. This is confirmed for Cape Prince of Wales where extensive economic grade beryllium deposits have been reported by Sainsbury, 1969, in the central York Mountains.

G. Other Miscellaneous Economic Elements

Au was not detected in any of the samples analyzed. This was to be expected because the lower limit of detection for Au using the emission spectographic method, is 7 ppm (7000 ppb). A study by Nelson and Hopkins, 1972, has shown that average Au concentrations in open Bering Sea sediments are about 2-3 parts per billion (ppb), and the highest nearshore concentrations found in relict gravel and selected ruby sands, ranged from 556 to 2,118 ppb.

Ag was detected in only 8 of the 180 samples and 3 of these samples could not be assigned a reasonable quantitative value. Some of the samples containing Ag concentrations were from off the NW Cape and the southern tip of St. Lawrence Island (Figs. 63 and 64). Mineralization containing appreciable amounts of Ag has been reported on both ends of St. Lawrence Island and could be the source for for Ag in these samples. Relatively high values were also found near Stuart Island and close in to the Yukon Delta. In addition, Ag was detected in a few samples from off Nome and Cape Nome. High concentrations of Ag (3 ppm) were found in beach samples from Bluff but these values were not plotted on the value-surface maps.

Mo concentrations in all but 5 samples were below the limit of detection of 2 ppm. The highest values were detected in Bluff beach samples (30 ppm) (Figs. 65 and 66). Another high value was found in a Stewart Island beach sample (2 pm) and the presence of Mo was detected off Cape Rodney. Mo mineralization has been reported inland from the coast of eastern Norton Sound and in the Nome area.

Bi was below the limit of detection of 7 ppm in all but 2 samples. The highest value of 70 ppm was in a sediment sample close to the Lost River Mining District on Cape Prince of Wales that also had an anomalously high Sn concentration. Bi is often found in association with Sn ores and is known to

occur in the form of bismuthinite as one of the main mineral constituents of a skarn zone associated with the Sn and Be deposits at Lost River (Sainsbury, 1969). A sample from off the known mineralized area of Bluff contained Bi; this sample also had high concentrations of Cu, Pb, Zn, Mn, Sb, and As.

H. Q- Mode Factor Analysis

Q-mode analysis was employed to discover possible relationships between groups of samples. The basic algorithms used in the Q-mode analysis are from Klovan and Imbrie (1971) and Imbrie (1963). A more complete description of the program is in Van Trump (1975).

The raw data was first transformed to proportions or the value range of each element so that the transformed values would lie between 0 and 1.

Four factors from the Q-mode varimax factor matrix were found to explain 92% of the variance between samples (see Table VII) and only these four factors seemed to be related to sediment characteristic and geologic background. Of these factors, Factor III was judged to include the most important sample group because it explained 33.4% of the variance between samples. Factor I explained 24.3%, Factor IV explained 22.5% and Factor II with a variance of 11.8%, encompassed the fewest samples.

Samples with the highest loadings (>.7) for Factor III were found in an apron around the Yukon Delta and in patches in the west-central part of Norton Sound and NNW of St. Lawrence Island and in Anadyr Strait (Fig. 4). Samples with intermediate loadings (.6 to .7) values were found in a wide apron around the Yukon Delta, throughout most of Norton Sound, around the northern, eastern, and southern coasts of St. Lawrence Island, and south of Cape Prince of Wales.

Samples with the highest loadings for Q-mode Factor I, which explained the second highest percentage of variance, were from an area that generally

has low loadings for Factor III, namely the Chirikov Basin region (Fig. 4). Samples with the highest loadings for Factor II are from along the coast between Cape Rodney and Golovnin Bay, just off Cape Prince of Wales and near King Island. Samples with the highest loadings for Factor IV are from patches north of St. Lawrence Island, from random areas throughout Norton Basin, and from areas just off the south coast of the Seward Peninsula.

Scaled varimax factor scores (Table VI) were computed for each element during the Q-mode analysis in order to determine the elements that are most correlative with each factor group. As an additional check of the relationship between samples and to highlight possible negative relationships between factors, correlation coefficients were computed between element values and factor loadings for all the samples (Tables III and V). Both the Q-mode scaled varimax factor scores and the correlation coefficients between varimax factor loadings and element values indicate that samples with high loadings for Factor III contain relatively high concentrations of Ba, Na, Sr, La, K, Ga, Al, and Sc. B, V, and Yb are concentrated in Factor I samples; Factor II loadings correlate most closely with Y, Fe, Mn, Ti, Yb, Zn, Co, Sc, and Cu. The only element that seems to correlate somewhat with Factor IV is Nb and its most negative r values (Table V) are almost the same as the elements that belong to Factor II which indicates it may simply be the negative of Factor II.

The area of sediments with high factor loadings for Factor III of the Q-mode analysis (0.5 and above) corresponds closely to the area covered predominantly by Yukon Holocene sediment, although samples with high loadings for Factor III are also found north of St. Lawrence Island and in Anadyr Strait. The elements used in grouping samples in this factor are primarily those elements that are most abundant in sialic rock types. Na cannot readily

be regarded as an artifact of residual pore water salts because it increases in concentration in sediments closer to the hyposaline runoff of the Yukon River. The occurrence of high loadings for Factor III in areas not covered by Yukon sediments probably indicates that the sediments in these areas are similar to Yukon-type sediment and that they also originated in sialic rock terrain.

Samples with high loadings for Q-mode Factor I are from areas where modern Yukon sediment is absent but where Holocene transgressive sands of mixed origin are found. This general area covers the region of Chirikov Basin, but there does not seem to be any clear relationship between the elements of this factor and the sediments of the region.

Samples with highest loadings for Factor II of the Q-mode analysis are from very close to the Nome-Bluff strand line and off of Cape Prince of Wales and King Island, regions of highly mineralized mafic rocks. Factor II is therefore grouping sediments derived from these terrains. This is borne out by the association of several mafic-related elements to Factor II, particularly Ti, Fe, Co, and Mn.

The contoured surface of Factor IV shows a rough correlation with areas reported to be covered by relict glacial debris and lag gravel, particularly in a lobe extending NE of St. Lawrence Island (McManus et al., 1977). Otherwise, its significance is not readily apparent, except as a negative factor to Factor II.

It is not altogether clear why some of the minor elements should be grouped with a particular factor or why, in some cases, they should be related to one another through their r values. These relationships should be regarded with caution.

VII. CONCLUSIONS AND NEED FOR FURTHER STUDY

Measured concentrations of Y, Ca, Ba, K, Cr, Cu, Na, Co, Nb, Ni, V, and Zn are within 30% of reported values for rock standards and are therefore reliable baseline data. Measured concentrations of Sr, Al, Sc, Zr, Ti, Ga, Pb, Fe, Mn, and Mg were within 35-65% of the reported values for rock standards and can probably be regarded as providing reasonable baseline data. The elements Ag, As, Bi, Mo, Sb, Sn, P, Ce, and Nd had too few concentrations above detection limits to say anything about the accuracy of their measurement. Concentrations of Si were higher than the upper limit of detection in every sample. All concentrations of Au, Cd, Pd, Pt, Te, U, W, Ge, Hf, In, Li, Re, Ta, Th, Tl, Pr, Sm, Eu, Gd, Tb, Dy, Ho, Er, Tm, and Lu were below limits of detection.

High concentrations of V and Ni have been noted in sediment in the areas of hydrocarbon seeps. Concentrations of these elements in samples from a grid covering a probable thermogenic gas seep 35 km south of Nome however, were no different than background concentrations for these elements in the northern Bering Sea. Lack of V and Ni anomalies for this gas seep may only mean that the seep source is of a light hydrocarbon gas type that does not result in high Ni and V values as do some heavy hydrocarbon petroleum seeps. Samples 40 km west of the southern tip of St. Lawrence Island contains high concentrations of V and Ni and their location warrants a closer study for hydrocarbon seeps. Other high concentrations of Ni occur in sediments in the vicinity of Stuart Island and off the north and south coasts of St. Lawrence Island and are related to the basaltic volcanics in these areas, not petroleum sources.

Pb, Cu, Zn, As, Sb, and Cd are considered to be potentially toxic when found in sufficient concentrations. Presently, the highest values of any of these elements are derived from highly mineralized onshore locations, for

example, Cu and Zn off St. Lawrence Island, Nome, and Bluff beaches, and high Cu values off Stuart Island. The few values detected for Sb and As are in sediment derived from areas of onshore mineralization near Bluff, the NE tip of St. Lawrence Island, and just off Stuart Island. Both Cu and Zn have relatively high values in areas off the Yukon Delta and in Norton Sound that correspond to the areas covered by Yukon Holocene sediment.

Concentrations of Pb vary little from the geometric mean but there are some relatively high concentrations off Bluff beach, Stuart Island, and the eastern tip of St. Lawrence Island.

Because Zr, Sn, Cr, and Ce are commonly found in heavy minerals, high concentrations of these elements may well indicate placer as well as primary lode occurrences of these minerals. Anomalously high Zr values were found off the NE Cape and the western portions of St. Lawrence Island and probably originated from zircon-containing quartz monzanitic rocks on the island. Concentrations generally above the mean were found in the area of Yukon Holocene sediment. The highest values for Sn are found close to Tin City and are related to the tin mineralization there. Detection of Sn in samples near Bluff and Cape Rodney-Nome areas again may be related to tin mineralization known to exist in these areas. Samples containing detectable concentrations of Sn in the areas of King Island, Port Clarence, and in the Anadyr Strait may be from tin placer deposits concentrated by the relatively high currents there. High Cr concentrations were found in sediment off Stuart Island, Cape Prince of Wales and north-central St. Lawrence Island and appear to be related to basalts or granites containing ultra-mafic dikes that are sources of chromite. Samples with high Ce values also have high La values and often have high Nd values, suggesting that the heavy mineral monazite concentrated as a placer mineral and may be the source of these elements. Because monazite is

probably the primary carrier of Ce and related elements and because it is concentrated in placer deposits, it promises to be a good indicator of sediment dispersal trends.

A sediment sample from 30 km south of Cape Prince of Wales contains the greatest amounts of Cr, Zr, Ce, Ti, Mn, La, Sc, Y, Yb, and Nd of all the samples analyzed and also contains a high concentration of tin. Because of these high concentrations and because the sample contains high values of La and Nd which are commonly found with Ce in the heavy mineral monazite, this sample may represent an area of placer deposits the existence and extent of which should be explored. Future studies of Sn, Zr, Cr, and Ce and associated heavy minerals should use sampling intervals close-spaced enough to detect significant variations caused by hydraulic concentration. Mechanical concentration of samples before analysis would also help to enhance existing trends.

Fe, Mn, Co, and Ba were considered together as chemically or environmentally-sensitive elements but in this study the evidence indicates their concentrations are source related. Fe, Mn, and Co all show high values near the volcanics of Stewart Island and north-central St. Lawrence Island. These elements also correlate with Cu, Zn, V, Y, and Zr, with generally high values in the areas of Yukon Holocene sedimentation and generally low values in Chirikov Basin. Co, however, does not follow this trend as closely as Fe and Mn. Concentrations of Ba above the mean are found generally throughout the area of Yukon sediment distribution but also are found close to Stuart Island and at various locations along the southern coast of the Seward Peninsula. The maximum concentration of Ba (.15%) is found in a sample from the Anadyr Strait and is unique in that other concentrations of other elements that usually correlate with Ba are not similarly high at this location.

Of the major elements, Ti is closely associated with Fe and Mn, discussed above, all of which have generally high concentrations in Yukon sediment with very high concentrations in areas close to the volcanics of Stuart Island and St. Lawrence Island. Ca and Mg are relatively high in Yukon sediment and sediment close to the volcanic areas mentioned. However, sediment with the highest concentrations of Ca and Mg was probably derived from the limestone formations in the Cape Prince of Wales and Port Clarence areas. Values for Na, K, and Al exhibit more erratic variation than values for the other major elements and the anomalies of Na, K and Al that appear to originate from land sources and are broader in areal extent. Concentrations of P occur in patches in eastern Norton Sound, Anadyr Strait, and surrounding the Yukon Delta. The highest concentration of P was in a sample from an enclosed basin NE of St. Lawrence Island and could be a result of reducing conditions in the basin.

Of the minor trace elements that are not usually regarded as potentially toxic, Sc correlates closest with Ti, Fe, V, La, and Mn. Yttrium correlates closest with Mn, Fe, and Ti. Yb correlates closest with Mn, Zn, and Y. Concentrations of Sc, Y, and Yb are all highest in Yukon sediment and lowest in Chirikov Basin sediment. Nb exhibited maximum concentrations in sediment off Cape Darby where the highest Nb anomalies on land in western Alaska have been found. Nd was detected in two samples from Norton Sound and in samples of sediment north of King Island, samples that also have high concentrations of La and Ce. These elements probably exist in the mineral monazite. Slightly higher values of Be can be found just off the coasts enclosing Norton Basin but maximum offshore values near Cape Prince of Wales correlate with economic Be deposits there.

Of the economically important elements, Ag, Mo, and Bi, detectable Ag concentrations occur in samples offshsore from terrestrial Ag mineralization

sites on St. Lawrence Island, near Stuart Island, and close to the Yukon Delta. Highest concentrations of Mo were found off the Bluff beach mineralization, Bi was detected in samples off the Cape Prince of Wales mineralization area that has associated Bi.

A contour map of the Q-mode factor loadings for Factor III outlines an area corresponding to the distribution of Yukon Holocene sediment plus areas in Anadyr Strait and north of St. Lawrence Island. Scaled varimax factor scores and cross correlation between factor loadings and element concentrations indicate that Factor III is best characterized by elevated concentrations of Ba, Na, Sr, La, K, Ga, Al, and Sc. The significance of this element grouping is that these elements tend to be concentrated in sialic rock types. Samples with high loadings for Factor I of the Q-mode analysis generally corresponds with the area of relict sediment in the Chirikov Basin. Samples with high loadings for Factor II of the Q-mode analysis occur off the coast from Bluff, Nome, and Tin City, suggesting a strong influence from the mineralization in these areas. This is confirmed by high correlations between loadings for this factor and concentrations of Fe, Mn, Ti, Co, Zn, Sc, Cu, Y, and V. Factor IV of the Q-mode analysis does not have any strong relation to sediment or mineral characteristics but shows some correlation with areas of known glacial debris.

REFERENCES

Bateman, A.M., 1965, Economic Mineral Deposits: John Wiley and Sons, Inc., New York, 916 p.

Cacchione, D.A., and Drake, D.E., 1978, Sediment transport in Norton Sound-Northern Bering Sea, Alaska, in: Environmental Assessment of the Alaskan Continental Shelf, Annual Report of Principal Investigators for the year ending March, 1978: Environmental Research Laboratory, Boulder, Colorado, NOAA, U.S. Dept. of Commerce, v. 12, p. 308-450.

Coachman, L.K., Aagaard, K., and Tripp, R.B., 1976, Bering Strait: The regional physical oceanography: Seattle, Washington, University Press, 186 p.

Cobb, E.H., 1960, Sb, bismuth and mercury occurrences in Alaska: U.S. Geological Survey, Mineral Investigations, Resource Map MR-11.

_____, 1960a, Chromite, cobalt, nickel, and platinum occurrences in Alaska: U.S. Geological Survey, Mineral Investigations Resource Map MR-8.

_____, 1960b, Copper, lead, and zinc occurrences in Alaska: U.S. Geological Survey, Mineral Investigations, Resource Map, MR-9.

_____, 1960c, Molybdenum, tin, tungsten occurrences in ALaska: U.S. Geological Survey, Mineral investigations, Resource Map MR-10

_____, 1962, Lode gold and silver occurrences in Alaska: U.S. Geological Survey, Mineral Investigations, Resource Map MR-32.

_____, 1964, Iron occurrences in Alaska: U.S. Geological Survey, Mineral Investigations, Resource Map MR-40.

_____, 1970, Uraniam, Thorium, and Rare-Earth elements of Alaska: U.S. Geological Surey, Mineral Investigations, Resources Map MR-56.

Cohen, A.C., Jr., 1959, Simplified estimators for the normal distribution when samples are singly censored or truncated: Technometrics, v. 1, no. 3, p. p. 217-237.

Dean, W., Gardner, J., and Vallier, T., 1978, Inorganic geochemistry and sedimentology of surface sediments, outer continental shelf, southern Bering Sea, Alaska: International Sedimentological Congress, Israel.

Eberlein, G.D., Chapman, R.M., Foster, H.L., Gassaway, J.S., 1977, Map with table showing known metalliferous and non--metalliferous mineral deposits in central Alaska: U.S. Geological Survey Open-file Report 77-168-D.

_____, Menzie, W.D., 1978, Maps and tables describing areas of metalliferous mineral resource potential of central Alaska: U.S. Geological Survey Open-file Report 78-1-0.

Fathauer, T.F., 1975, The great Bering Sea storms of 9-19 November, 1974 Weatherwise Magazine, American Meterological Society, v. 28, p. 76-83.

Flores, R.M., Shideler, G.L., 1978, Factors controlling heavy-mineral variations on the south Texas outer continental shelf, Gulf of Mexico: Journal of Sedimentary Petrology, v. 48, p. 269.

Grimes, D.J., and Marinzino, A.P., 1968, U.S. Geological Survey, Circular 591.

Hudson, T., Miller, M.L., Pickthorn, W.J., 1977, Map showing metalliferous and selected non-metalliferous mineral deposits, Seward Peninsula, Alaska: U.S. Geological Survey, Open-file Report 77-796B, 46 p.

_____, DeYoung, J.H., Jr., 1978, Maps and tables describing areas of mineral resource potential, Seward Peninsula, Alaska: U.S. Geological Survey, Open-file Report 78-1-C, 62 p.

Hummel, C.L., 1977, Review of exploration geochemical surveys on Seward Peninsula, Western Alaska: U.S. Geological Survey Open-file Report 77-796D, 28 p.

Imbrie, J., 1963, Factor and vector analysis programs for analyzing geologic data: Office of Naval Research Technical Report 6, Geography Branch, p. 83.

Klovan, J.E. and Imbrie, J., 1971, Algorithm and FORTRAN IV Program for large-scale Q-mode Factor analysis and calculations of Factor scores: Mathematical Geol. 3, p. 61-77.

Kvenvolden, K.A., Weliky, K., Nelson, C.H., DesMarais, D.J., 1979, Submarine seep of carbon dioxide in Norton Sound, Alaska: Science, v. 205, No. 4412, p. 1264.

Mason, B., 1966, Principles of Geochemistry: John Wiley and Sons, Inc., New York, 329 p.

_____, Berry, L.G., 1968, Elements of Mineralogy: W. H. Freeman and Company, San Francisco, California, 550 p.

McManus, D.A., Venkatarathnam, K., Hopkins, D.M., Nelson, C.H., 1977, Distribution of bottom sediments on the continental shelf, northern Bering Sea: U.S. Geological Survey Professional Paper 759-C, p. C1-C31.

Meisch, A.T., 1967, Methods of computation for estimating geochemical abundance: U.S. Geological Survey Professional Paper 574-B, p. B1-B15.

Miller, T.P., Grybeck, D., 1973, The geochemical survey of the eastern Solomon and southeastern Bendeleben Quadrangles, Seward Peninsula, Alaska: U.S. Geological Survey Open-file Report.

Nelson, C.H., Hopkins, D.M., 1972, Sedimentary processes and distribution of partiulate gold in the northern Bering Sea: U.S. Geological Survey Professional Paper 689, 27 p.

_____, Pierce, D.E., Leong, K.W., Wang, F., 1975, Mercury distribution in ancient and modern sediment of northeastern Bering Sea: Marine Geology 18C, p. 91-104.

_____, and Creager, J.S., 1977, Sediment budgets and displacement of Yukon River sediments from Berng Sea in the late Holocene.

_____, Larsen, B.R., Larsen, M., Thor, D.R., Sedimentary characteristics of the Norton Basin sea floor, U.S. Geological Survey Open-file Report (in prep.).

Overstreet, W.C., Hamilton, J.C., Boerngen, J.G., Rosenblum, S., Marsh, W.R., and Sainsbury, C.L., 1974, Minor elements in nonmagnetic concentrates from Alaska: U.S. Geological Survey/G.D. 74-039, National Technical Information Service, PB-238'989, 434 p.

Patry, J.J., Larsen, B.R., Nelson, C.H., Heropoulos, C., 1977, Trace metal content of bottom sediment in northern Bering Sea: Quarterly Report of Principal Investigators, April-June 1, in: Environmental Assessment of the Alaskan Continental Shelf, Environmental Research Laboratory, Boulder, Colorado, NOAA, U.S. Dept. of Commerce, Contract RK6-6074, 10 p.

Patton, W.W., Jr., and Csejtey, B., Jr., 1971, Preliminary Geologic Investigations of eastern St. Lawrence Island, Alaska: U.S. Geological Survey Open-file report 52 p.

_____, _____, 1971, Preliminary Geologic Investigations of western St. Lawrence Island, Alaska: U.S. Geological Survey Professional Paper 684-C, p. C1-C15.

_____, _____, 1972, Analysis of stream-sediment and rock samples from St. Lawrence Island, Alaska, 1966-1971: U.S. Geological Survey Open-file Report, 78 p.

Peratis, A., et al., 1978, User Manual for the Surface Display Library: Dynamic Graphics, Inc., Berkeley, California.

_____, et al., 1978, User Manual for the Surface Gridding Library: Dynamic Graphics, Inc., Berkeley, California.

Reed, W.E., Kaplan, I.R., 1977, The chemistry of marine petroleum seeps: Journal of Geochemical Exploration, No. 7., p. 255-293.

Sainsbury, C.L., 1969, Geology and Ore Deposits of the Central York Mountains, western Seward Peninsular, Alaska: U.S. Geological Survey Bulletin 1287, 101 pages.

_____, 1975, Geology, ore deposits, and mineral potential of the Seward Peninsula, Alaska: U.S. Bureau of Mines, Open-file Report, 108 p.

Sheth, M., 1971, A heavy mineral study of Pleistocene and Holocene sediments near Nome, Alaska: U.S. Geological Survey Open-file Report, 82 p.

Sichel, H.S., 1947, An experimental and theoretical investigation of bias error in mine sampling, with special reference to narrow gold reefs: Laudon, Inst. Mining Metallulrgy Trans., v. 56, p. 403-474.

Sienko, M.J., Plane, R.A., 1961, Chemistry: McGraw Hill Book COmpany, Inc., New York, 673 p.

Van Trump Jr., G., 1975, Factor analysis (Q-mode)-STATPAC, Program D0097: U.S. Geological Survey Computer Program Documentation (unpub.).

Venkatarathnam, K., 1971, Heavy minerals on the continental shelf of the northern Berng Sea: U.S. Geological Survey Open-file report, 93 p.

Yen, T.F., 1975, The role of trace metals in petroleum: Ann Arbor Science Publishers, Ann Arbor, Michigan, 221 p.

TABLE I

Geometric means, geometric deviations, central and expected value ranges, and maximum and minimum values for different element groups in the Northern Bering Sea.

Element Group	Element	Geometric Mean	Geometric Deviation	Central Range*	Expected range**	Minimum Values	Maximum Values
Petroleum Index Elements	Ni	22.7 ppm	2.01	11.3 - 45.6	5.6 - 91.6	7.0	1500.0
	V	87.3 ppm	1.51	57.8 - 131.8	38.3 - 198.9	30.0	200.0
Heavy Metal Element	Sn	too few values				N	100.0
	Zr	162.4 ppm	1.56	104.2 - 253.1	66.8 - 394.5	50.0	2000.0 G
	Cr	45.2 ppm	1.82	24.8 - 82.5	13.6 - 150.4	10.0	1000.0
	Ce	too few values				N	300.
Toxic Elements	Pb	20.5 ppm	1.66	12.3 - 34.0	7.4 - 56.5	N	500.0
	Cu	12.6 ppm	2.17	5.8 - 27.4	2.7 - 59.5	3.0	700.0
	Zn	72.8 ppm	1.70	42.8 - 124.0	25.1 - 211.0	N	1000.0
	As	too few values				N	3000.0 ppm
	Sb	too few values				N	1000.0 ppm
Chemically or Environmentally Sensitive Elements	Fe	2.29%	1.63	1.4 - 3.7	.86 - 6.1	.7	10.0 G
	Mn	462.5 ppm	1.88	245.7 - 870.6	130.5 - 1638.8	150.0	7000.0
	Co	11.6 ppm	1.80	6.4 - 20.9	3.6 - 37.7	5.0	100.0
	Ba	551.3 ppm	1.70	323.6 - 939.3	189.9 - 1600.3	100.0	1500.0
Major Elements	Al	5.6%	1.40	4.0 - 7.9	2.9 - 11.0	.7	10.0
	Na	1.7%	1.72	1.0 - 3.0	.6 - 5.2	.07	3.0
	K	1.5%	1.74	.9 - 2.7	.5 - 4.6	.1	5.0
	Ca	1.6%	2.06	.8 - 3.4	.4 - 7.0	.2	10.0 G
	Mg	.8%	2.08	.4 - 1.7	.2 - 3.5	.15	10.0 G
	Ti	.4%	1.59	.3 - .7	.2 - 1.1	.1	2.0
	P	too few values				N	.7%
Minor Elements	Sr	227.7 ppm	1.81	123.1 - 402.5	68.2 -727.5	30.0	1000.0
	Y	26.9 ppm	1.50	17.9 - 40.5	11.9 - 60.9	10.0	150.0
	Sc	12.1 ppm	1.50	8.0 - 18.2	5.3 - 27.4	5.0	50.0
	Nb	11.3 ppm	1.47	7.6 - 16.6	5.2 - 24.5	N	30.0
	B	73.7 ppm	1.72	42.8 - 126.9	24.9 -218.6	N	150.0
	La	41.4 ppm	1.63	25.5 - 67.3	15.7 -109.5	10.0	100.0
	Ga	10.3 ppm	2.45	4.2 - 25.3	1.7 - 62.1	N	30.0
	Yb	3.4 ppm	1.52	2.2 - 5.1	1.5 - 7.8	1.0	10.0
	Be	2.4 ppm	1.51	1.6 - 3.7	1.1 - 5.6	N	10.0
	Nd	too few values			N	150.0 ppm	
Miscellaneous Economic Elements	Ag	too few values				N	3.0 ppm
	Bi	too few values				N	70.0 ppm
	Mo	too few values			N	30.0 ppm	

* Central Range = geom.mean/geom. dev. to geom. mean x geom. dev.

**Expected Range = geom. mean/(geom.dev.)^2 to geom. mean x (geom. dev.)^2

G = > greater than accompanying value (upper limit of detection)

L = > less than accompanying value (lower limit of detection)

N = > not detected in a sample

TABLE II

Analytic results for miscellaneous elements not shown in general element groups of TABLE I.

Element	Number of samples element was detected in	Limit of detection (lower limit except for Si)	Element	Number of samples element was detected in	Limit of detection (lower limit except for Si)
Ag	5	0.7 ppm	Hf	0	50.0 ppm
As	3	100.0 ppm	In	0	1.0 ppm
Au	0	7.0 ppm	Li	0	100.0 ppm
Bi	2	7.0 ppm	Re	0	7.0 ppm
Cd	0	7.0 ppm	Ta	0	50.0 ppm
Mo	5	2.0 ppm	Th	0	150.0 ppm
P	54	0.1 %	Tl	0	3.0 ppm
Pd	0	1.0 ppm	Pr	0	20.0 ppm
Pt	0	5.0 ppm	Nd *	3	20.0 ppm
Sb	8	20.0 ppm	Sm	0	50.0 ppm
Sn	23	2.0 ppm	Eu	0	1.5 ppm
Te	0	300.0 ppm	Gd	0	5.0 ppm
U	0	150.0 ppm	Tb	0	100.0 ppm
W	0	10.0 ppm	Dy**	0	20.0 ppm
Si***	179	10.0% upper limit	Ho	0	5.0 ppm
Ce	19	50.0 ppm	Er	0	30.0 ppm
Ga	151	0.7 ppm	Tm	0	2.0 ppm
Ge	0	7.0 ppm	Lu	0	15.0 ppm

* Looked for only when La or Ce is found

** Looked for only when Y is >50 ppm

***Si was a major component in all samples analyzed, i.e., >10.0%. However, exact values cannot be assigned above this limit.

TABLE III

Lists most closely related or disrelated elements according to the correlation coefficients between their log values.

Ga	Fe	Mg	Ca	Ti	Mn	B
La .4950	Cu .8323	Ca .5861	Mg .5861	Fe .7251	Fe .7738	K .4929
Sc .4047	Ni .8101	Co .5151	Sr .5469	Sc .7180	Zn .6657	Ba .4508
Ti .3806	Zn .7868	Ni .4949	Sc .3371	Mn .6617	Ti .6617	Al .4328
	Mn .7738	Fe .3884	Nb -.3232*	Ni .6153	Cu .6612	Na .4109
	Co .7503	Ti .3884		Zn .5717	Y .6103	Nb .2884
	Ti .7251	Sc .3565		Cu .5682	Ni .5954	La .2815
	Sc .6326	Cr .3331		Cr .5623	Yb .5729	Ni -.5464*
	B-.3164*			Y .5435	Sc .5571	Co -.4110*
				Yb .5181		Fe -.3164*
				Co .5067		

Ba	Be	Co	Cr	Cu	La	Nb
K .8040	La .3720	Ni .8263	Ni .6132	Fe .8823	Sc .5572	B .2884
Na .6847	Yb .3388	Fe .7503	Ti .5623	Zn .8023	Sn .5539	Ca-.3232*
Sr .6241	Sc .3351	Cu .6296	Sc .5274	Ni .6833	Ba .5508	
Al .6092	Cu .3211	Zn .5982	Fe .4796	Mn .6612	V .5189	
	Ti .3058	B -.4110*	Co .3879	Co .6296	K .5171	
		K -.3177*			Ga .4950	
					Zr .4933	
					Ti .4473	

Ni	Pb	Sc	Sr	V	Y	Zn
Co .8263	Cu .5114	Ti .7180	K .6994	Sc .5790	Mn .6103	Cu .8023
Fe .8101	Zn .4194	Fe .6326	Na .6863	La .5189	Yb .5678	Fe .7868
Cu .6833	Y .3701	V .5790	Al .6140	Cu .4801	Fe .5563	Mn .6657
Ti .6153	Fe .3106	La .5572	Ba .6241	Yb .4589	Ti .5435	Ni .6142
Zn .6142	Mn .2615	Mn .5571	La .5539	Zn .4584	Cu .4842	Co .5982
Cr .6132	Na-.4041*	Cu .5470	Cu .5469	Ti .4352	Zr .4552	Ti .5717
Mn .5954		Cr .5274		Fe .4039	Sc .4335	Yb .5713
B -.5464*						

Zr	Al	Na	K	Yb
La .4933	Na .8348	Al .8348	Ba .8040	Mn .5729
Y .4552	K .6999	K .7935	Na .7935	Zn .5713
Ti .4059	Sr .6140	Sr .6863	Al .6999	Y .5678
K .3778	Ba .6092	Ba .6847	Sr .6994	Fe .5294
Ba .3694	B .4328	B .4109	La .5171	Cu .5112
		Pb-.4041*	B .4929	Ti .5181
			Co .3177*	V .4589
				Sc .4278

*Extreme negative correlation.

TABLE IV

Correlation coefficients between element log values

D0101 CORRELATION ANALYSIS - USGS STATPAC (04/27/77) DATE 4/11/79

ARRAY OF CORRELATION COEFFICIENTS -

		1 GA PPM-S	2 FE %-S	3 MG %-S	4 CA %-S	5 TI %-S	6 MN PPM-S	7 B PPM-S	8 BA PPM-S	9 CO PPM-S	10 CR PPM-S
1	GA PPM-S	1.0000	0.3289	0.1181	0.1505	0.3806	0.1154	-0.0253	0.1866	0.2649	0.3128
2	FE %-S	0.3289	1.0000	0.3884	0.2678	0.7251	0.7738	-0.3164	-0.0398	0.7503	0.4796
3	MG %-S	0.1181	0.3884	1.0000	0.5861	0.3884	0.2669	-0.2313	-0.1395	0.5151	0.3331
4	CA %-S	0.1505	0.2678	0.5861	1.0000	0.2823	0.1458	-0.0424	0.0475	0.2837	0.2014
5	TI %-S	0.3806	0.7251	0.3884	0.2823	1.0000	0.6617	-0.1365	0.0932	0.5067	0.5623
6	MN PPM-S	0.1154	0.7738	0.2669	0.1458	0.6617	1.0000	-0.2643	-0.1461	0.5187	0.3113
7	B PPM-S	-0.0253	-0.3164	-0.2313	-0.0424	-0.1365	-0.2643	1.0000	0.4508	-0.4110	-0.2177
8	BA PPM-S	0.1866	-0.0398	-0.1395	0.0475	0.0932	-0.1461	0.4508	1.0000	-0.2254	0.2336
9	CO PPM-S	0.2649	0.7503	0.5151	0.2837	0.5067	0.5187	-0.4110	-0.2254	1.0000	0.3879
10	CR PPM-S	0.3128	0.4796	0.3331	0.2014	0.5623	0.3113	-0.2177	0.2336	0.3879	1.0000
11	CU PPM-S	0.2418	0.8323	0.2714	0.2434	0.5682	0.6612	-0.2482	0.0008	0.6296	0.3522
12	LA PPM-S	0.4950	0.3369	0.0688	0.2879	0.4473	0.2424	0.2815	0.5508	0.1032	0.3629
13	NB PPM-S	0.1875	-0.0777	-0.2974	-0.3232	0.0435	-0.0686	0.2884	0.1651	-0.1894	-0.0059
14	NI PPM-S	0.3090	0.8101	0.4949	0.2480	0.6153	0.5954	-0.5464	-0.1467	0.8263	0.6132
15	PB PPM-S	0.0227	0.3106	-0.2186	0.0812	-0.0118	0.2615	-0.0271	-0.0241	0.2152	-0.2529
16	SC PPM-S	0.4047	0.6326	0.3565	0.3371	0.7180	0.5571	0.0724	0.3589	0.3984	0.5276
17	SR PPM-S	0.3097	0.0081	0.1979	0.5469	0.1885	-0.1694	0.1981	0.6241	-0.0661	0.3323
18	V PPM-S	0.0446	0.4039	0.2333	0.1561	0.4352	0.3714	0.2196	0.3529	0.2090	0.3407
19	Y PPM-S	0.2224	0.5563	0.1480	0.2392	0.5435	0.6103	0.0590	-0.0607	0.4272	0.1015
20	ZN PPM-S	0.2140	0.7868	0.1528	0.0466	0.5717	0.6657	-0.1722	0.0552	0.5982	0.2692
21	ZR PPM-S	0.2732	0.2547	0.1485	0.2224	0.4059	0.2388	0.1497	0.3694	0.1450	0.3005
22	AL %-S	0.2245	0.0585	0.2193	0.2679	0.2162	-0.1887	0.4328	0.6092	0.0046	0.2365
23	NA %-S	0.2528	-0.0524	0.1963	0.2352	0.1629	-0.2520	0.4109	0.6847	-0.1178	0.3354
24	K %-S	0.1800	-0.1536	0.0225	0.2076	0.0296	-0.2734	0.4929	0.8040	-0.3177	0.1947
25	YB PPM-S	-0.0617	0.5294	-0.0234	0.0692	0.5181	0.5729	0.1397	0.1760	0.2138	0.1956
26	BE PPM-S	0.1098	0.2741	-0.0618	0.0194	0.3058	0.2558	0.0945	0.2710	0.0144	0.1313

Table IV cont.

00101 CORRELATION ANALYSIS - USGS STATPAC (04/27/77) DATE 4/11/79

ARRAY OF CORRELATION COEFFICIENTS - CONT.

		11 CU PPM-S	12 LA PPM-S	13 NB PPM-S	14 NI PPM-S	15 PB PPM-S	16 SC PPM-S	17 SR PPM-S	18 V PPM-S	19 Y PPM-S	20 ZN PPM-S
1	GA PPM-S	0.2418	0.4950	0.1875	0.3090	0.0227	0.4047	0.3097	0.0446	0.2224	0.2160
2	FE %-S	0.8323	0.3369	-0.0777	0.8101	0.3106	0.6326	0.0081	0.4039	0.5563	0.7868
3	MG %-S	0.2714	0.0688	-0.2974	0.4969	-0.2186	0.3565	0.1979	0.2333	0.1480	0.1528
4	CA %-S	0.2434	0.2879	-0.3232	0.2480	0.0812	0.3371	0.5469	0.1561	0.2392	0.0466
5	TI %-S	0.5682	0.4473	0.0435	0.6153	-0.0118	0.7180	0.1885	0.4352	0.5435	0.5717
6	MN PPM-S	0.6612	0.2424	-0.0686	0.5954	0.2615	0.5571	-0.1694	0.3714	0.6103	0.6657
7	B PPM-S	-0.2482	0.2815	0.2884	-0.5464	-0.0271	0.0724	0.1981	0.2196	0.0590	-0.1722
8	BA PPM-S	0.0008	0.5508	0.1651	-0.1467	-0.0241	0.3589	0.6241	0.3529	-0.0607	0.0552
9	CO PPM-S	0.6296	0.1032	-0.1894	0.8263	0.2152	0.3984	-0.0661	0.2090	0.4272	0.5982
10	CR PPM-S	0.3522	0.3629	-0.0039	0.6132	-0.2529	0.5274	0.3323	0.3407	0.1015	0.2692
11	CU PPM-S	1.0000	0.4102	-0.1300	0.6833	0.5114	0.5470	0.0144	0.4801	0.4842	0.8023
12	LA PPM-S	0.4102	1.0000	0.1089	0.1760	0.2100	0.5572	0.5539	0.5189	0.3886	0.3333
13	NB PPM-S	-0.1300	0.1089	1.0000	-0.0983	-0.0720	-0.0297	-0.0829	0.0931	0.0139	0.0700
14	NI PPM-S	0.6833	0.1760	-0.0983	1.0000	0.1626	0.4481	0.0041	0.2766	0.3516	0.6142
15	PB PPM-S	0.5114	0.2100	-0.0720	0.1626	1.0000	-0.0439	-0.0772	0.0053	0.3701	0.4194
16	SC PPM-S	0.5470	0.5572	-0.0297	0.4481	-0.0439	1.0000	0.3238	0.5790	0.4335	0.5294
17	SR PPM-S	0.0144	0.5539	-0.0829	0.0041	-0.0772	0.3238	1.0000	0.2163	-0.0675	-0.1362
18	V PPM-S	0.4801	0.5189	0.0931	0.2766	0.0053	0.5790	0.2163	1.0000	0.2237	0.4584
19	Y PPM-S	0.4842	0.3886	0.0139	0.3516	0.3701	0.4335	-0.0675	0.2237	1.0000	0.4121
20	ZN PPM-S	0.8023	0.3333	0.0700	0.6142	0.4194	0.5294	-0.1362	0.4584	0.4121	1.0000
21	ZR PPM-S	0.1452	0.4933	0.1213	0.2615	0.0857	0.3509	0.3286	0.2401	0.4552	0.1914
22	AL %-S	-0.0534	0.3294	0.2116	-0.0162	-0.2630	0.3365	0.6140	0.3314	-0.0457	-0.0332
23	NA %-S	-0.1747	0.3754	0.2021	-0.0615	-0.4041	0.3212	0.6863	0.2713	-0.1440	-0.1644
24	K %-S	-0.1474	0.5171	0.1445	-0.1998	-0.1277	0.2040	0.6994	0.2661	-0.1034	-0.1840
25	YB PPM-S	0.5112	0.3746	0.1340	0.3027	0.2547	0.4278	-0.0703	0.4589	0.5678	0.5713
26	BE PPM-S	0.3211	0.3720	0.0378	0.0884	0.1790	0.3351	0.2056	0.2900	0.2444	0.2771

Table IV. cont.

D0101 CORRELATION ANALYSIS - USGS STATPAC (04/27/77) DATE 4/11/79

ARRAY OF CORRELATION COEFFICIENTS - CONT.

		21	22	23	24	25	26
		ZR PPM-S	AL %-S	NA %-S	K %-S	YB PPM-S	BE PPM-S
1	GA PPM-S	0.2732	0.2245	0.2528	0.1800	-0.0617	0.1098
2	FE %-S	0.2547	0.0585	-0.0524	-0.1536	0.5294	0.2741
3	MG %-S	0.1485	0.2193	0.1963	0.0225	-0.0234	-0.0618
4	CA %-S	0.2224	0.2679	0.2352	0.2076	0.0692	0.0194
5	TI %-S	0.4059	0.2162	0.1629	0.0296	0.5181	0.3058
6	MN PPM-S	0.2388	-0.1887	-0.2520	-0.2734	0.5729	0.2558
7	B PPM-S	0.1497	0.4328	0.4109	0.4929	0.1397	0.0965
8	BA PPM-S	0.3694	0.6092	0.6847	0.8040	0.1760	0.2710
9	CO PPM-S	0.1450	0.0046	-0.1178	-0.3177	0.2138	0.0144
10	CR PPM-S	0.3005	0.2365	0.3354	0.1947	0.1956	0.1313
11	CU PPM-S	0.1452	-0.0534	-0.1747	-0.1474	0.5112	0.3211
12	LA PPM-S	0.4933	0.3294	0.3756	0.5171	0.3746	0.3720
13	NB PPM-S	0.1213	0.2116	0.2021	0.1445	0.1340	0.0378
14	NI PPM-S	0.2615	-0.0162	-0.0615	-0.1998	0.3027	0.0884
15	PB PPM-S	0.0857	-0.2630	-0.4041	-0.1277	0.2547	0.1790
16	SC PPM-S	0.3509	0.3365	0.3212	0.2040	0.4278	0.3351
17	SR PPM-S	0.3286	0.6140	0.6863	0.6994	-0.0703	0.2056
18	V PPM-S	0.2401	0.3314	0.2713	0.2661	0.4589	0.2900
19	Y PPM-S	0.4552	-0.0457	-0.1440	-0.1034	0.5678	0.2444
20	ZN PPM-S	0.1914	-0.0332	-0.1644	-0.1840	0.5713	0.2771
21	ZR PPM-S	1.0000	0.2784	0.3000	0.3778	0.3322	0.2169
22	AL %-S	0.2784	1.0000	0.8348	0.6999	0.0953	0.1454
23	NA %-S	0.3000	0.8348	1.0000	0.7935	0.0077	0.0699
24	K %-S	0.3778	0.6999	0.7935	1.0000	0.0875	0.2228
25	YB PPM-S	0.3322	0.0953	0.0077	0.0875	1.0000	0.3388
26	BE PPM-S	0.2169	0.1454	0.0699	0.2228	0.3388	1.0000

TABLE V

Correlation coefficients between Q-mode Factor loading values and non-log element values.

D0101 CORRELATION ANALYSIS - USGS STATPAC (04/27/77) DATE 3/23/78

ARRAY OF CORRELATION COEFFICIENTS -

		1 factor1	2 factor2	3 factor3	4 factor4	5 GA PPM-S	6 FE %-S	7 MG %-S	8 CA %-S	9 TI %-S	10 MN PPM-S
1	factor1	1.0000	-0.3258	-0.1758	0.0181	-0.5480	-0.5093	-0.4750	-0.4209	-0.3586	-0.3352
2	factor2	-0.3258	1.0000	-0.2785	-0.4808	0.0926	0.6616	0.1630	0.1168	0.6328	0.6527
3	factor3	-0.1758	-0.2785	1.0000	-0.1591	0.5729	-0.1304	-0.0144	0.1668	0.2239	-0.2894
4	factor4	0.0181	-0.4808	-0.1591	1.0000	0.1481	-0.4933	-0.1958	-0.2655	-0.4254	-0.4867
5	GA PPM-S	-0.5480	0.0926	0.5729	0.1481	1.0000	0.2323	0.0767	0.1157	0.3607	0.0346
6	FE %-S	-0.5093	0.6616	-0.1304	-0.4933	0.2323	1.0000	0.3534	0.1270	0.6022	0.8405
7	MG %-S	-0.4750	0.1630	-0.0144	-0.1958	0.0767	0.3534	1.0000	0.4199	0.2847	0.0851
8	CA %-S	-0.4209	0.1168	0.1668	-0.2655	0.1157	0.1270	0.4199	1.0000	0.2017	0.0055
9	TI %-S	-0.3586	0.6328	0.2239	-0.4254	0.3607	0.6022	0.2847	0.2017	1.0000	0.4216
10	MN PPM-S	-0.3352	0.6527	-0.2894	-0.4867	0.0346	0.8405	0.0851	0.0055	0.4216	1.0000
11	B PPM-S	0.5392	-0.1656	-0.0089	0.1728	0.1575	-0.2368	-0.2685	-0.1292	-0.1006	-0.2229
12	BA PPM-S	0.1990	-0.3470	0.7106	-0.1613	0.4000	-0.1194	-0.2644	-0.1561	0.0600	-0.1898
13	CO PPM-S	-0.6072	0.5020	-0.1428	-0.2790	0.1962	0.7835	0.5335	0.1775	0.3948	0.6020
14	CR PPM-S	-0.3911	0.2104	0.1073	-0.2136	0.1573	0.4351	0.6329	0.1227	0.4659	0.1229
15	CU PPM-S	-0.3316	0.4444	-0.2692	-0.3765	0.0312	0.6852	0.0005	-0.0025	0.1593	0.6637
16	LA PPM-S	-0.0977	0.1546	0.6073	-0.4107	0.5193	0.1447	-0.0687	0.1215	0.3360	0.0496
17	NB PPM-S	0.1628	-0.0266	-0.1231	0.4103	0.1705	-0.1652	-0.2389	-0.3283	-0.0241	-0.1743
18	NI PPM-S	-0.4219	0.2246	-0.1548	-0.2109	0.0263	0.5145	0.6984	0.0401	0.2242	0.2827
19	PB PPM-S	-0.3033	0.3939	-0.3279	-0.3356	-0.0372	0.5928	-0.0839	0.0072	0.0383	0.6280
20	SC PPM-S	-0.2070	0.4598	0.4683	-0.5150	0.4777	0.4371	0.1420	0.1943	0.6401	0.3225
21	SR PPM-S	-0.2944	-0.2621	0.6476	-0.1438	0.3909	-0.0342	0.1171	0.5443	0.1646	-0.1729
22	V PPM-S	0.2703	0.2858	0.2886	-0.5579	0.1720	0.1910	0.0242	-0.0143	0.3205	0.1154
23	Y PPM-S	-0.2662	0.7176	-0.1753	-0.3921	0.1518	0.5309	-0.0513	0.2354	0.4335	0.6178
24	ZN PPM-S	-0.3199	0.5440	-0.2229	-0.4407	0.1069	0.7869	0.0044	-0.0616	0.2700	0.7980
25	ZR PPM-S	-0.0689	0.0418	0.0825	-0.0516	0.1167	0.0155	-0.0335	0.0277	0.1798	-0.0307
26	AL %-S	0.0527	-0.2436	0.5707	0.0729	0.4666	-0.0257	0.0199	0.1024	0.2603	-0.2648
27	NA %-S	-0.0308	-0.3275	0.6474	0.0416	0.5404	-0.0169	0.0233	0.0863	0.2389	-0.2490
28	K %-S	0.0796	-0.4179	0.5948	-0.0583	0.4125	-0.1496	-0.1554	0.0003	0.0118	-0.2329
29	YB PPM-S	0.1620	0.5663	-0.1618	-0.5081	0.3283	0.4684	-0.1307	-0.0357	0.4097	0.5124

TABLE VI

A. Q-mode scaled varimax factor scores relating which elements are most correlative with each factor (in order of descending importance).

B. Lists elements most closely related to the first four factor loadings according to the correlations among their non-log values.

A.

Factor I	Factor II	Factor III	Factor IV
B 2.74	Y 2.05	La -2.02	Nb -2.40
V 2.10	Yb 1.78	Na -1.98	Ga -2.35
Yb 1.62	Ti 1.75	Ga -1.70	B -1.97
Ba 1.22	Fe 1.52	Ba -1.70	Al -1.67
Al 1.05	Sc 1.49	Sr -1.67	Na -1.38
	Cu 1.28	Sc -1.46	
	V 1.08	K 1.29	
	Mn 1.04	V -.93	
		Al -.86	

B.

Factor I	Factor II	Factor III	Factor IV
B .54	Y .72	Ba .71	Nb .41
V .27	Fe .66	Na .67	
Ba .20	Mn .65	Sr .65	*V -.56
Yb .16	Ti .63	La .61	*Sc -.52
	Yb .57	K .59	*Yb -.51
*Co -.61	Zn .54	Ga. 57	*Fe -.49
*Ga -.55	Co .50	Al .57	*Mn -.49
*Fe -.51	Sc .46	Sc .47	*Zn -.44
*Mg -.48	Cu .44	*Pb -.33	*Ti -.43
*Ni -.42			*La -.41
*Ca -.42	*K -.42		
*Cr -.39	*Ba-.35		
*Ti -.36	*Na-.33		
*Mn -.34			
*Cu -.33			
*Zn -.32			

*Extreme negative correlation.

TABLE VII

Q-mode varimax factor matrix associating samples into factor groupings.

00097 FACTOR ANALYSIS (Q-MODE) - U S G S STATPAC 06/07/77

Q Factor analysis on 25 col bu

VARIMAX FACTOR MATRIX

		COMM.	1	2	3	4
1	69ANC100	0.9484	0.4232	0.3825	-0.6168	-0.4924
2	69ASC101	0.9440	0.4416	0.3271	-0.6588	-0.4562
3	69ASC105	0.9773	0.4202	0.2779	-0.5858	-0.6167
4	69ANC107	0.9481	0.4572	0.1810	-0.5552	-0.6310
5	69ANC114	0.9585	0.4006	0.2533	-0.7559	-0.4031
6	69ANC116	0.9727	0.4459	0.3677	-0.6634	-0.4455
7	69ANC121	0.9322	0.4167	0.3968	-0.6592	-0.4082
8	69ASC155	0.9613	0.5693	0.1800	-0.5227	-0.5758
9	69ANC200	0.9300	0.5289	0.3561	-0.3572	-0.6292
10	69ANC206	0.9646	0.4538	0.2277	-0.5654	-0.6222
11	69ANC208	0.9632	0.4163	0.2146	-0.7042	-0.4980
12	69ANC209	0.9499	0.4636	0.1901	-0.6528	-0.5221
13	69ANC220	0.9368	0.4127	0.1696	-0.6747	-0.5315
14	69ANC221	0.9680	0.3569	0.1194	-0.7602	-0.4984
15	69ANC224	0.9364	0.3438	0.2519	-0.7037	-0.5095
16	69ANC227	0.9097	0.3356	0.1820	-0.7413	-0.4632
17	69ANC229	0.9336	0.4468	0.0843	-0.6401	-0.5632
18	69ANC232	0.9720	0.4616	0.3126	-0.6604	-0.4745
19	69ANC235	0.9514	0.4560	-0.0240	-0.5355	-0.6753
20	69ANC247	0.9029	0.5502	0.2904	-0.5967	-0.3998
21	70ANC78	0.9609	0.5759	0.2251	-0.6379	-0.4144
22	70ANC118	0.8948	0.4364	0.2424	-0.5643	-0.5719
23	70ANC138	0.9458	0.5066	0.2030	-0.5994	-0.5372
24	70ANC148	0.9156	0.5066	0.2986	-0.6510	-0.3821
25	70ANC155	0.9610	0.5425	0.2433	-0.6660	-0.4050
26	70ANC165	0.9303	0.4445	0.0799	-0.7395	-0.4235
27	70ASC205	0.9261	0.4357	0.1942	-0.6840	-0.4804
28	70ANC245	0.9578	0.4122	0.1384	-0.6691	-0.5666
29	70ANC278	0.9337	0.5181	0.2702	-0.6696	-0.3794
30	70ANC295	0.9383	0.5582	0.3855	-0.6325	-0.2792
31	70ANC328	0.9757	0.4818	0.3486	-0.6964	-0.3701
32	70ANC355	0.9597	0.5424	0.3971	-0.5493	-0.4540
33	70ANC408	0.9432	0.4999	0.3090	-0.6018	-0.4854
34	70ANC455	0.9362	0.5548	0.3249	-0.5934	-0.4131
35	70ANC478	0.9337	0.5830	0.3417	-0.5284	-0.4448
36	70ANC488	0.9373	0.5555	0.3395	-0.6292	-0.3428
37	70ANC535	0.8663	0.4755	0.3627	-0.6375	-0.3199
38	70ANC545	0.9484	0.5384	0.2752	-0.5928	-0.4811
39	70ANC568	0.9460	0.4945	0.3379	-0.6486	-0.4083
40	70ANC59T	0.9532	0.4870	0.3153	-0.6643	-0.4188
41	70ANC61T	0.9266	0.4721	0.1501	-0.5394	-0.6247
42	67ANC30	0.8690	0.5279	0.4974	-0.4106	-0.4176
43	68AWF310	0.8950	0.4137	0.4762	-0.2763	-0.6486
44	68AWF327	0.8661	0.4049	0.5763	-0.3370	-0.5065
45	68AWF338	0.9619	0.3472	0.4583	-0.5557	-0.5680
46	68AWF343	0.9319	0.3005	0.3751	-0.4177	-0.7256
47	68AWF344	0.9537	0.3296	0.2750	-0.3425	-0.8076
48	68AWF345	0.9547	0.3733	0.4562	-0.4144	-0.6599
49	68AWF346	0.9133	0.3573	0.3553	-0.3988	-0.7073

Table VII cont.

50	68AWF350	0.9629	0.4113	0.4042	-0.6142	-0.5031
51	68AWF354	0.9516	0.3836	0.3658	-0.4953	-0.6522
52	68AWF355	0.9614	0.2864	0.3079	-0.4429	-0.7671
53	68AWF357	0.9739	0.4131	0.4332	-0.5483	-0.5612
54	68AWF410	0.9652	0.4131	0.3524	-0.6053	-0.5514
55	68AWF430	0.9464	0.4607	0.4339	-0.5155	-0.5292
56	68AWF440	0.9318	0.3728	0.3901	-0.5148	-0.6128
57	68AWF505	0.8597	0.4819	0.2095	-0.4516	-0.6161
58	68ANC308	0.9547	0.4479	0.2959	-0.2083	-0.7894
59	68ANC618	0.7867	0.2441	0.4051	-0.6690	-0.3398
60	68ANC708	0.7790	0.3230	0.2936	-0.6989	-0.3161
61	68ANC958	0.9286	0.3070	0.0497	-0.6824	-0.6052
62	68ANC105	0.9189	0.2003	0.2794	-0.6621	-0.6020
63	68ANC112	0.9572	0.3260	0.1645	-0.7143	-0.5601
64	68ANC115	0.8643	0.0644	0.3589	-0.7140	-0.4706
65	68ANC118	0.9271	0.2252	0.3215	-0.7242	-0.4985
66	68ANC120	0.9278	0.3284	0.3170	-0.6561	-0.5377
67	68ANC126	0.9013	0.3785	0.1983	-0.6157	-0.5828
68	68ANC140	0.9207	0.3305	0.2739	-0.7270	-0.4561
69	68ANC154	0.9565	0.3945	0.1499	-0.5947	-0.6517
70	68ANC166	0.9550	0.5444	0.1272	-0.3336	-0.7289
71	68ANC179	0.9630	0.4315	0.4627	-0.5643	-0.4943
72	68ANC181	0.6896	0.3151	0.2304	-0.4730	-0.5599
73	68ANC182	0.7059	0.6045	0.1876	-0.3397	-0.4358
74	68ANC187	0.9552	0.7767	0.3260	-0.3369	-0.3636
75	68ANC190	0.2377	0.2429	0.0879	-0.3757	-0.2547
76	68ANC200	0.9855	0.7714	0.2255	-0.3393	-0.4738
77	68ANC212	0.9527	0.7923	0.2554	-0.2870	-0.4212
78	68ANC215	0.9290	0.6878	0.0987	-0.5117	-0.4293
79	68ANC231	0.9559	0.6885	0.2961	-0.5342	-0.3299
80	68ANC233	0.9644	0.7502	0.3190	-0.4152	-0.3557
81	68ANC234	0.9749	0.7168	0.4826	-0.4212	-0.2255
82	68ANC240	0.9616	0.6988	0.3902	-0.5404	-0.1703
83	68ANC241	0.9604	0.7254	0.3452	-0.4834	-0.2852
84	68ANC244	0.9608	0.7342	0.4107	-0.3938	-0.3132
85	68ANC248	0.9450	0.6889	0.3396	-0.5418	-0.2480
86	68ANC251	0.9441	0.7140	0.4263	-0.3571	-0.3536
87	68ANC768	0.9643	0.7788	0.1157	-0.3990	-0.4303
88	68ANC798	0.9259	0.7315	0.0777	-0.4545	-0.4221
89	68ANC839	0.8958	0.6669	0.1483	-0.5800	-0.3045
90	68ANC148	0.9128	0.6197	0.2206	-0.6148	-0.3195
91	68ANC156	0.9196	0.6771	0.0916	-0.4854	-0.4660
92	68ANC158	0.9298	0.6897	0.0385	-0.5289	-0.4158
93	68ANC160	0.9347	0.7136	0.0897	-0.4858	-0.4260
94	68ANC163	0.9380	0.7013	0.1127	-0.4868	-0.4433
95	69ANC169	0.9581	0.7503	0.2086	-0.2989	-0.5121
96	68ANC194	0.9382	0.7383	0.2261	-0.4120	-0.4151
97	68ANC214	0.9341	0.7696	0.1105	-0.2665	-0.5086
98	68ANC218	0.9431	0.7240	0.2095	-0.3586	-0.4964
99	69ANC221	0.9782	0.5222	0.2021	-0.5020	-0.6424
100	68ANC223	0.8672	0.5486	0.2991	-0.4402	-0.5320
101	68ANC225	0.9577	0.4280	0.4083	-0.6715	-0.3960
102	69ANC102	0.9520	0.5282	0.3186	-0.5835	-0.4806
103	69ANC104	0.9427	0.5190	0.2885	-0.6475	-0.4134
104	69ANC110	0.9483	0.4746	0.3688	-0.5990	-0.4778
105	69ANC111	0.9826	0.5322	0.2469	-0.7074	-0.3714
106	69ANC112	0.9611	0.4927	0.4057	-0.6827	-0.2960
107	69ANC113	0.9761	0.5112	0.2272	-0.7182	-0.3838
108	69ANC115	0.9590	0.4929	0.3073	-0.6860	-0.3888
109	69ANC117	0.9817	0.4617	0.3162	-0.5951	-0.5607

Table VII cont.

110	69ANC119	0.9573	0.4507	0.3894	-0.6482	-0.4270
111	69ANC205	0.9750	0.3932	0.2409	-0.6342	-0.6002
112	69ANC211	0.9485	0.4283	0.1794	-0.6123	-0.5983
113	69ANC218	0.9444	0.3355	0.0940	-0.7666	-0.4851
114	70ANC28	0.9794	0.4698	0.2444	-0.6582	-0.4737
115	70ANC381	0.9619	0.5256	0.2684	-0.4585	-0.6352
116	70ANC421	0.9727	0.5306	0.2564	-0.5538	-0.5646
117	70ANC51	0.9664	0.5337	0.3643	-0.5537	-0.4922
118	70ANC521	0.9699	0.4673	0.3150	-0.6362	-0.4975
119	70ANC571	0.9510	0.5293	0.3472	-0.5384	-0.5103
120	70ANC60	0.9771	0.4312	0.2763	-0.5677	-0.6221
121	69ANC120	0.9785	0.4103	0.3880	-0.6828	-0.4398
122	68ANC38	0.9534	0.5340	0.4619	-0.5668	-0.3655
123	68ANC89	0.9299	0.3639	0.0614	-0.6984	-0.5531
124	68ANC15	0.6726	0.4328	0.3754	-0.3558	-0.4666
125	68ANC23	0.8771	0.4001	0.1929	-0.3137	-0.7627
126	68PR23	0.7044	0.3410	0.5527	-0.4380	-0.3013
127	69ANC127	0.9288	0.5259	0.5832	-0.2720	-0.4880
128	69ANC130	0.9336	0.4827	0.6779	-0.2361	-0.4310
129	69ANC145	0.8808	0.5048	0.2053	-0.4436	-0.6221
130	69ANC147	0.9073	0.4125	0.4665	-0.3157	-0.6480
131	68AWF801	0.3641	0.2954	0.8409	-0.1481	-0.2185
132	68AWF807	0.7666	0.1953	0.8215	-0.2112	-0.0950
133	68AWF807	0.8339	0.0931	0.8944	-0.1429	-0.0717
134	68AWF827	0.5930	0.0293	0.7592	-0.1209	-0.0338
135	69ANC85	0.7732	0.0829	0.4862	-0.6355	-0.3551
136	69ANC86	0.3821	-0.1003	0.4880	-0.2841	-0.2307
137	69ANC95	0.7883	0.1965	0.4825	-0.6085	-0.3829
138	69ASC97	0.8668	0.2828	0.4972	-0.6231	-0.3891
139	5PANC307	0.7034	0.3949	0.3192	-0.4779	-0.4660
140	68ANC304	0.8314	0.4120	0.2272	-0.6094	-0.4885
141	68ANC307	0.8992	0.3947	-0.0038	-0.6653	-0.5485
142	68ANC309	0.9053	0.3274	0.0545	-0.7469	-0.4871
143	68ANC216	0.9539	0.5533	0.2698	-0.4974	-0.5723
144	68ANC235	0.9410	0.5004	0.4194	-0.5074	-0.5072
145	69ANC204	0.9306	0.5730	0.1613	-0.5032	-0.5684
146	69ANC207	0.9716	0.4669	0.2338	-0.7072	-0.4459
147	69ANC223	0.9668	0.4421	0.1071	-0.7505	-0.4434
148	69ANC230	0.9778	0.5789	0.0915	-0.4893	-0.6283
149	69ANC245	0.9505	0.5858	0.2288	-0.5193	-0.5343
150	69ANC252	0.9125	0.5596	0.3766	-0.5227	-0.4292
151	69ANC255	0.9838	0.5897	0.1446	-0.4297	-0.6561
152	70ANC58H	0.9349	0.5320	0.3934	-0.6332	-0.3100
153	M131032	0.9666	0.4302	0.4735	-0.7269	-0.1703
154	M131033	0.8864	0.5580	0.5431	-0.4786	-0.2260
155	M131034	0.9500	0.6335	0.2132	-0.3338	-0.6260
156	M131036	0.5672	0.1702	0.2717	-0.6376	-0.2405
157	M131037	0.9312	0.6037	0.3913	-0.3729	-0.5239
158	M131038	0.9499	0.4790	0.4085	-0.6896	-0.2791
159	M131039	0.9473	0.5429	0.2660	-0.5197	-0.5583
160	M131040	0.9628	0.4795	0.4457	-0.6432	-0.3469
161	M131041	0.9207	0.3196	0.4762	-0.7256	-0.2555
162	M131042	0.9703	0.4903	0.4222	-0.6961	-0.2590
163	M131043	0.9545	0.4090	0.4931	-0.6481	-0.3522
164	M131044	0.9611	0.4793	0.4695	-0.6693	-0.2510
165	M131045	0.9821	0.4390	0.4919	-0.7040	-0.2277
166	M131046	0.9843	0.4023	0.3589	-0.7529	-0.3561
167	M131047	0.9418	0.3364	0.4083	-0.7642	-0.2792
168	M131048	0.9797	0.3698	0.3793	-0.7891	-0.2766
169	M131049	0.9728	0.4587	0.3965	-0.7315	-0.2648

Table VII cont.

170	M131050	0.9535	0.5231	0.3978	-0.6951	-0.1961
171	M131051	0.9812	0.4966	0.4042	-0.7183	-0.2348
172	M131052	0.8930	0.4699	0.3032	-0.7200	-0.2489
173	M131053	0.9741	0.4610	0.3655	-0.7673	-0.1993
174	M131054	0.9671	0.4966	0.2958	-0.6839	-0.4065
175	M131055	0.9704	0.3906	0.2975	-0.7991	-0.3139
176	M131056	0.9670	0.5309	0.2372	-0.6532	-0.4497
177	M131057	0.9307	0.4832	0.2691	-0.6349	-0.4709
178	M131059	0.9561	0.4526	0.4419	-0.6690	-0.3292
179	M131064	0.9384	0.4293	0.3203	-0.7186	-0.3693
	VARIANCE	24.232	11.842	13.379	22.489	
	CUM. VAR	24.232	36.074	69.453	91.942	

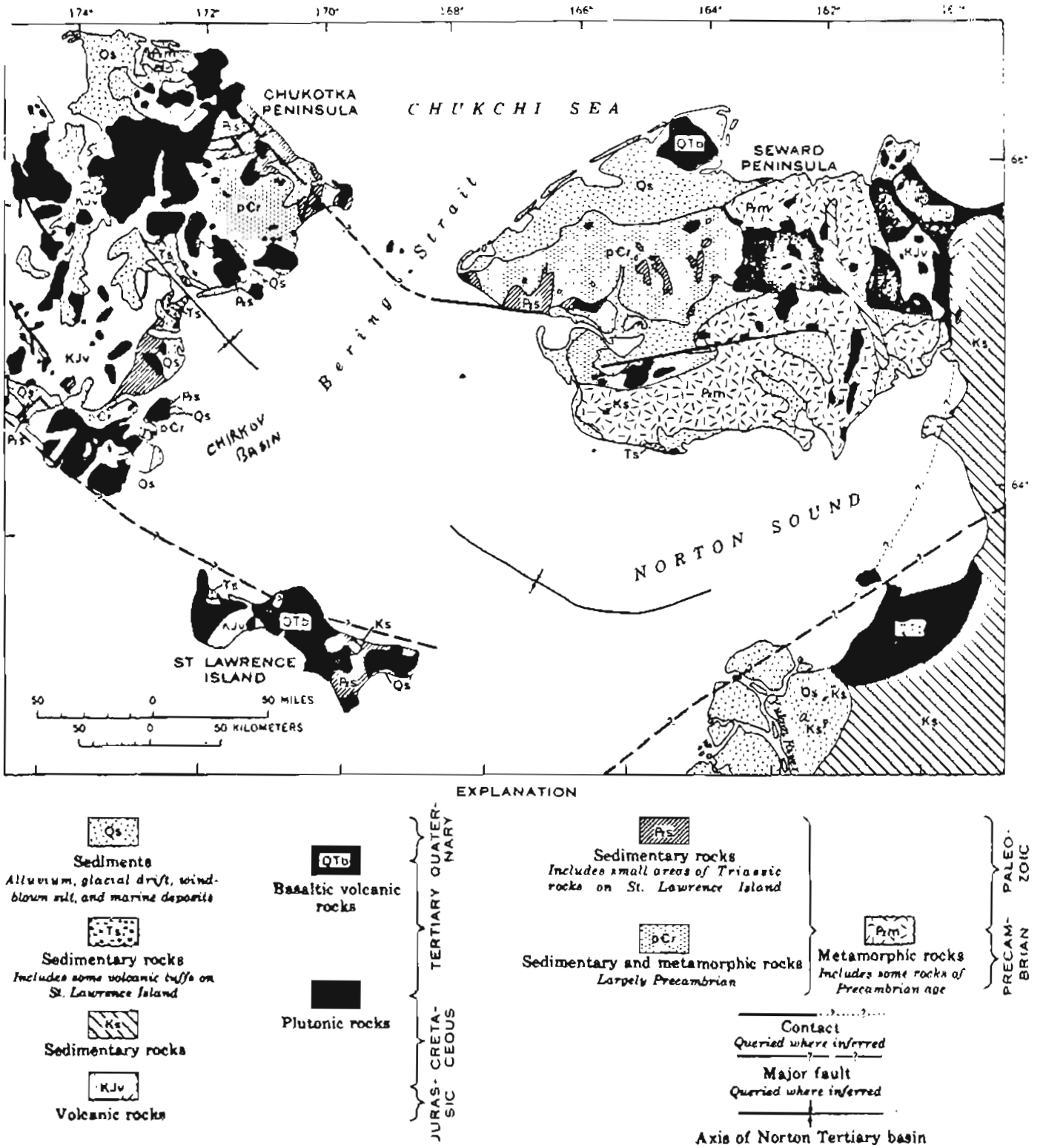

Figure 1. Generalized map of the northern Bering Sea region, (Nelson and Hopkins, 1972).

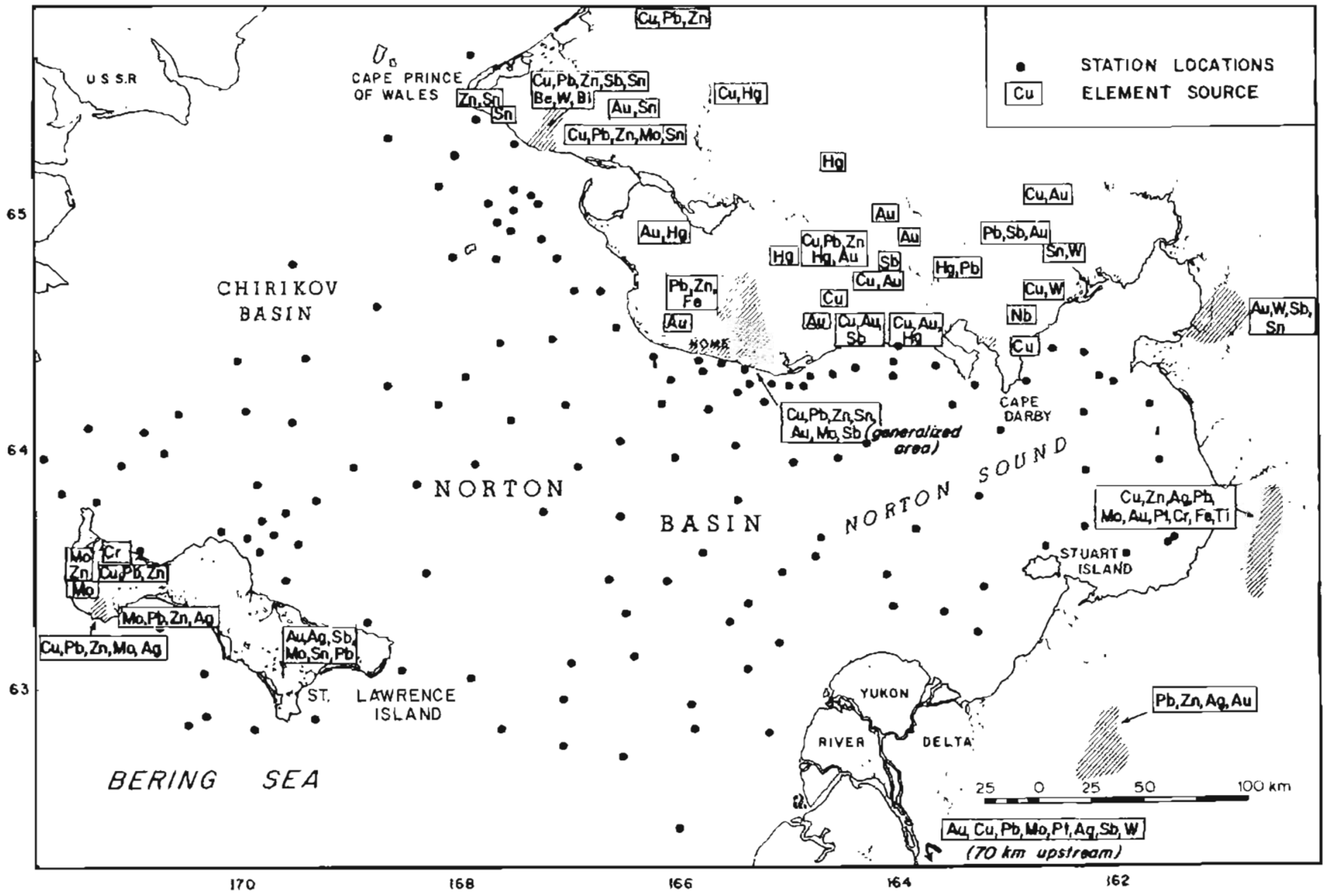

Figure 2. Offshore sampling locations and terrestrial sites of known mineralization for various elements.

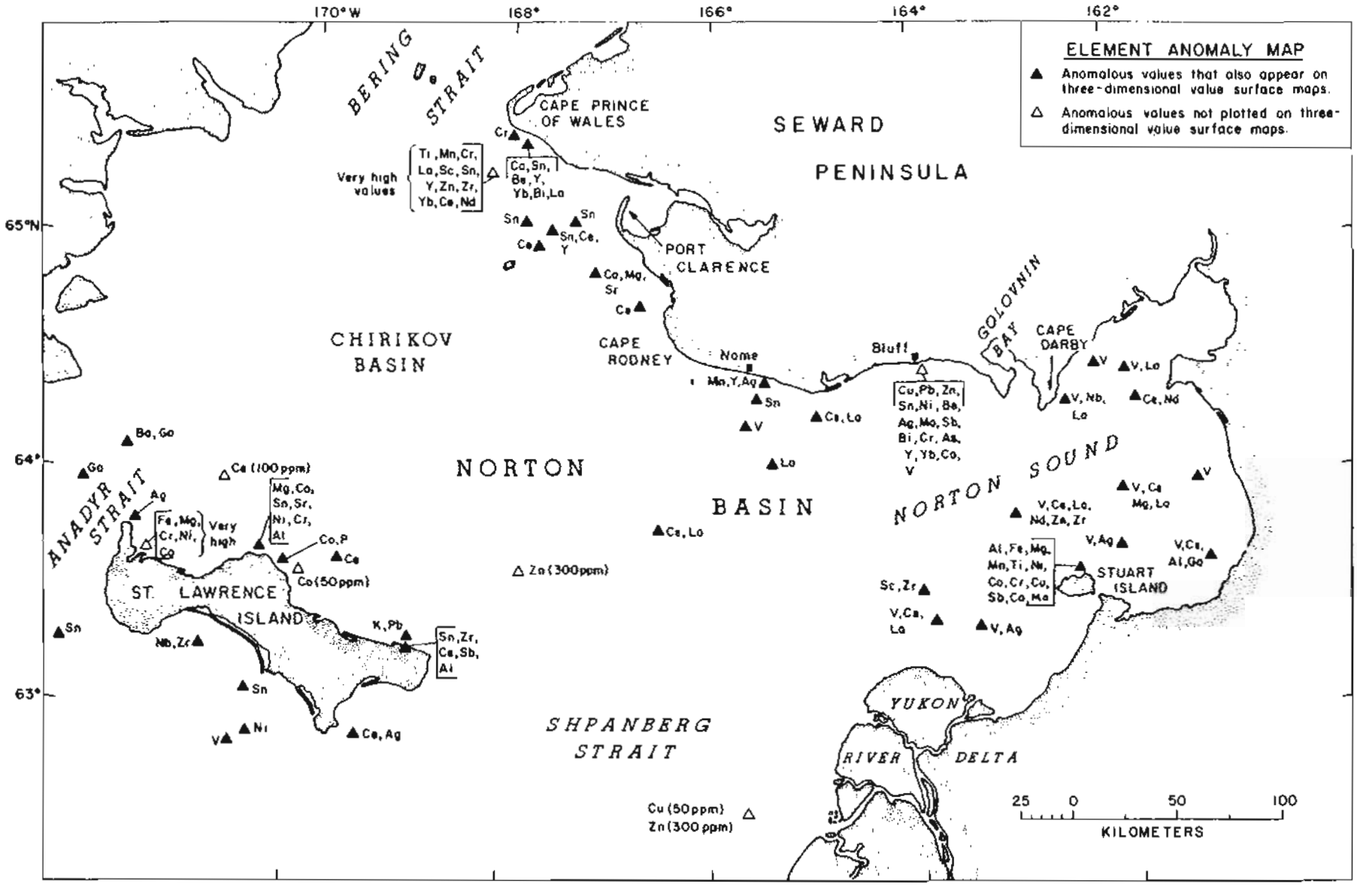

Figure 3. Map depicting significant anomalies defined as values falling outside the upper limit of the expected value range or as the highest few values (see Table I).

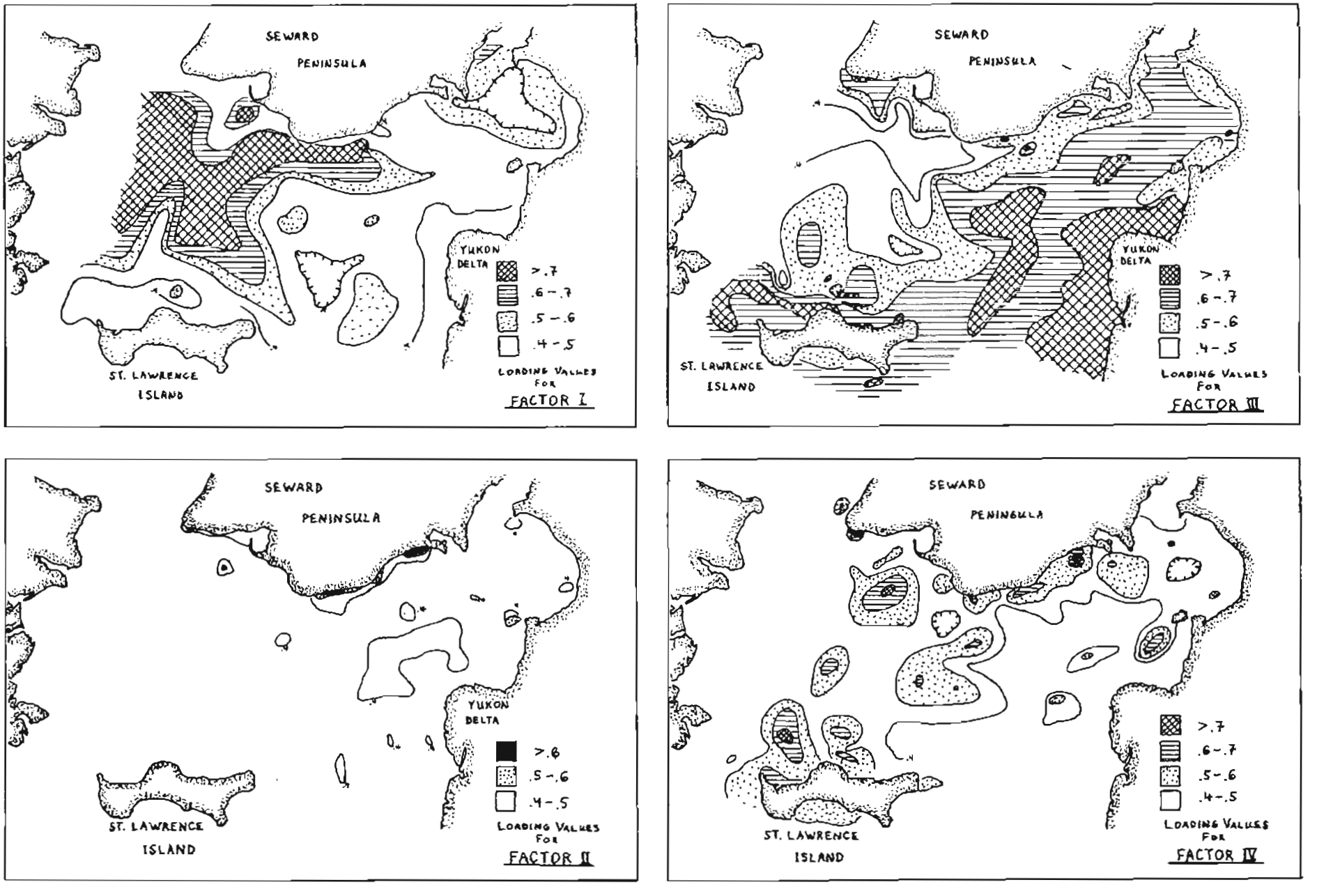

Figure 4. Distribution of Q-mode Factor loadings for the first four factors.

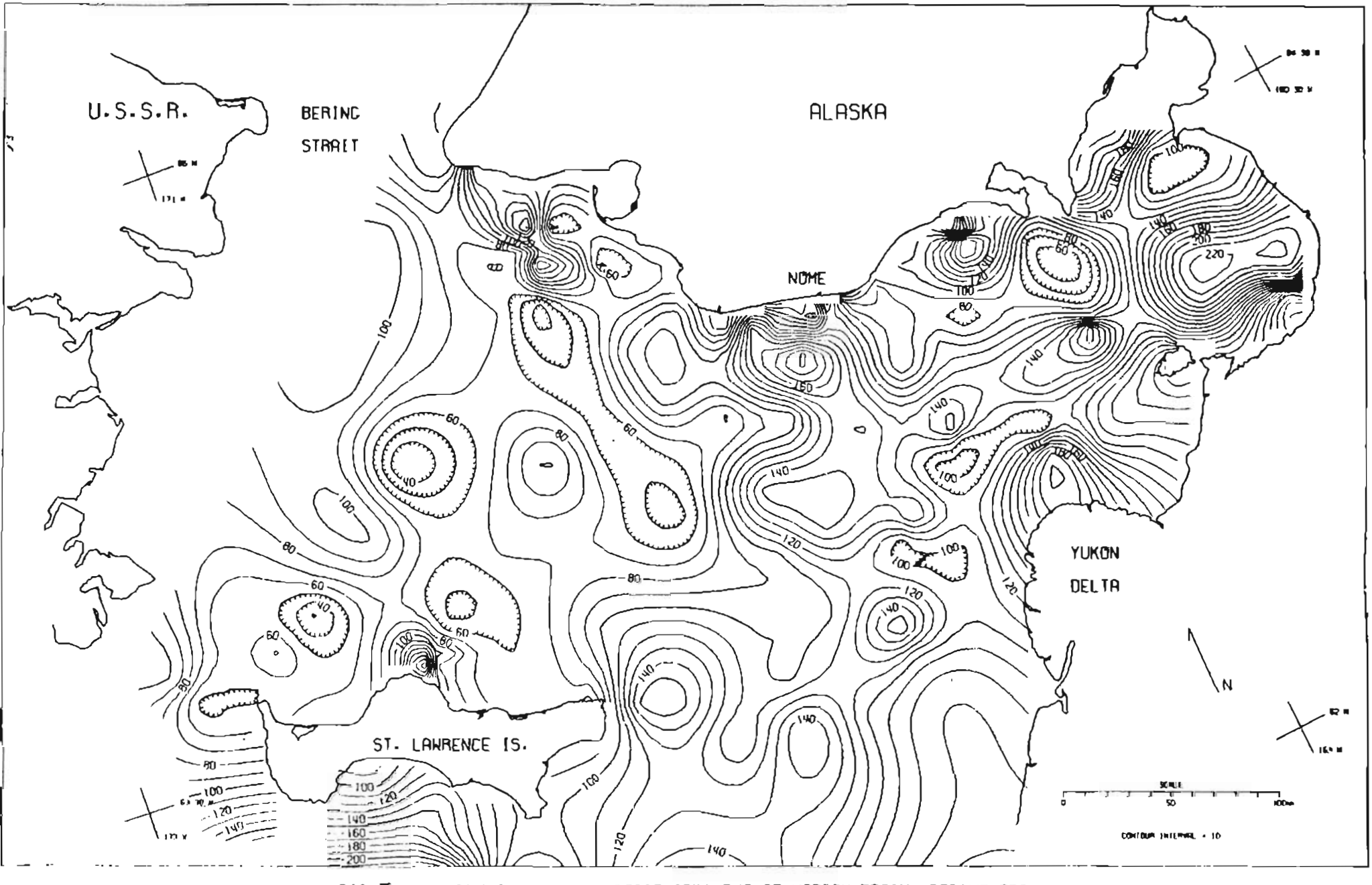

FIG 5 V PPM IN BOTTOM SURFACE SEDIMENT OF NORTON BASIN, BERING SEA

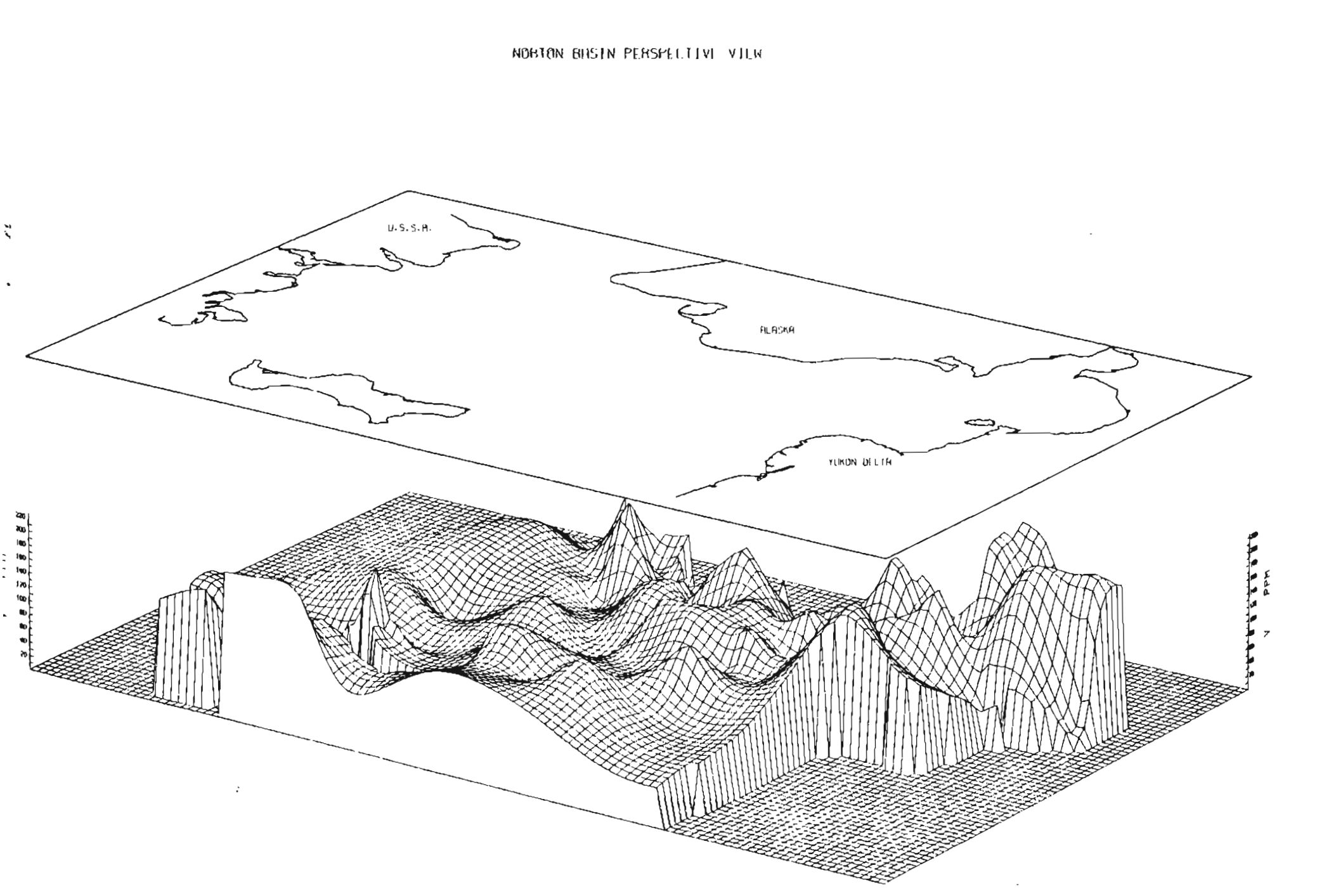

FIG 6 V PPM IN BOTTOM SURFACE SEDIMENT OF NORTON BASIN, BERING SEA

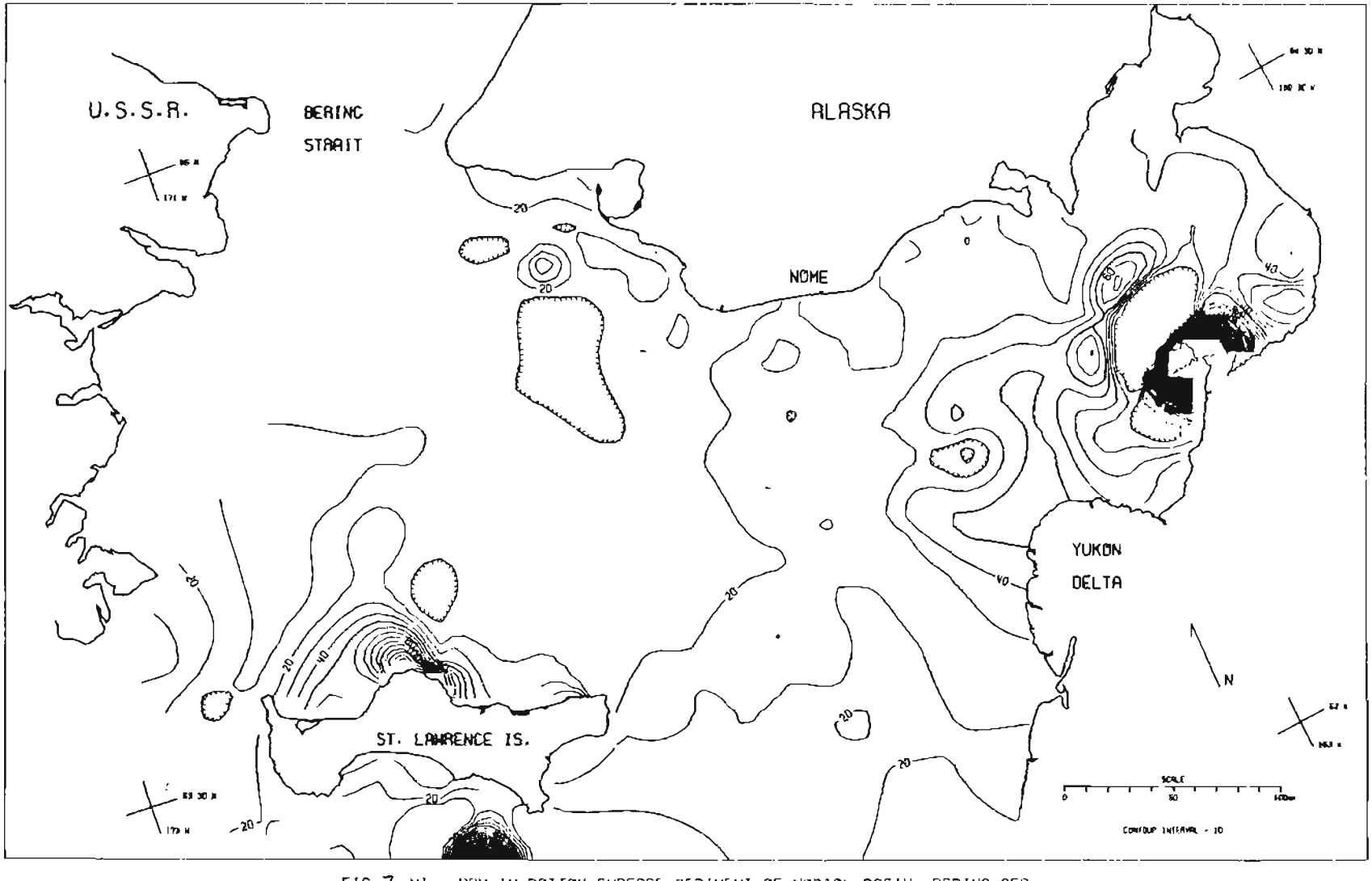

FIG 7 NI PPM IN BOTTOM SURFACE SEDIMENT OF NORTON BASIN, BERING SEA

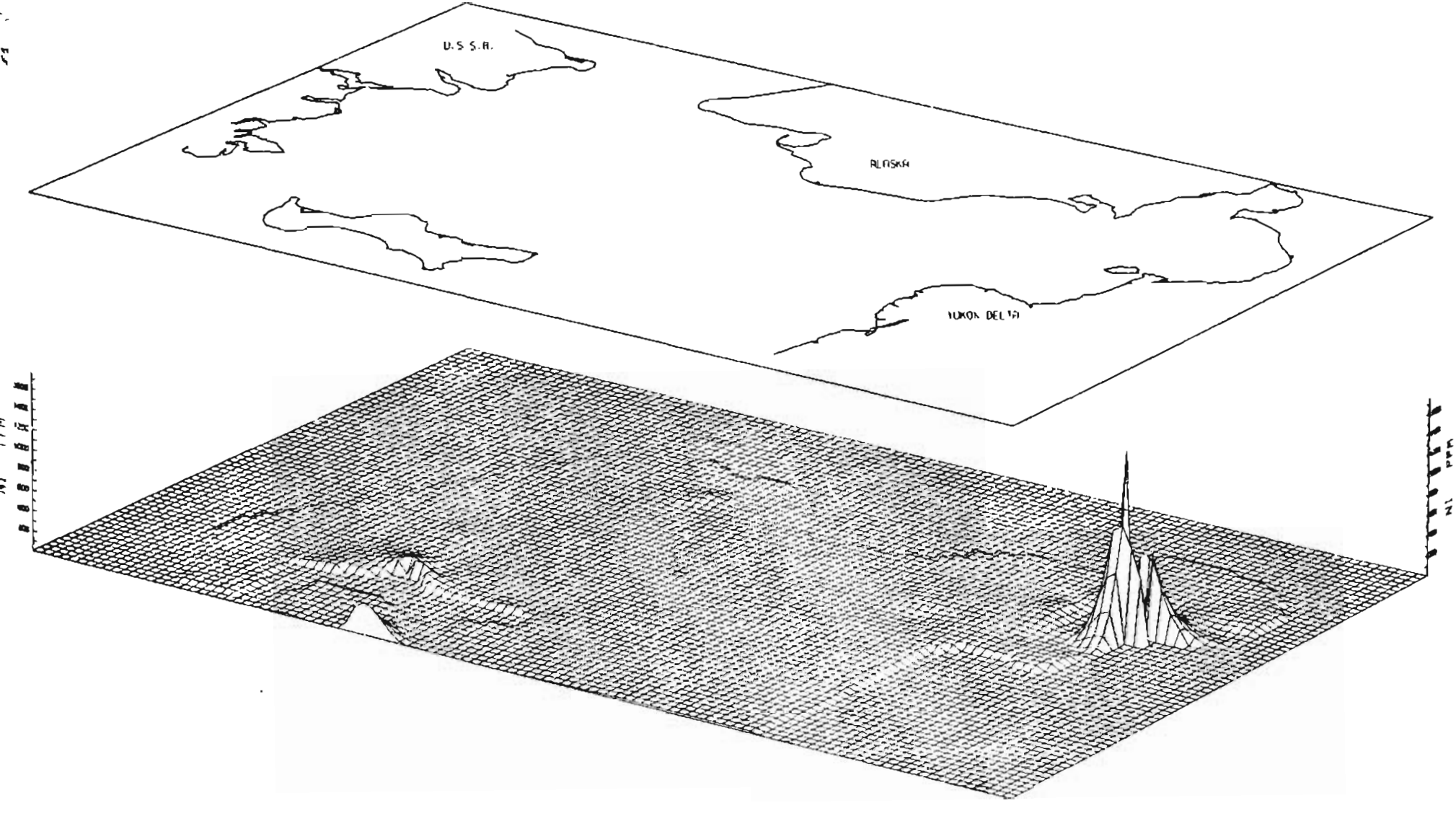

FIG 8 NI PPM IN BOTTOM SURFACE SEDIMENT OF NORTON BASIN, BERING SEA

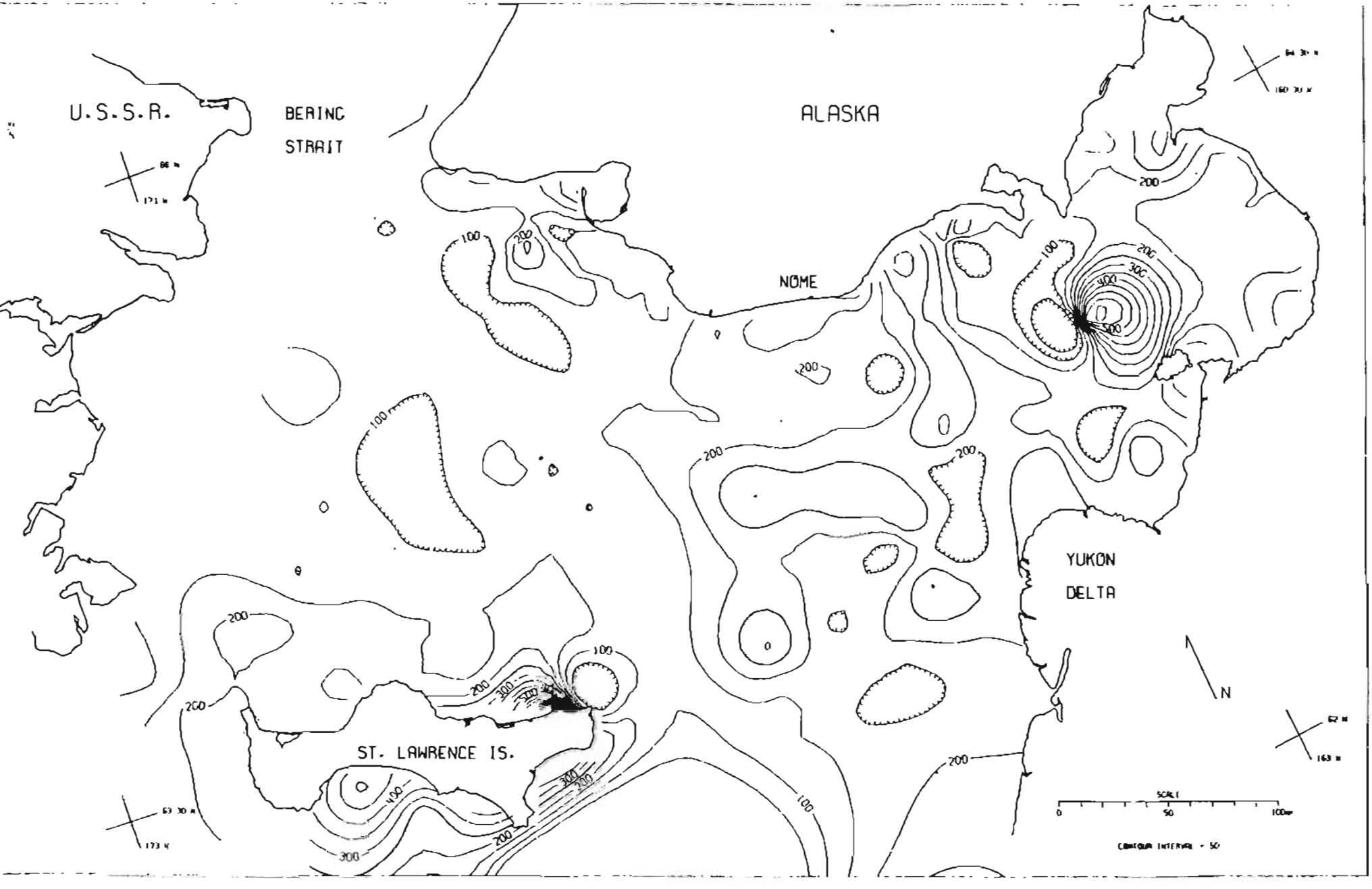

FIG 9 ZR PPM IN BOTTOM SURFACE SEDIMENT OF NORTON BASIN, BERING SEA

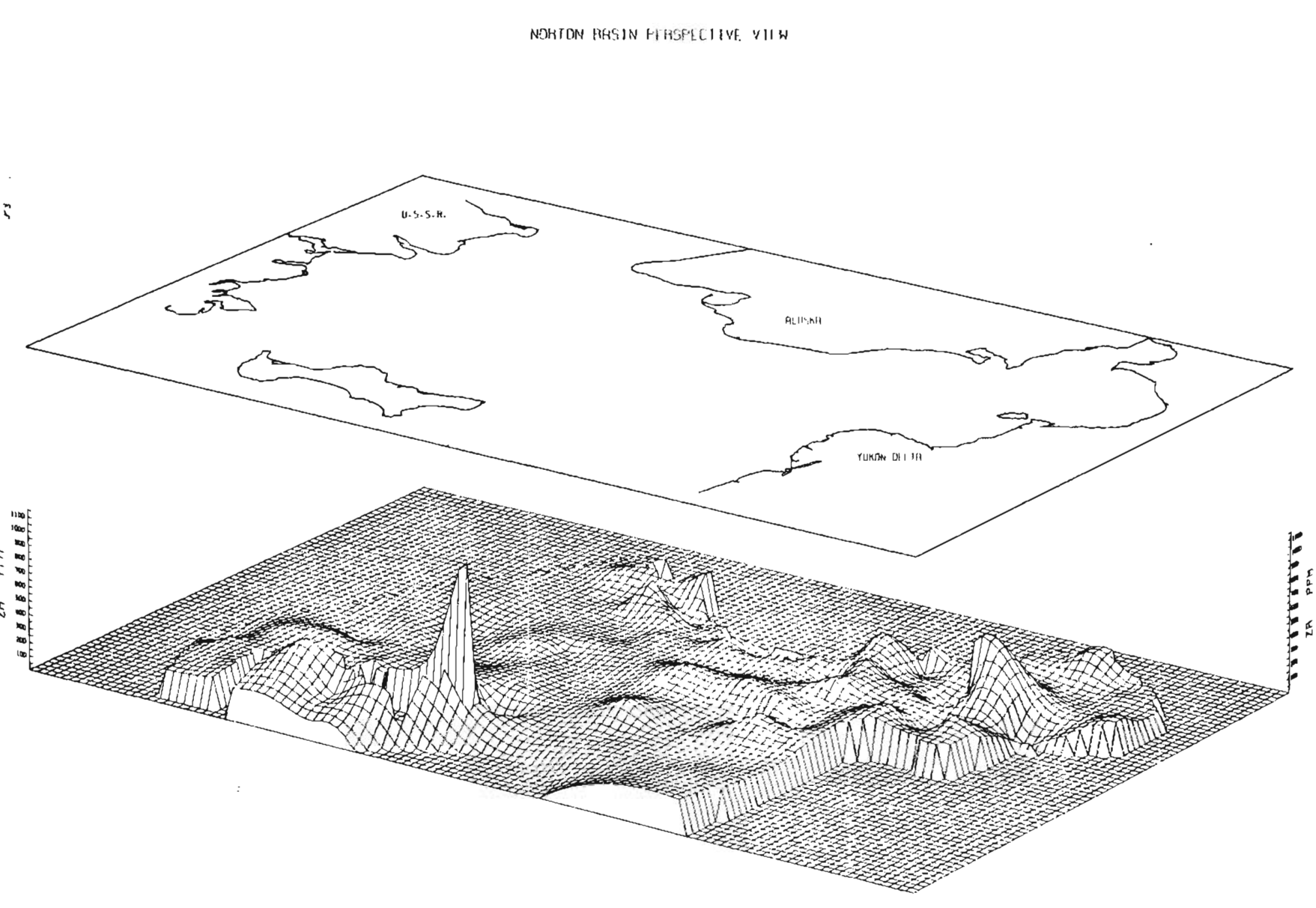

FIG 10 ZR PPM IN BOTTOM SURFACE SEDIMENT OF NORTON BASIN, BERING SEA

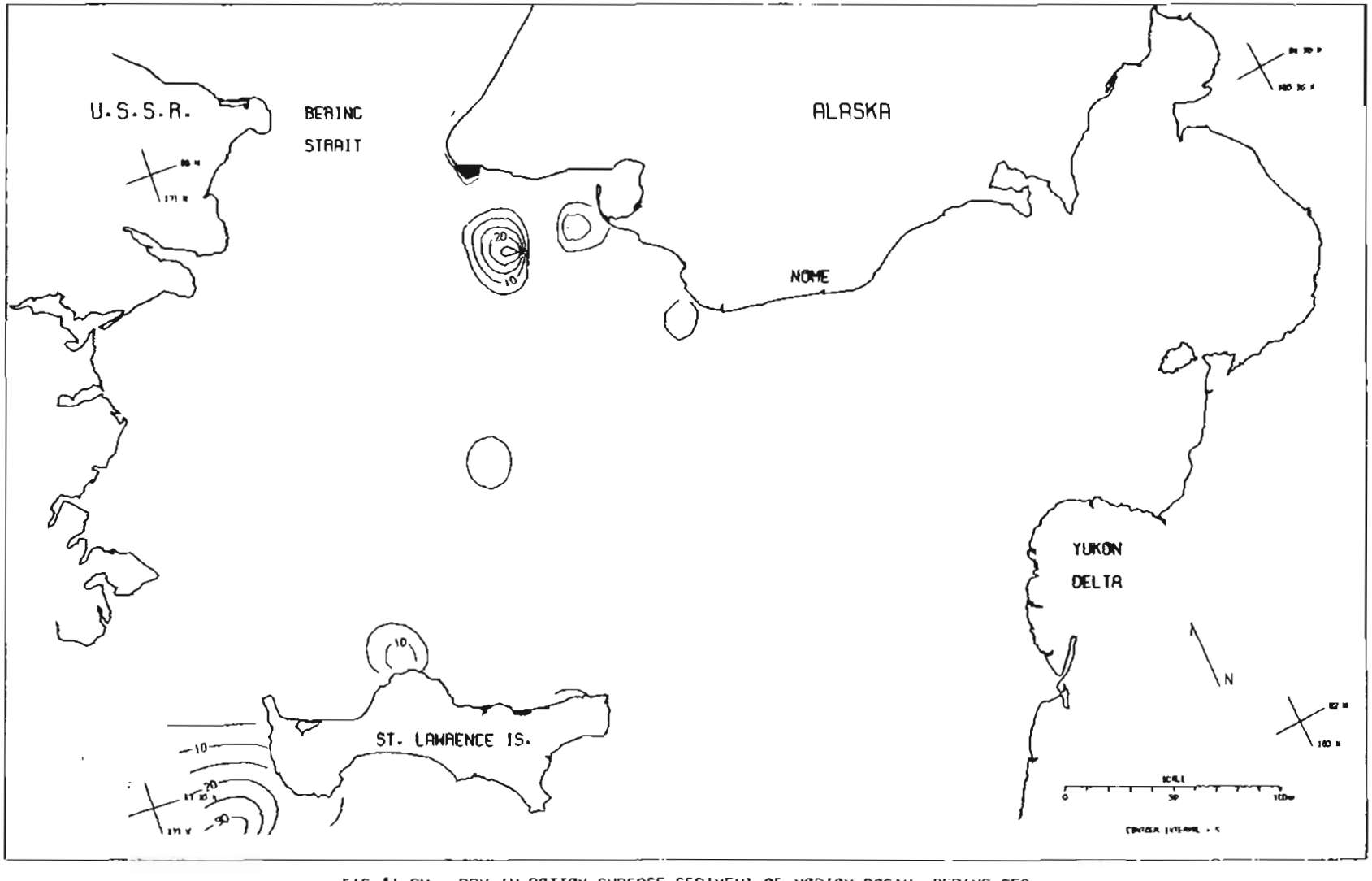

FIG 1| SN PPM IN BOTTOM SURFACE SEDIMENT OF NORTON BASIN, BERING SEA

NORTON BASIN PERSPECTIVE VIEW

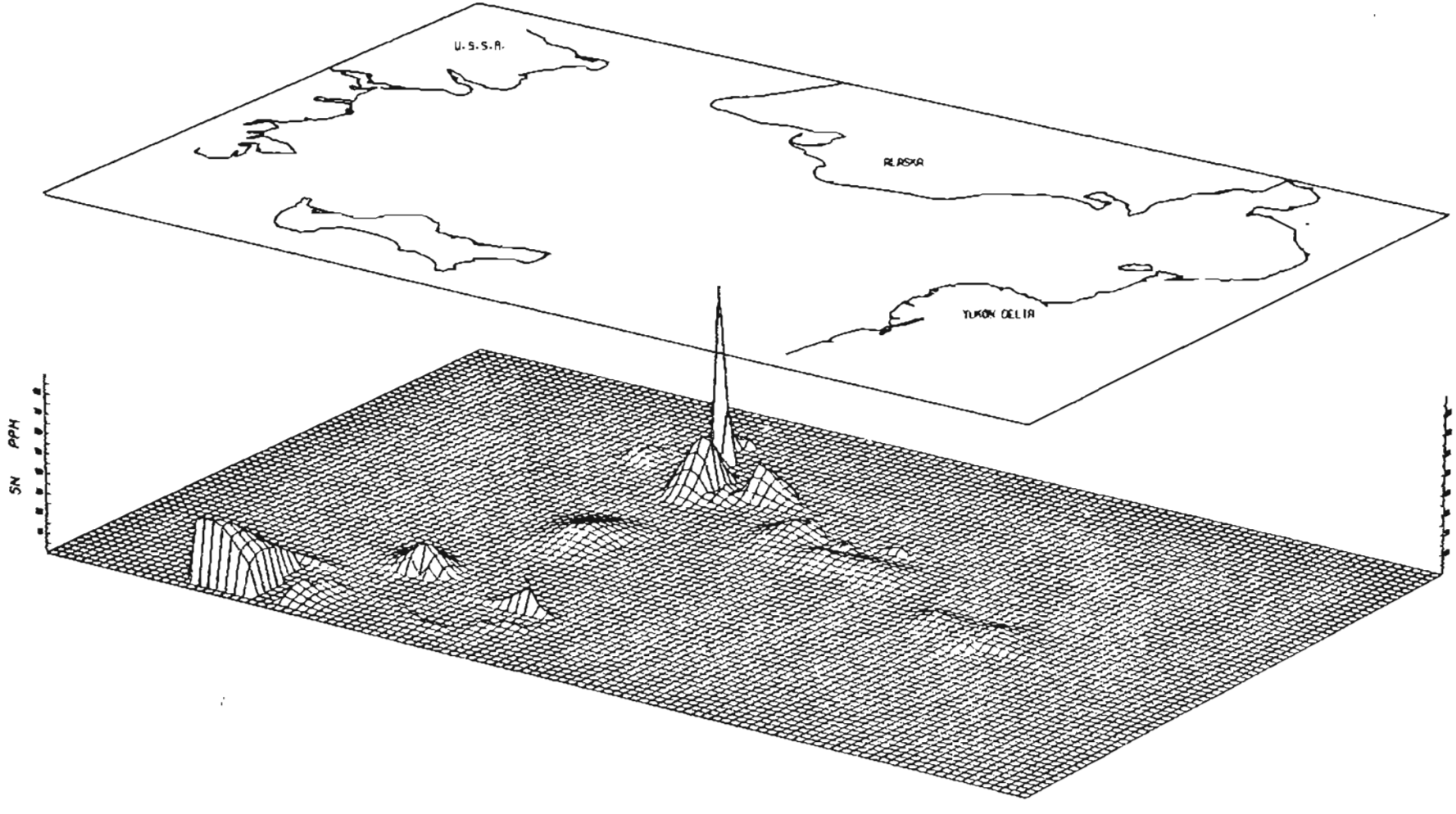

FIG 12 SN PPM IN BOTTOM SURFACE SEDIMENT OF NORTON BASIN, BERING SEA

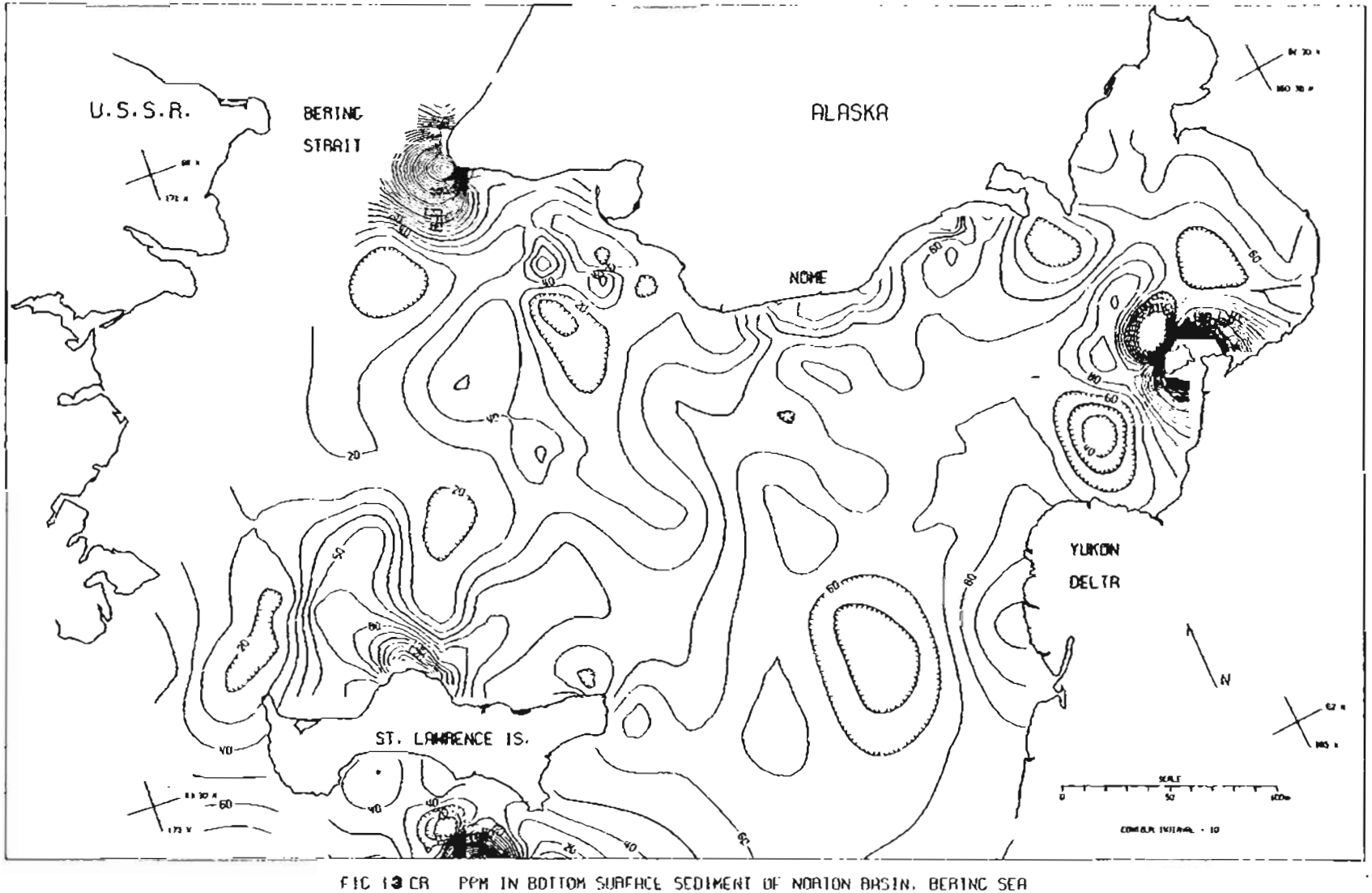

FIG 13 CR PPM IN BOTTOM SURFACE SEDIMENT OF NORTON BASIN, BERING SEA

NORTON BASIN PERSPECTIVE VIEW

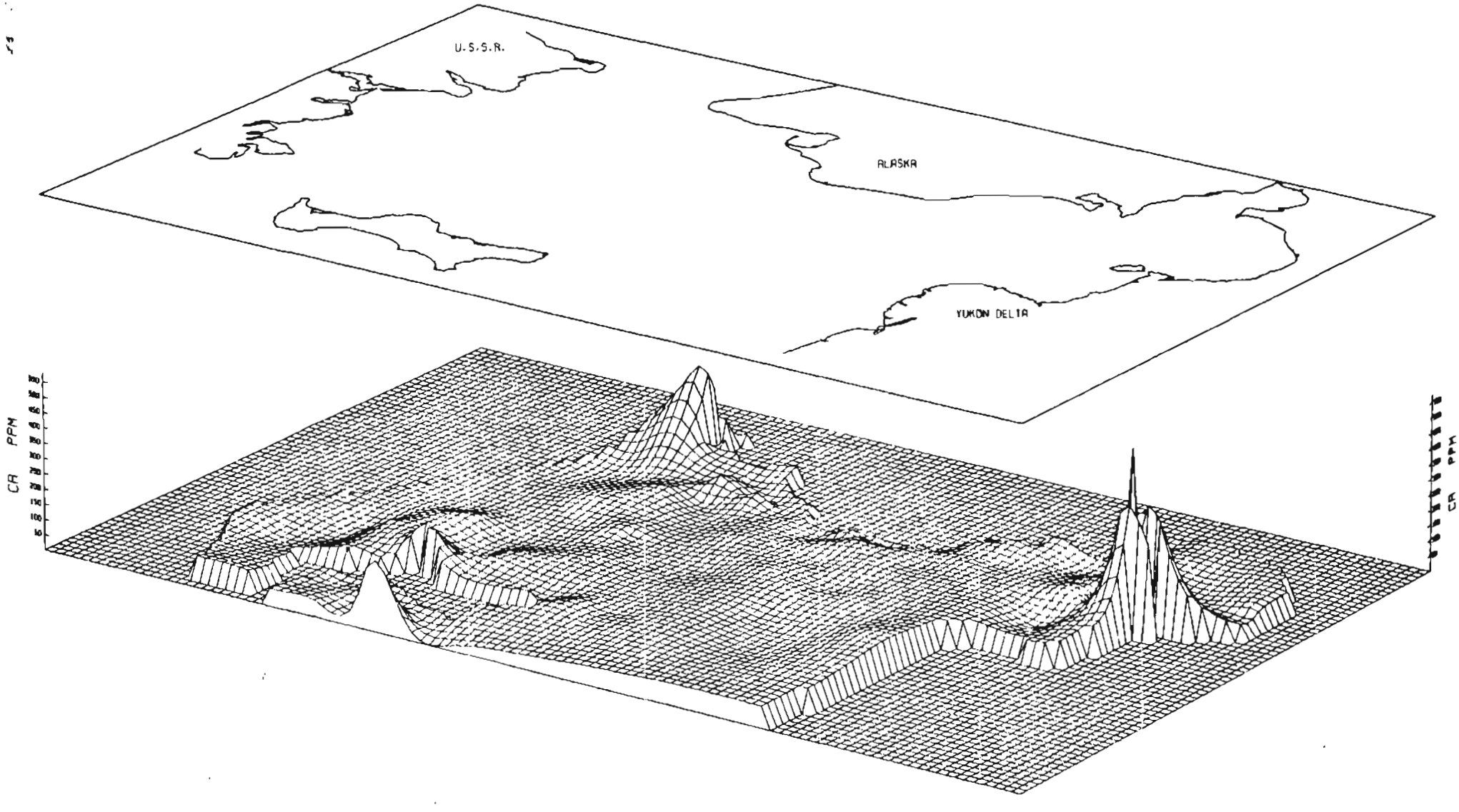

FIG 14 CR PPM IN BOTTOM SURFACE SEDIMENT OF NORTON BASIN, BERING SEA

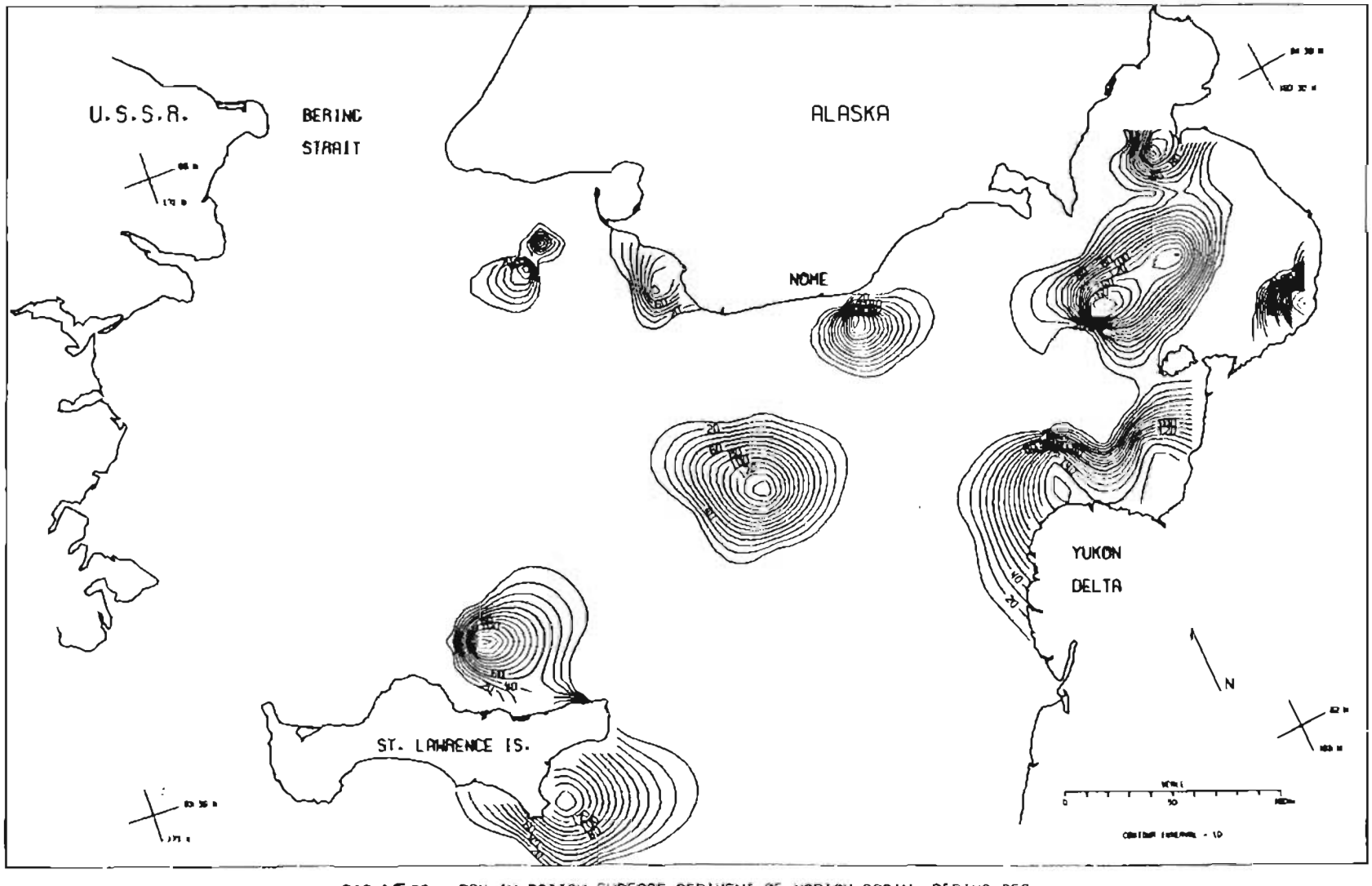

FIG 15 CE PPM IN BOTTOM SURFACE SEDIMENT OF NORTON BASIN, BERING SEA

NORTON BASIN PERSPECTIVE VIEW

FIG 16 CC PPM IN BOTTOM SURFACE SEDIMENT OF NORTON BASIN, BERING SEA

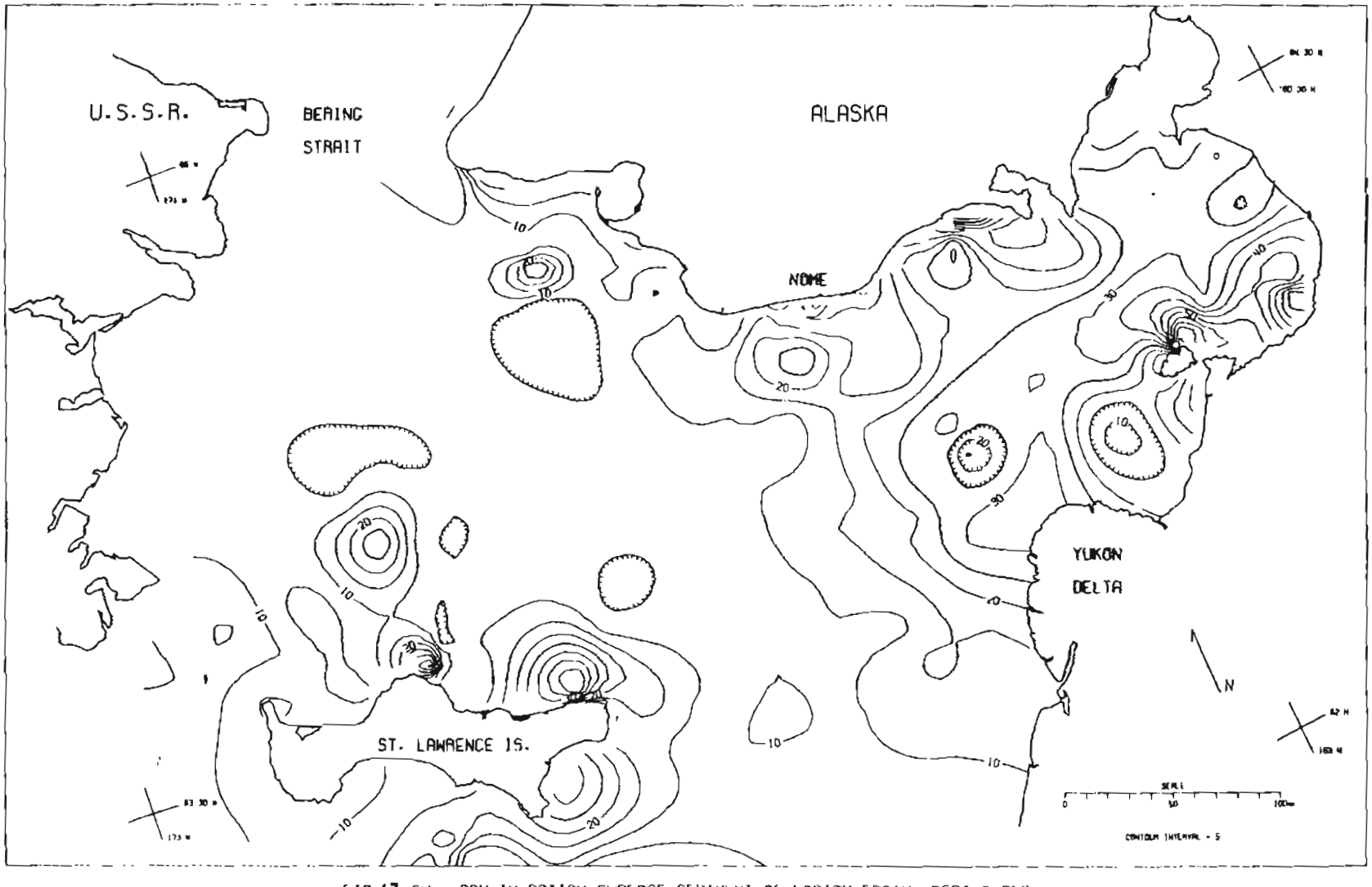

FIG 17 CU PPM IN BOTTOM SURFACE SEDIMENT OF NORTON BASIN, BERING SEA

NORTON BASIN PERSPECTIVE VIEW

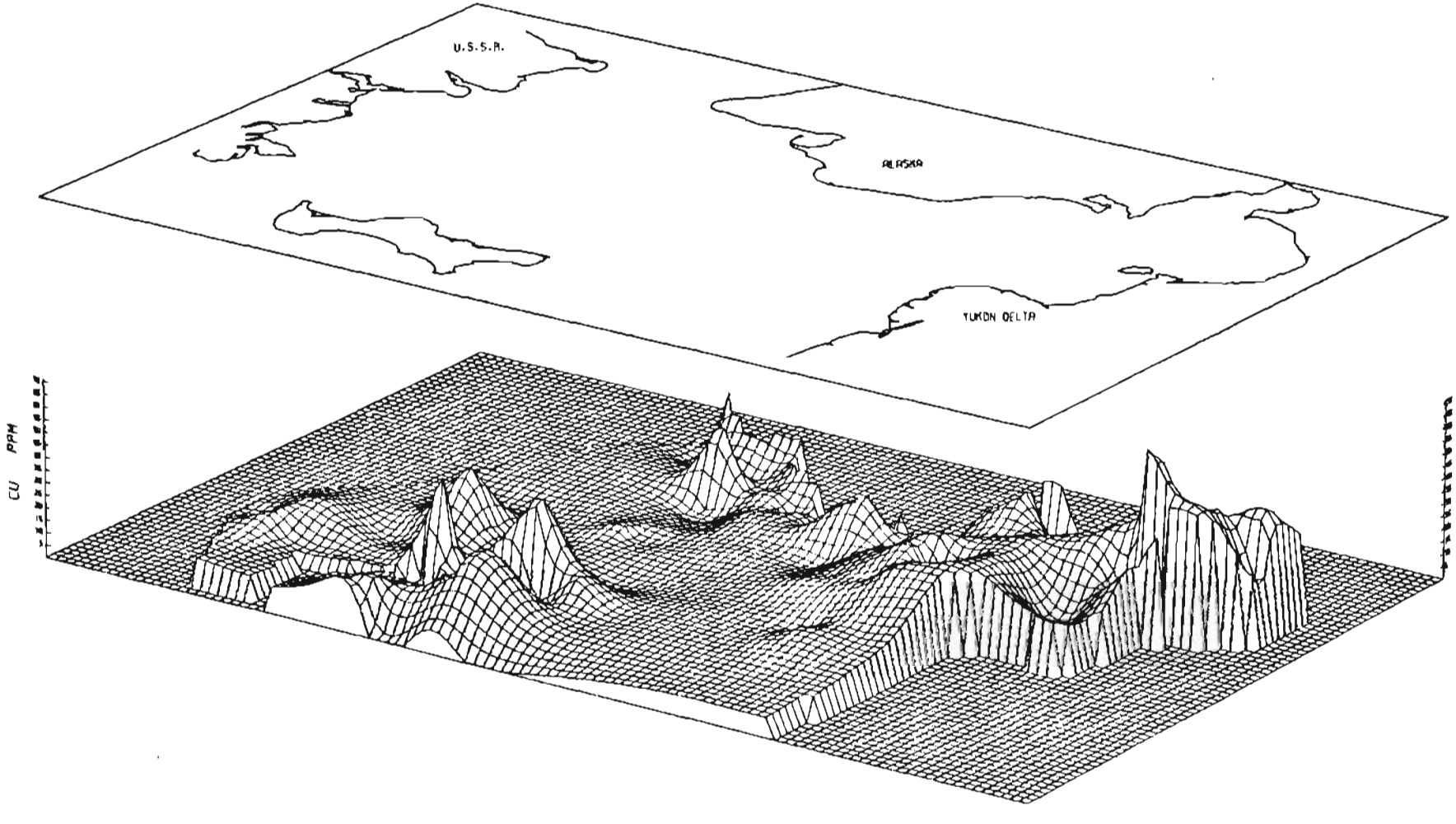

FIG 18 CU PPM IN BOTTOM SURFACE SEDIMENT OF NORTON BASIN, BERING SEA

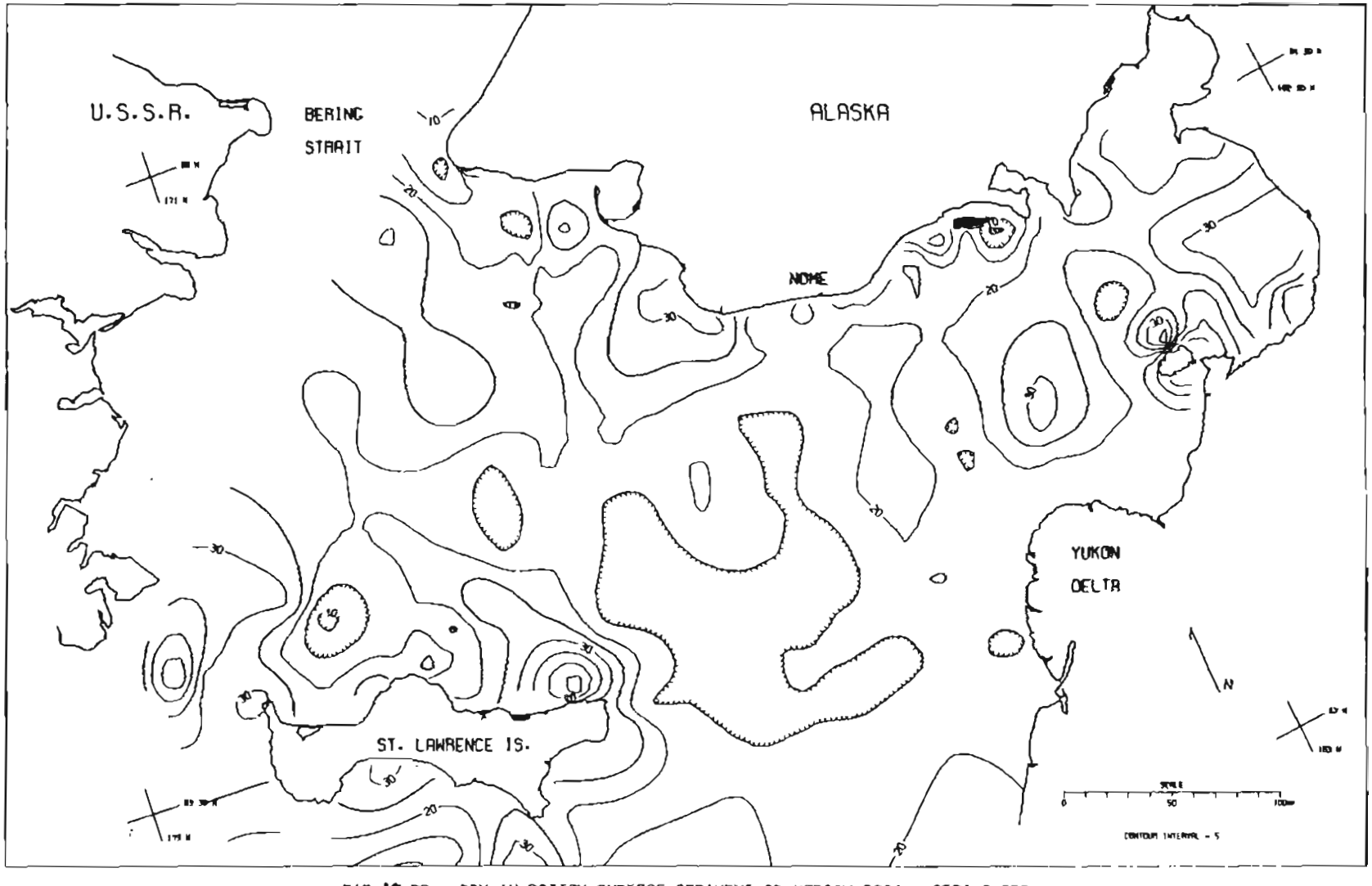

FIG 19 P8 PPM IN BOTTOM SURFACE SEDIMENT OF NORTON BASIN, BERING SEA

NORTON BASIN PERSPECTIVE VIEW

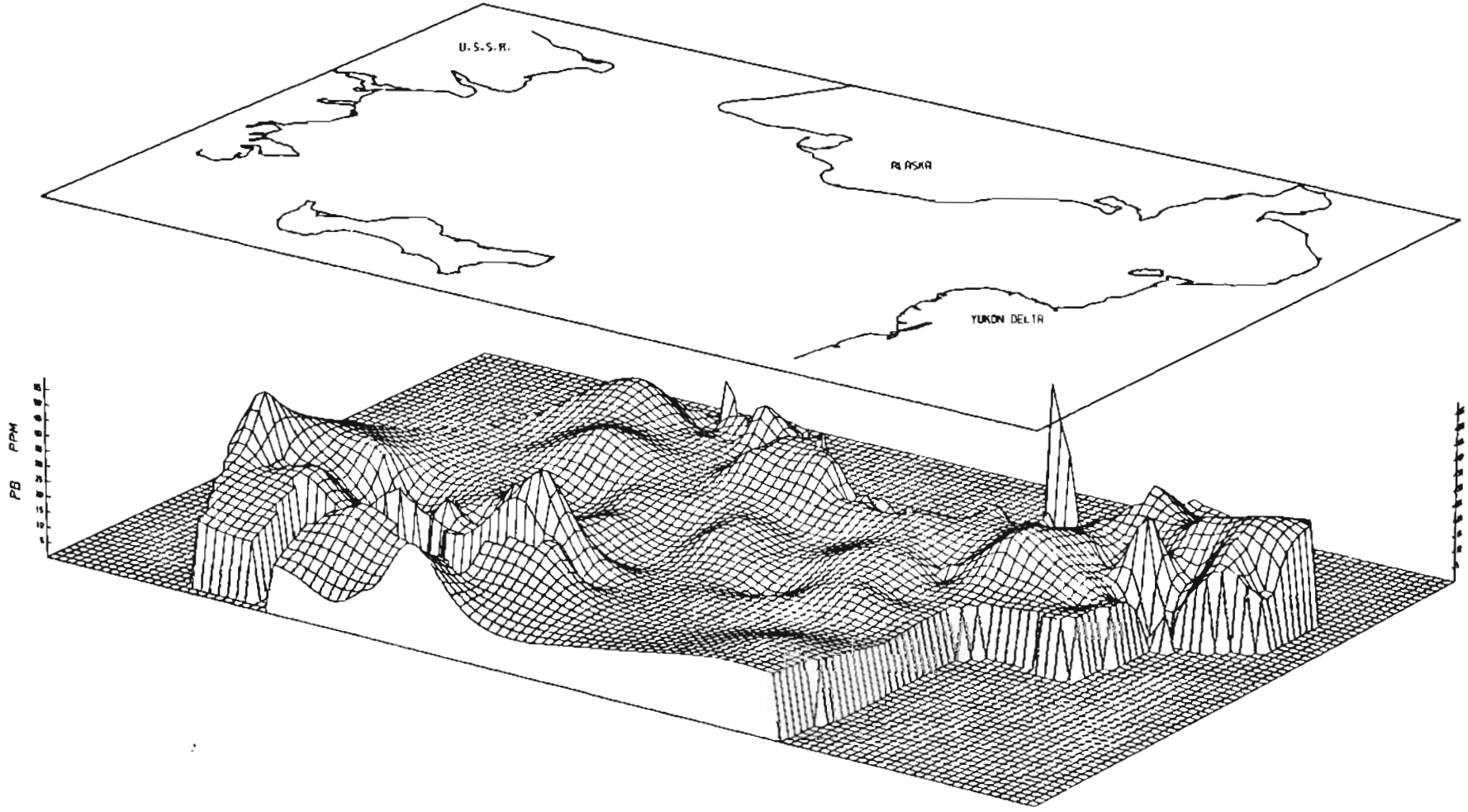

FIG 20 PB PPM IN BOTTOM SURFACE SEDIMENT OF NORTON BASIN, BERING SEA

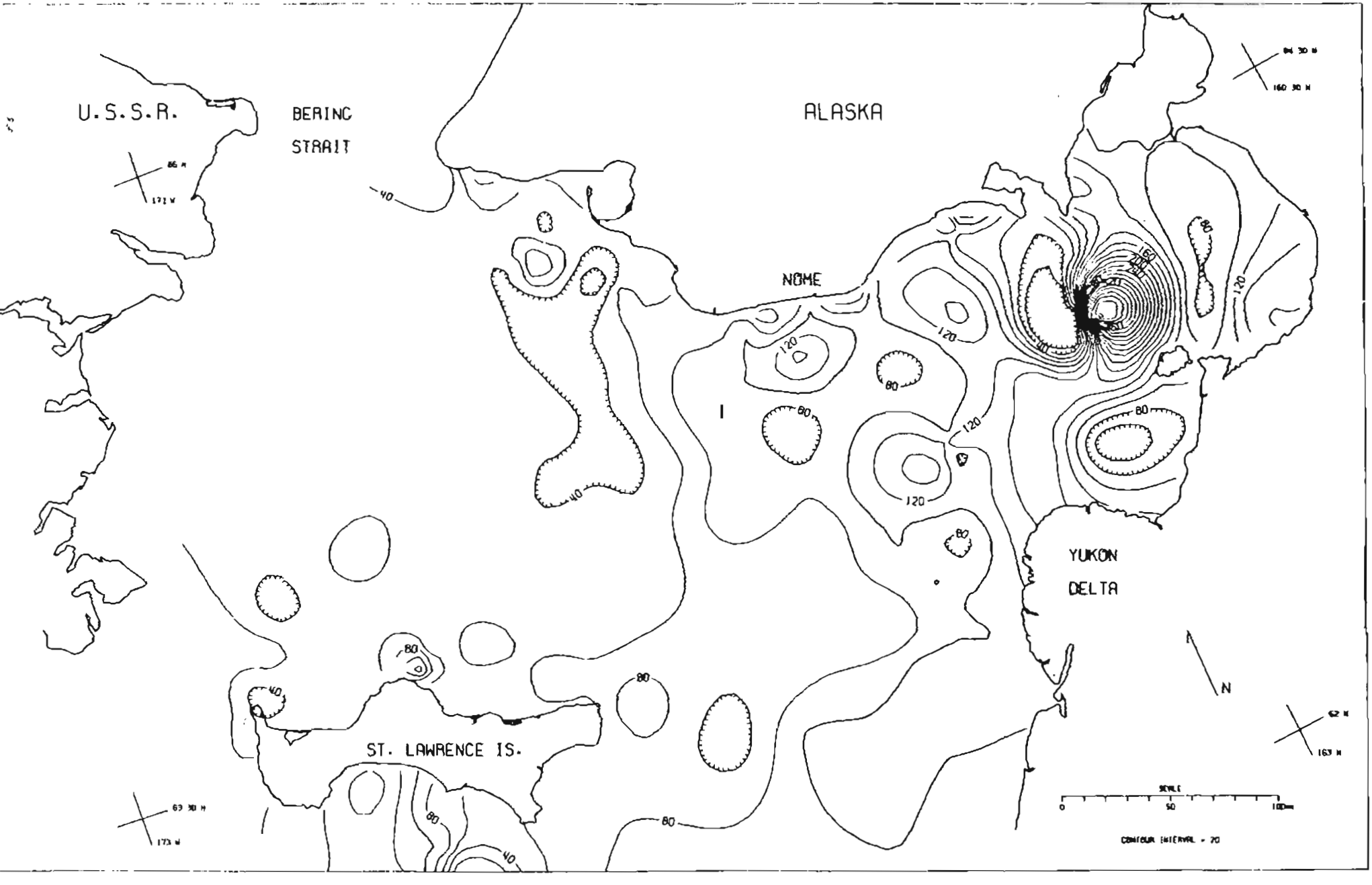

FIG 21 ZN PPM IN BOTTOM SURFACE SEDIMENT OF NORTON BASIN, BERING SEA

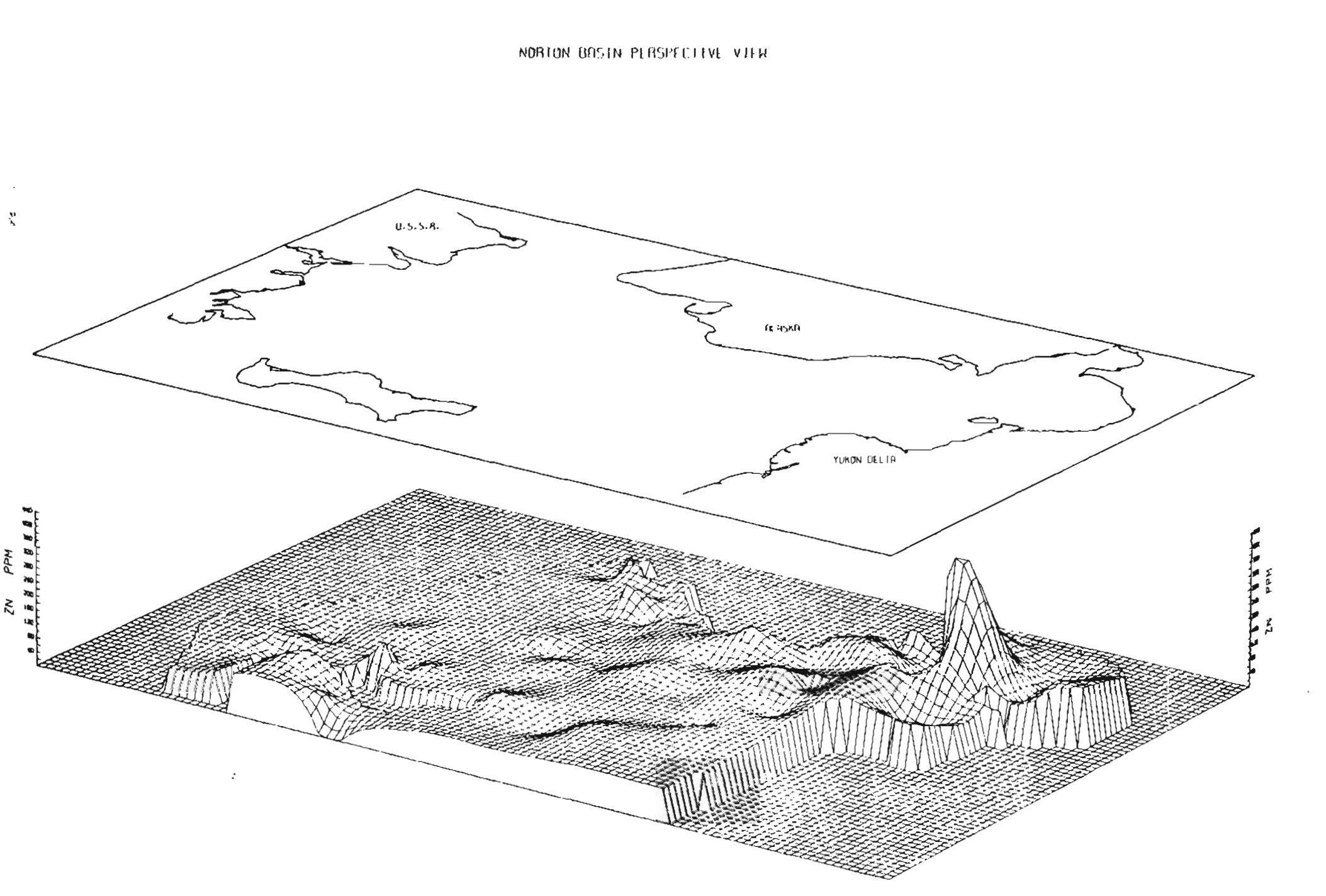

FIG 22 ZN PPM IN BOTTOM SURFACE SEDIMENT OF NORTON BASIN, BERING SEA

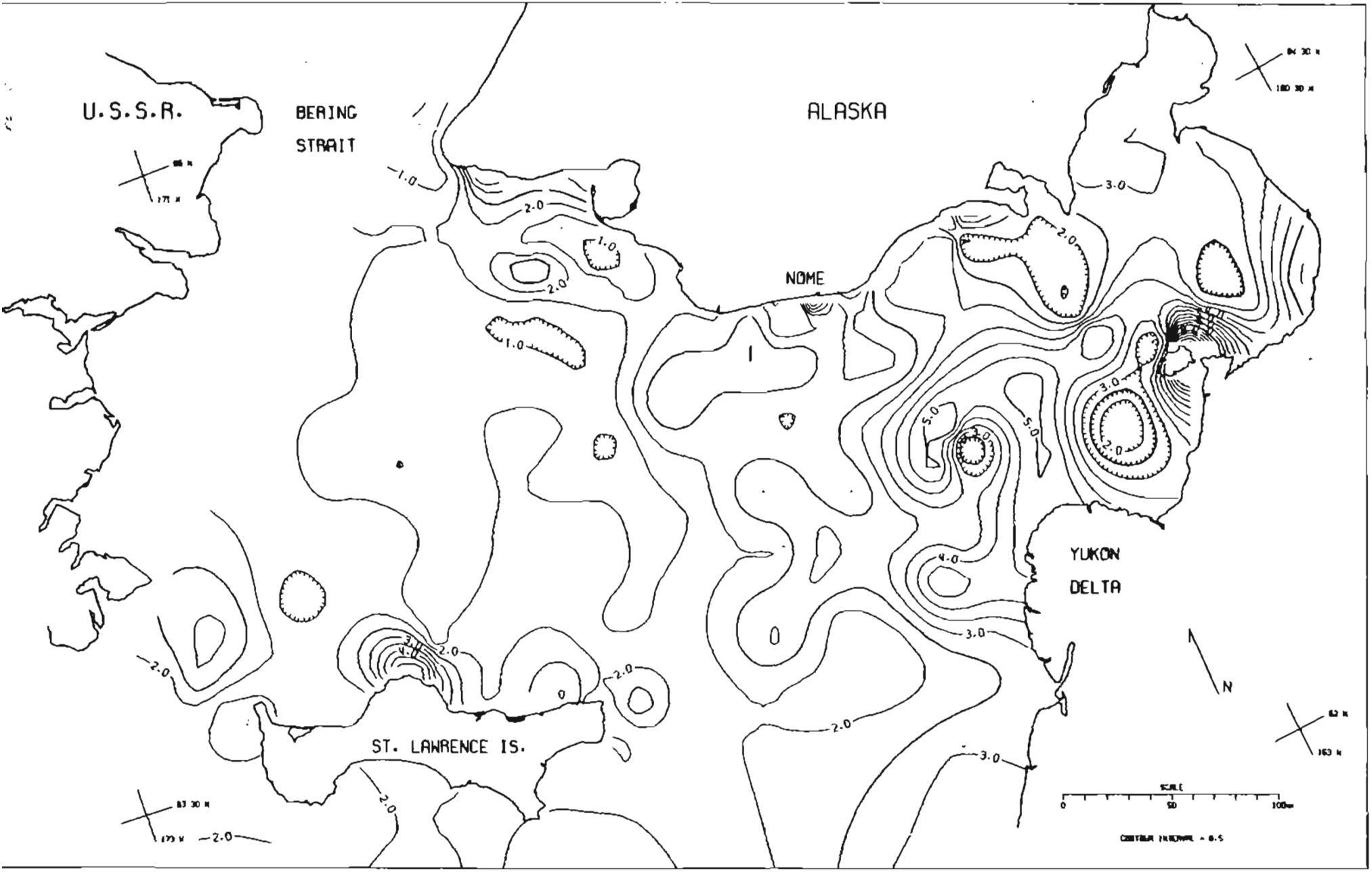

FIG 23 FE % IN BOTTOM SURFACE SEDIMENT OF NORTON BASIN, BERING SEA

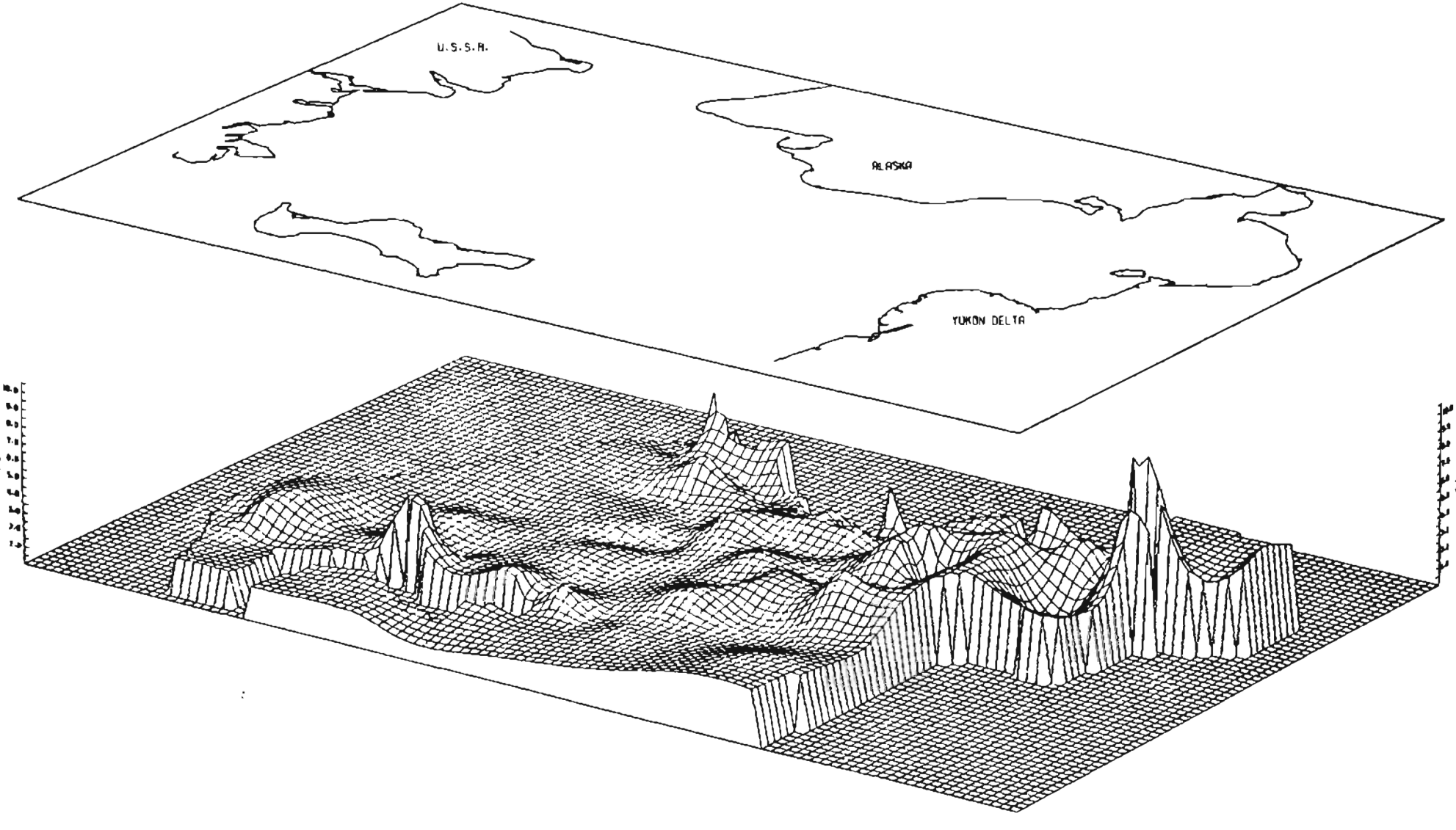

FIG 24 FE % IN BOTTOM SURFACE SEDIMENT OF NORTON BASIN, BERING SEA

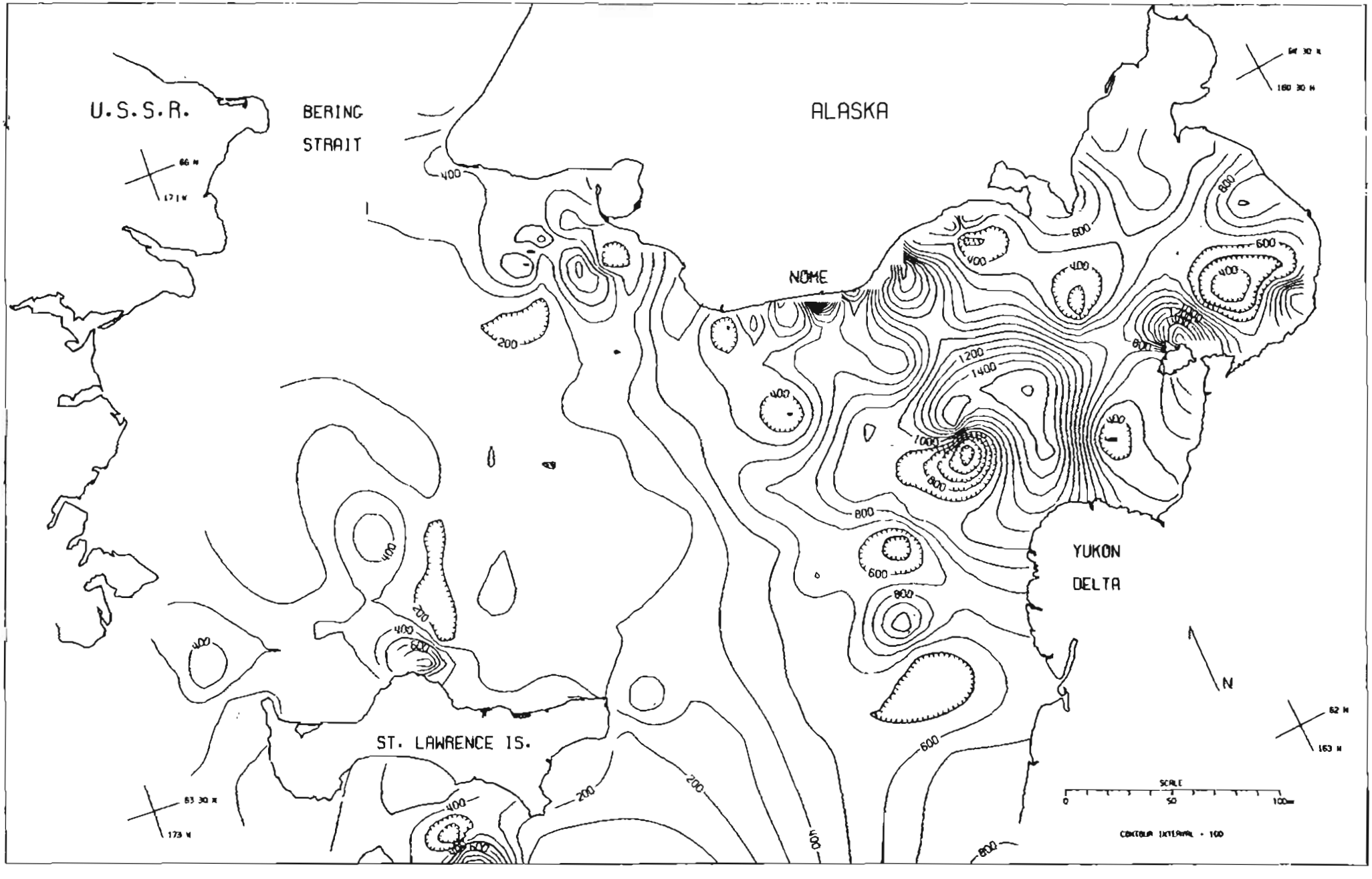

FIG 25 MN PPM IN BOTTOM SURFACE SEDIMENT OF NORTON BASIN, BERING SEA

NORTON BASIN PERSPECTIVE VIEW

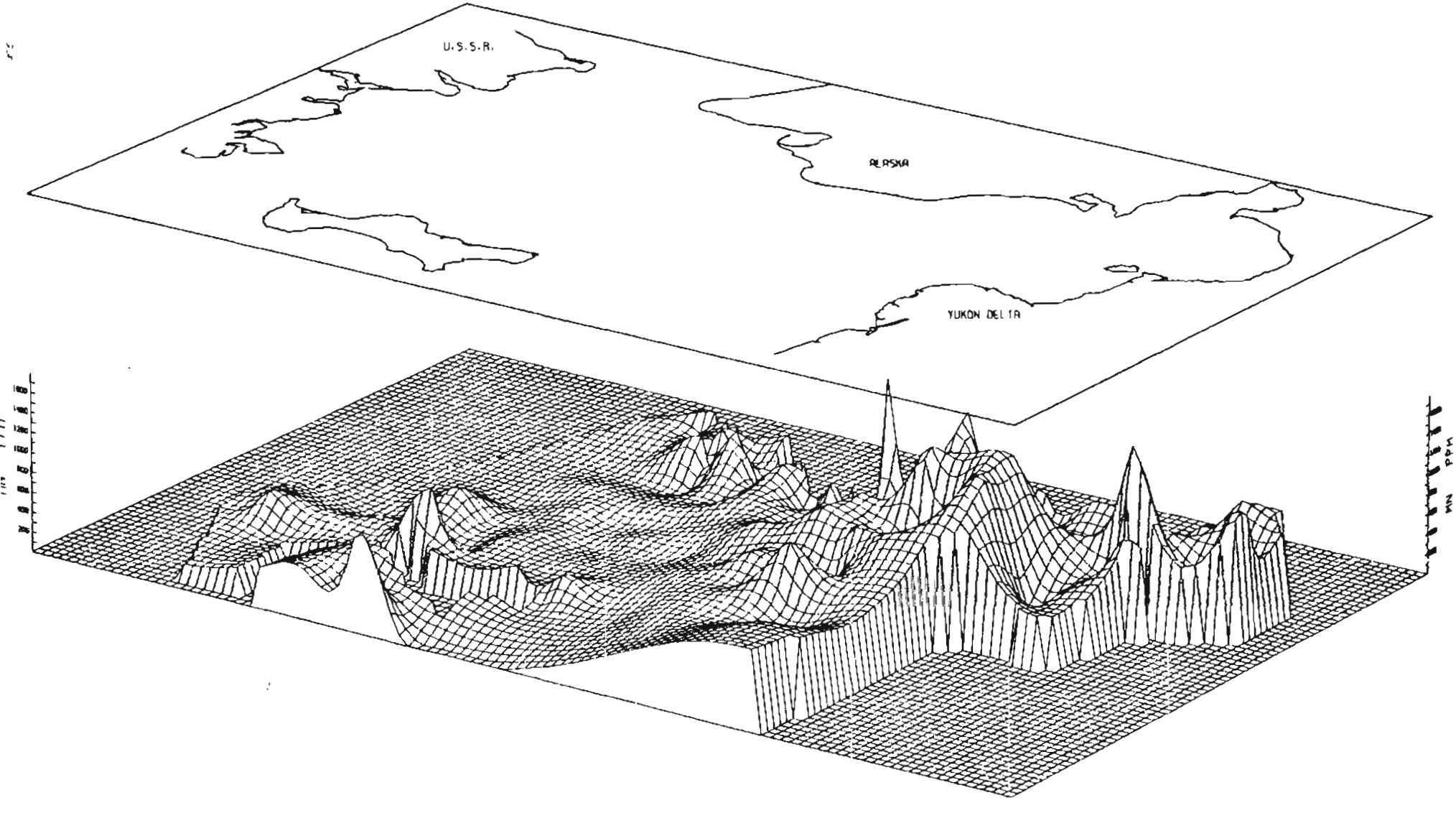

FIG 26 MN PPM IN BOTTOM SURFACE SEDIMENT OF NORTON BASIN, BERING SEA

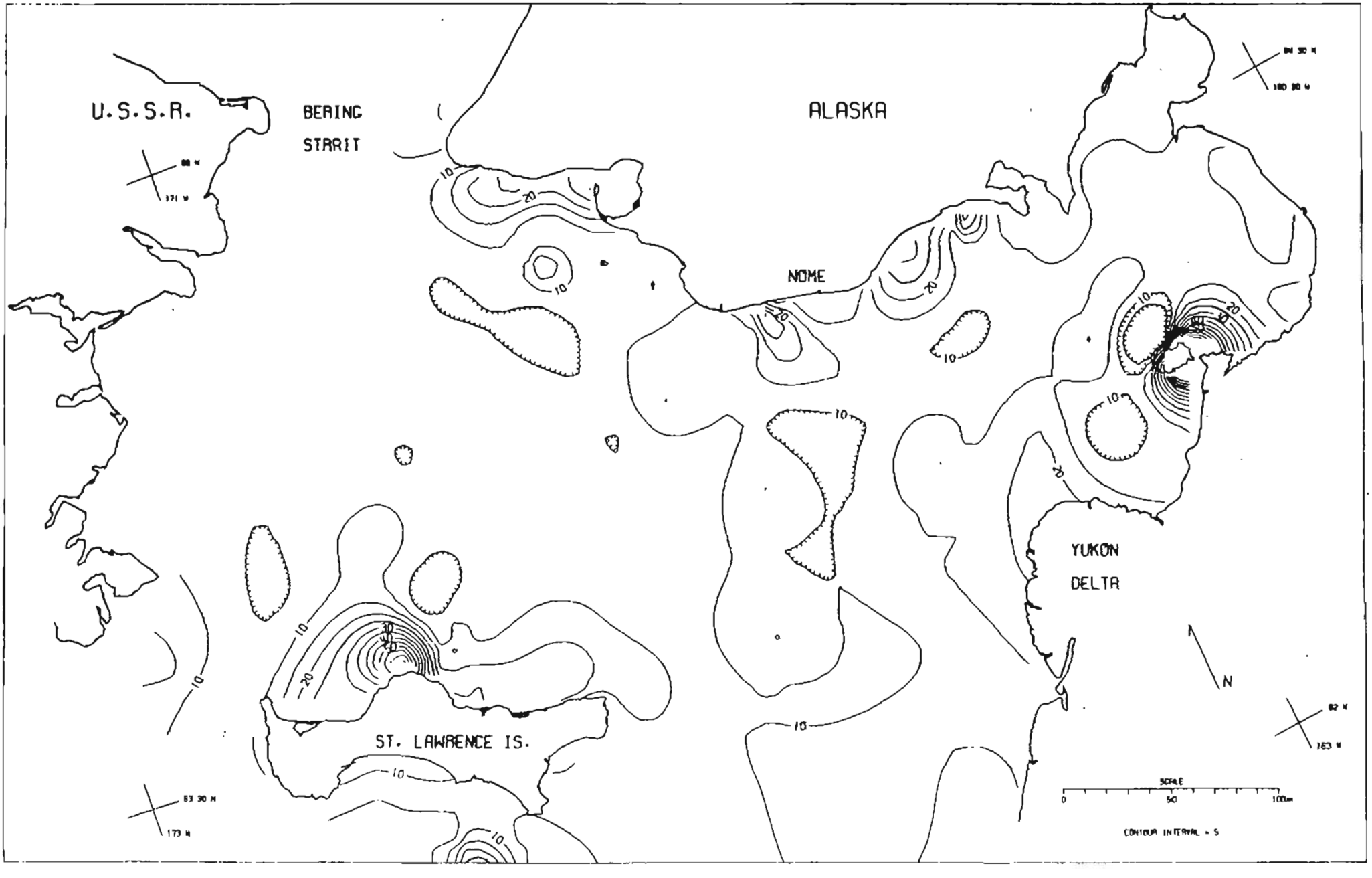

FIG 27 CO PPM IN BOTTOM SURFACE SEDIMENT OF NORTON BASIN, BERING SEA

NORTON BASIN PERSPECTIVE VIEW

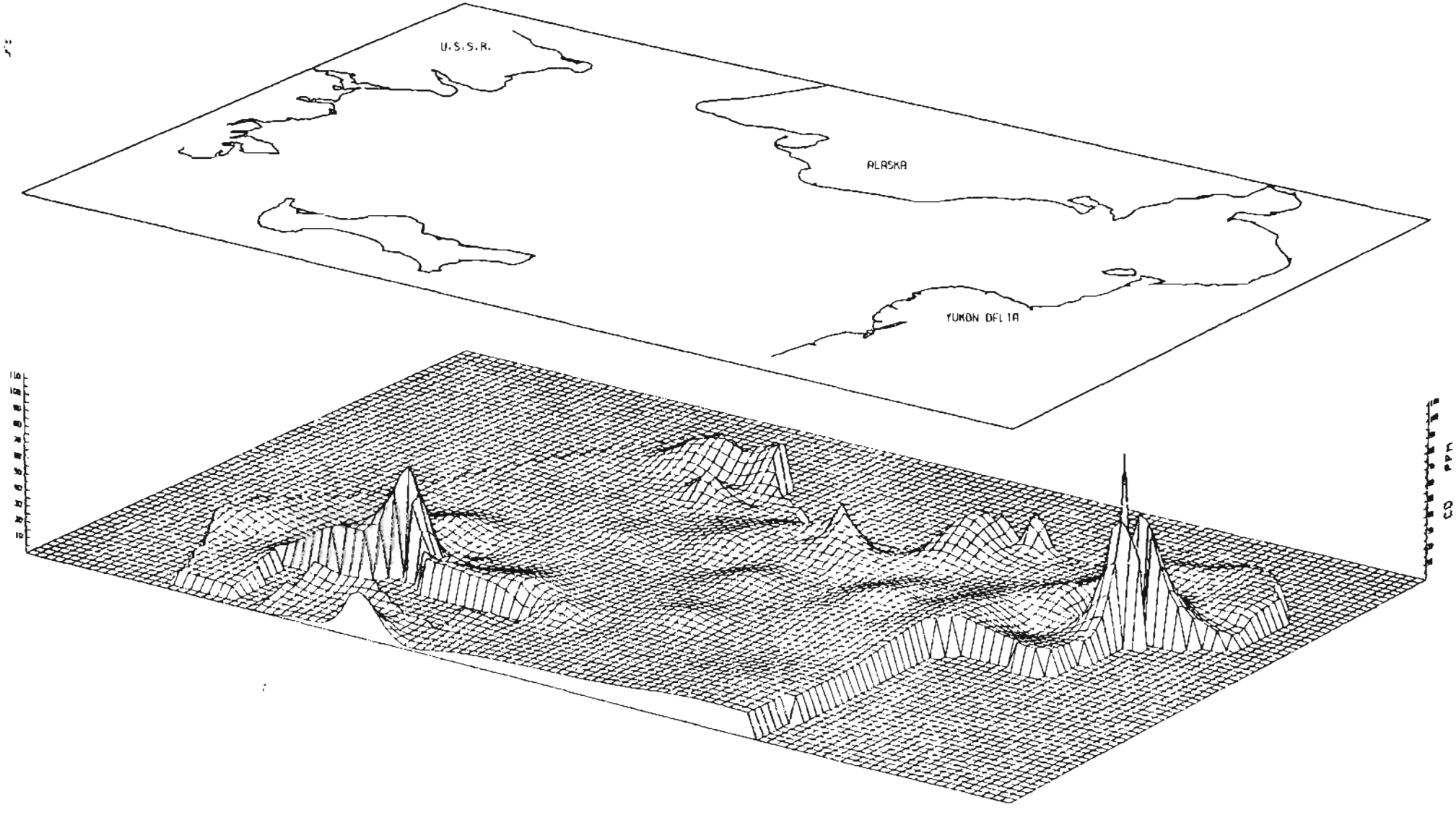

FIG 28 CO PPM IN BOTTOM SURFACE SEDIMENT OF NORTON BASIN, BERING SEA

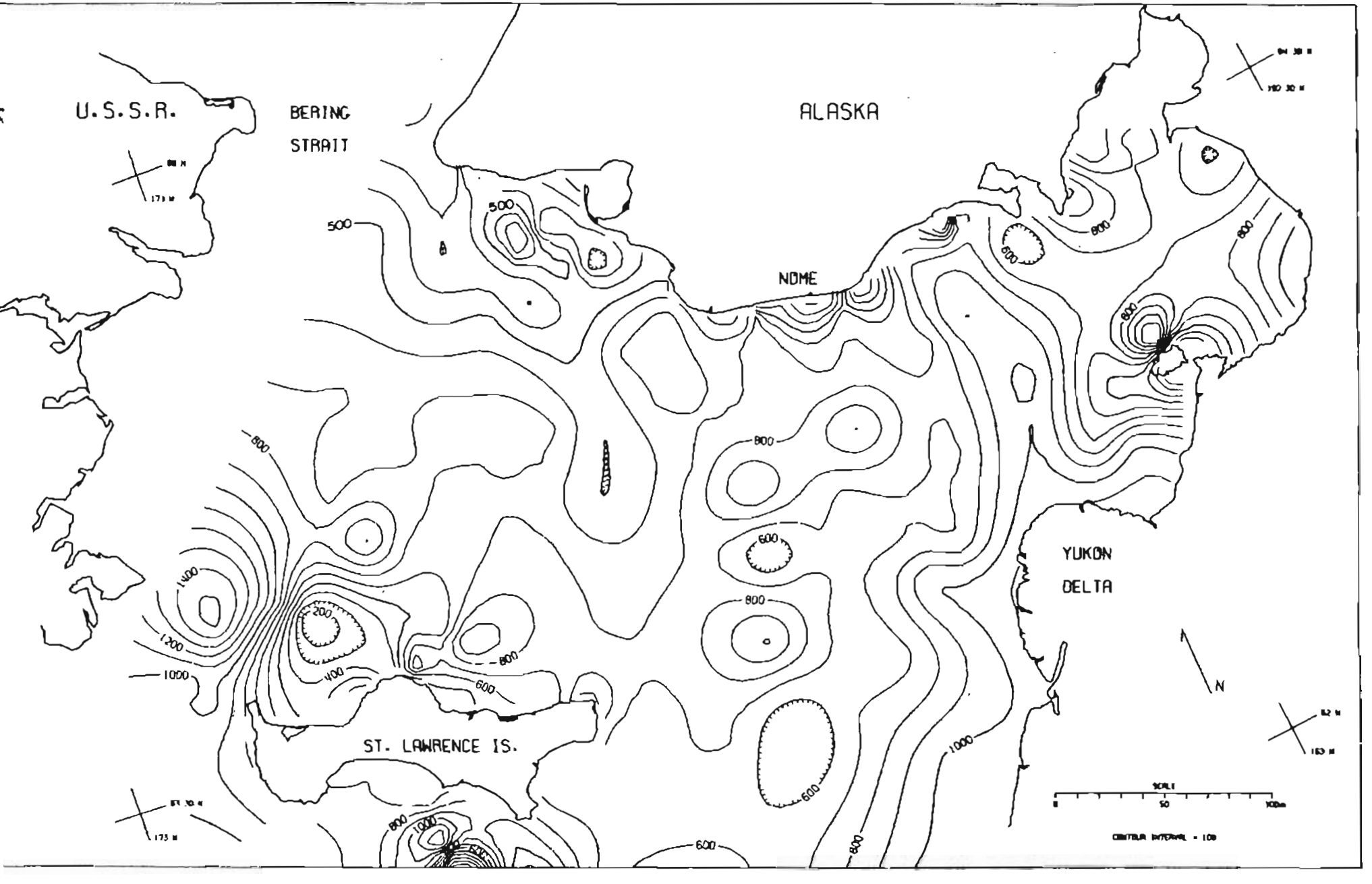

FIC 29 BA PPM IN BOTTOM SURFACE SEDIMENT OF NORTON BASIN, BERING SEA

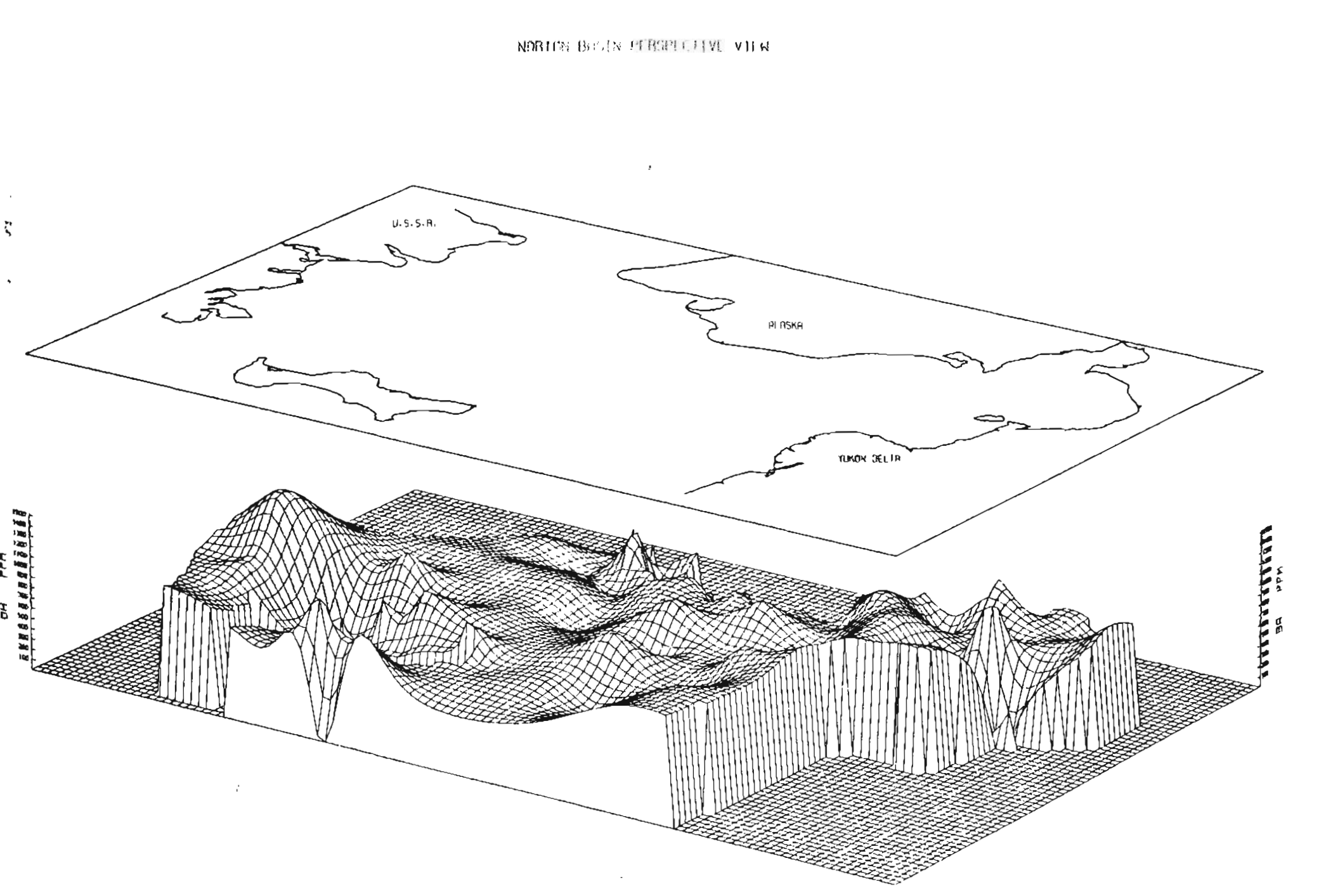

FIG 30 BA PPM IN BOTTOM SURFACE SEDIMENT OF NORTON BASIN, BERING SEA

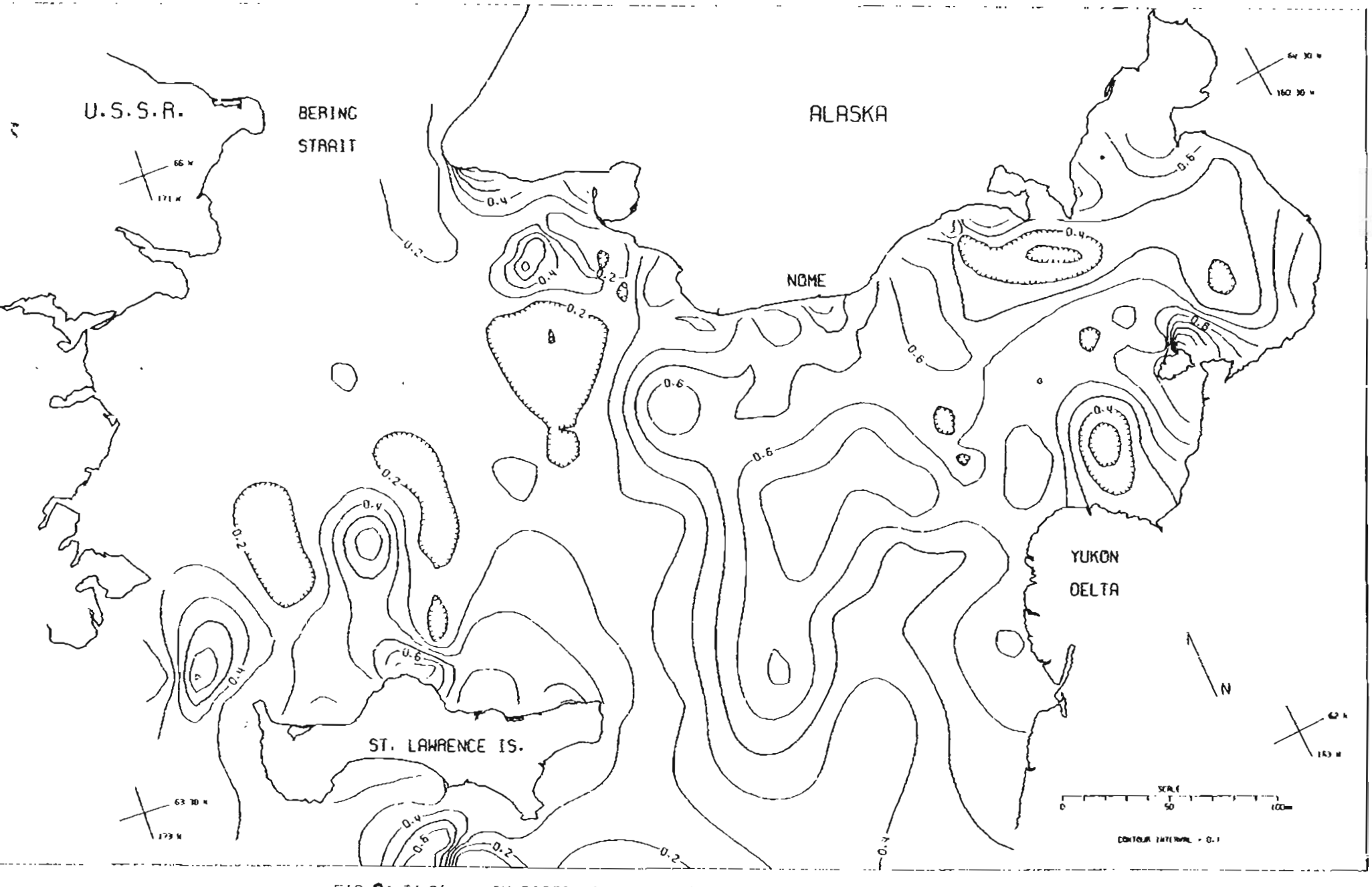

FIG 31 Ti % IN BOTTOM SURFACE SEDIMENT OF NORTON BASIN, BERING SEA

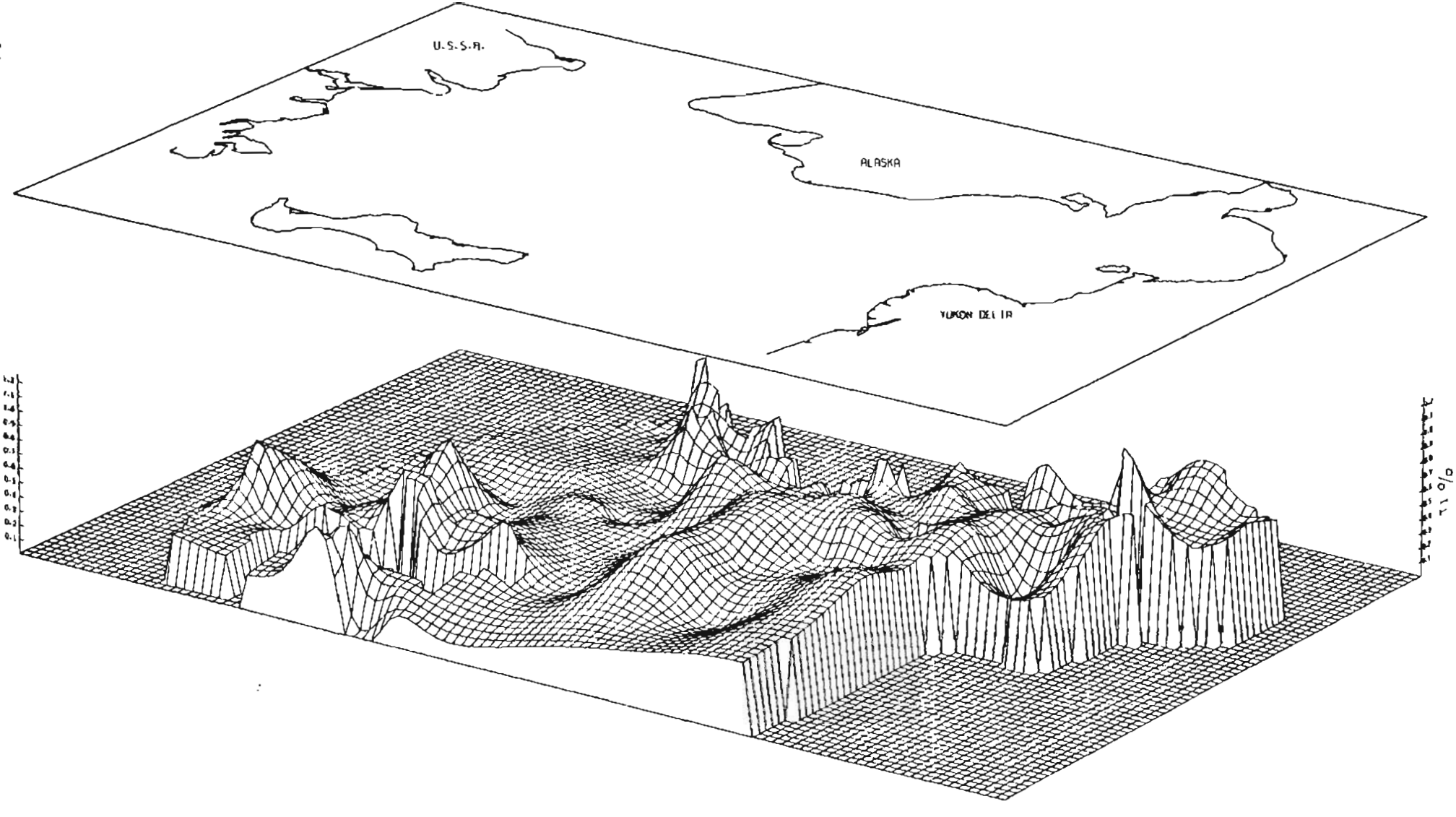

FIG 32 Ti % IN BOTTOM SURFACE SEDIMENT OF NORTON BASIN, BERING SEA

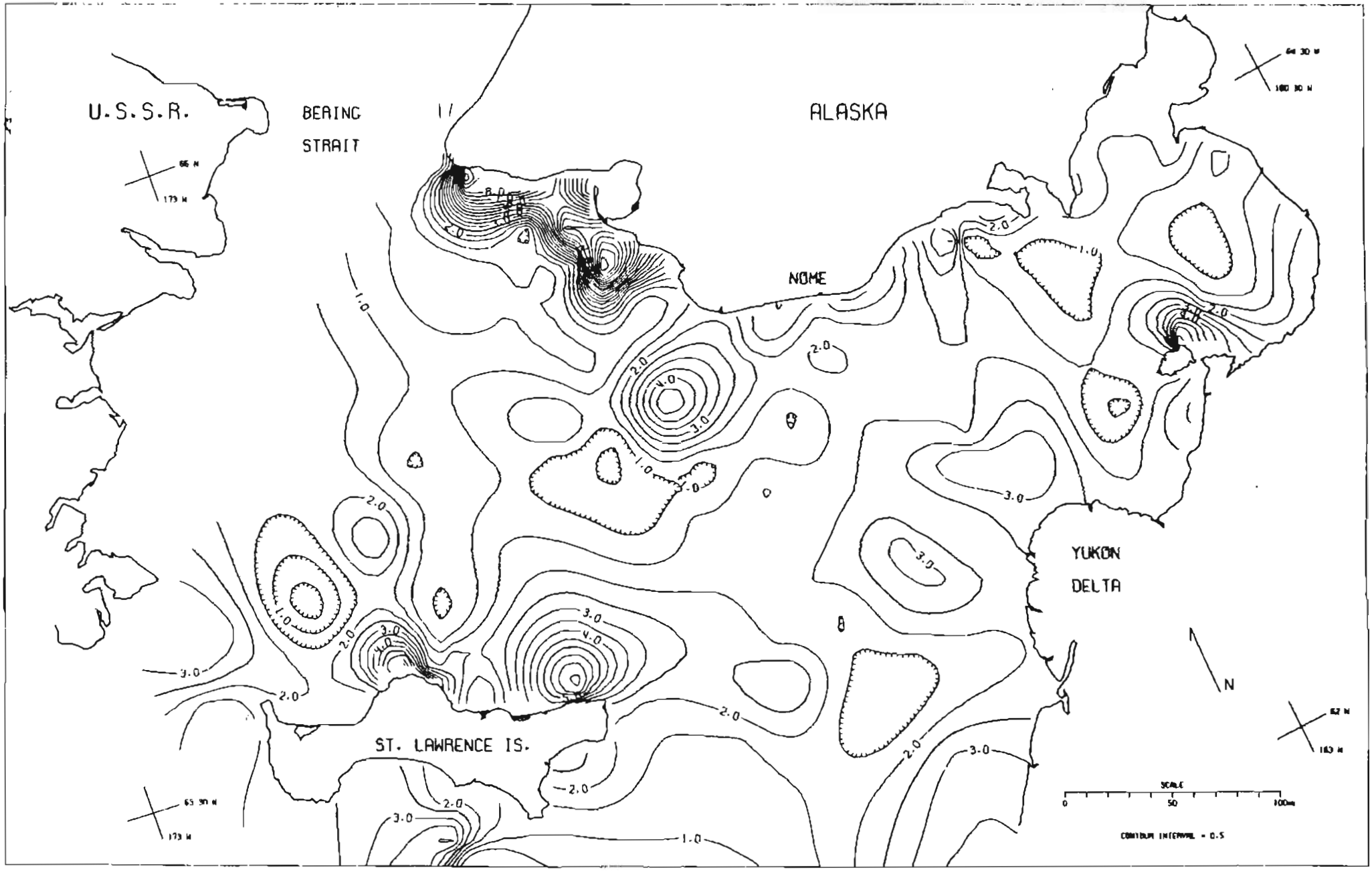

FIG 33 CA IN BOTTOM SURFACE SEDIMENT OF NORTON BASIN, BERING SEA

NORTON BASIN PERSPECTIVE VIEW

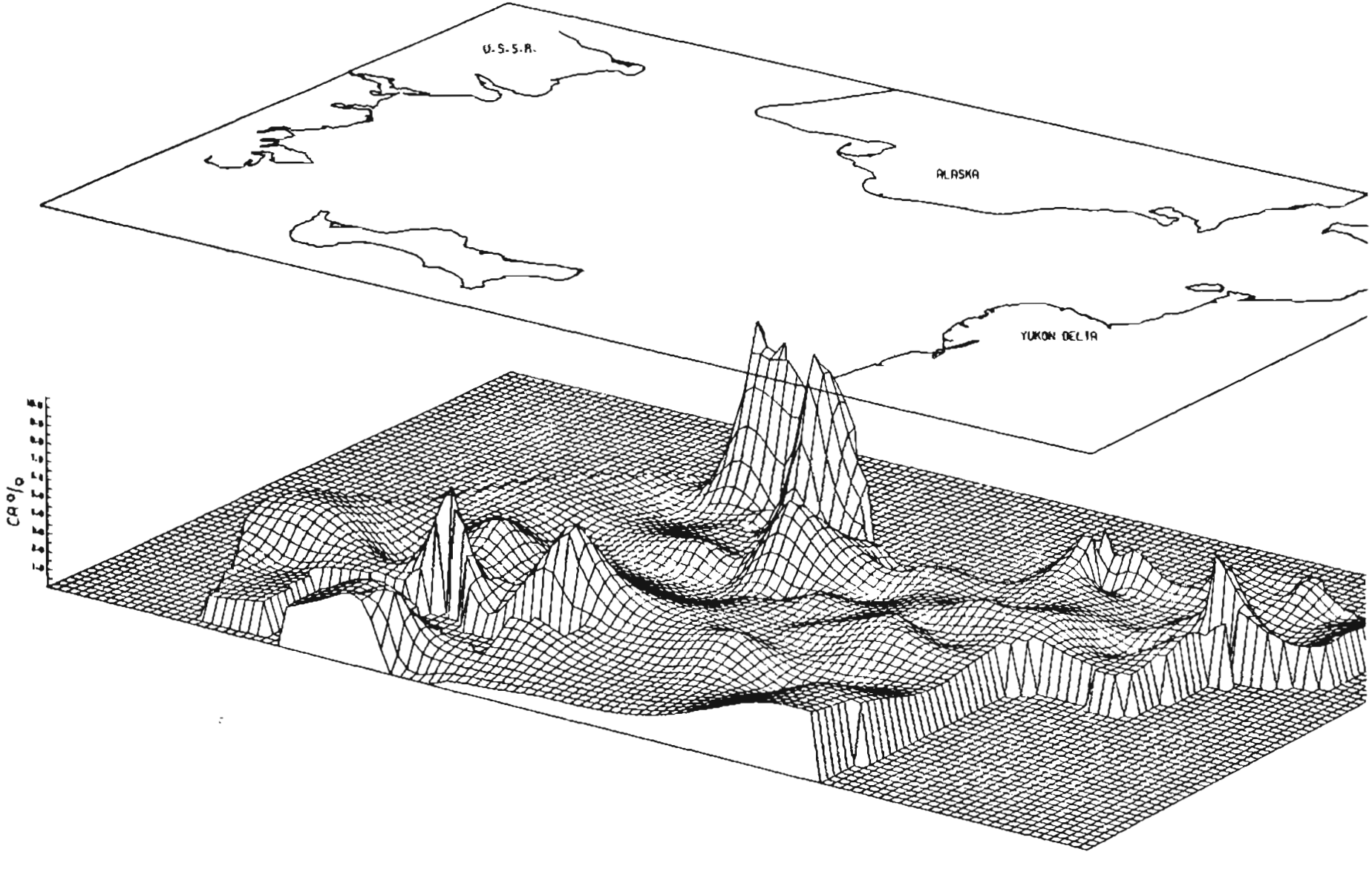

FIG 34 CA % IN BOTTOM SURFACE SEDIMENT OF NORTON BASIN, BERING SEA

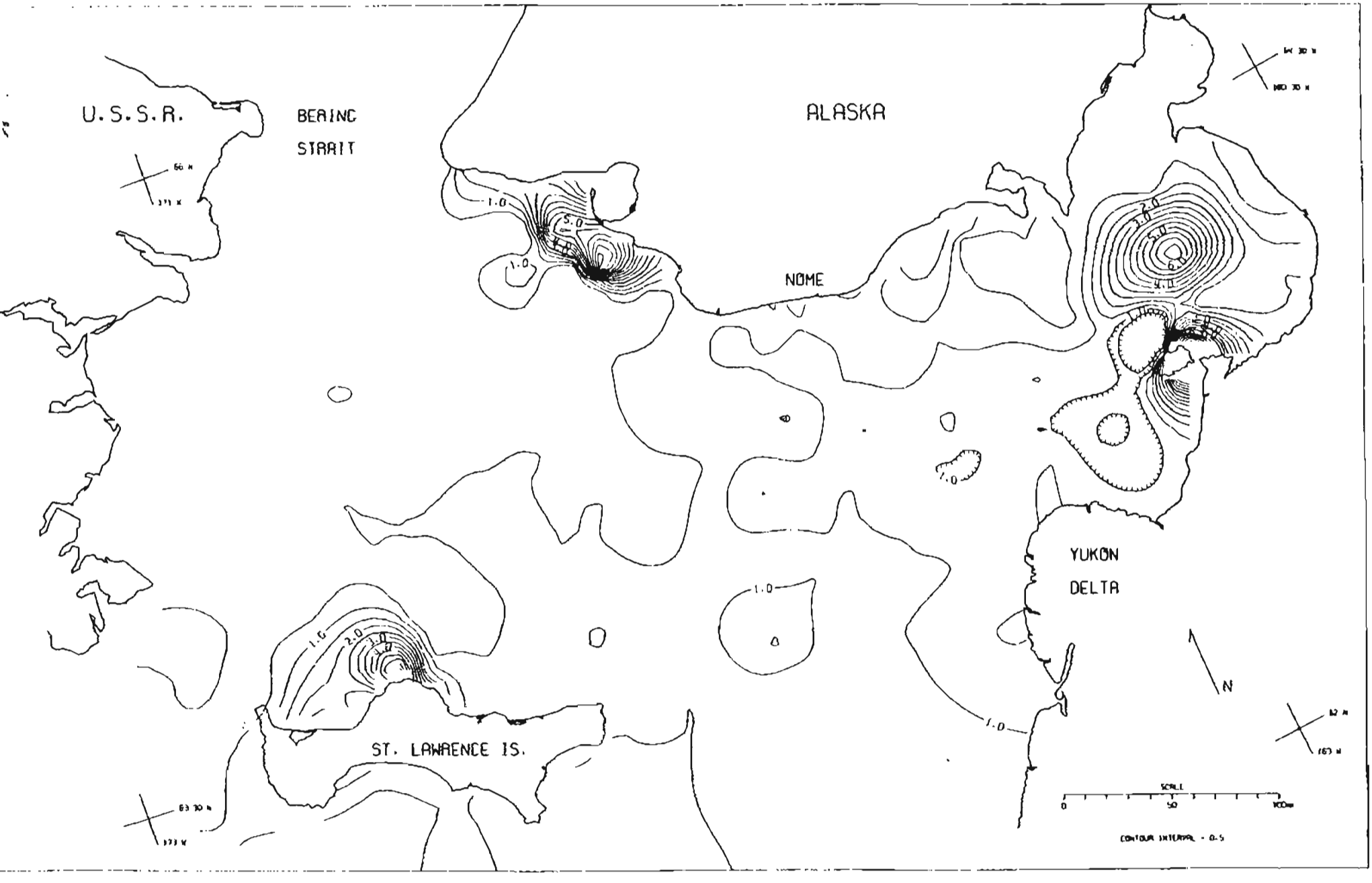

FIG 35 MC % IN BOTTOM SURFACE SEDIMENT OF NORTON BASIN, BERING SEA

NORTON BASIN PERSPECTIVE VIEW

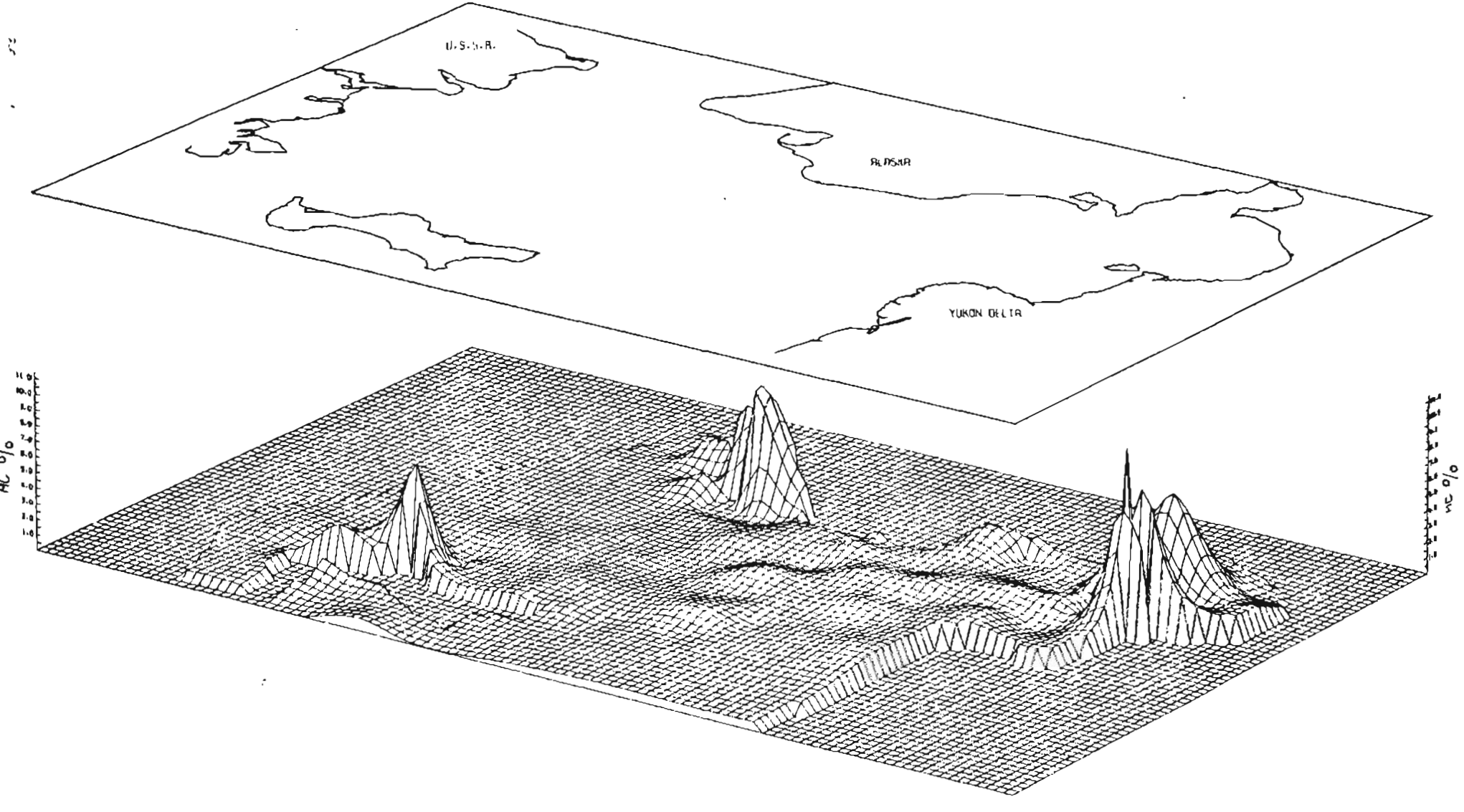

FIG 36 MC % IN BOTTOM SURFACE SEDIMENT OF NORTON BASIN, BERING SEA

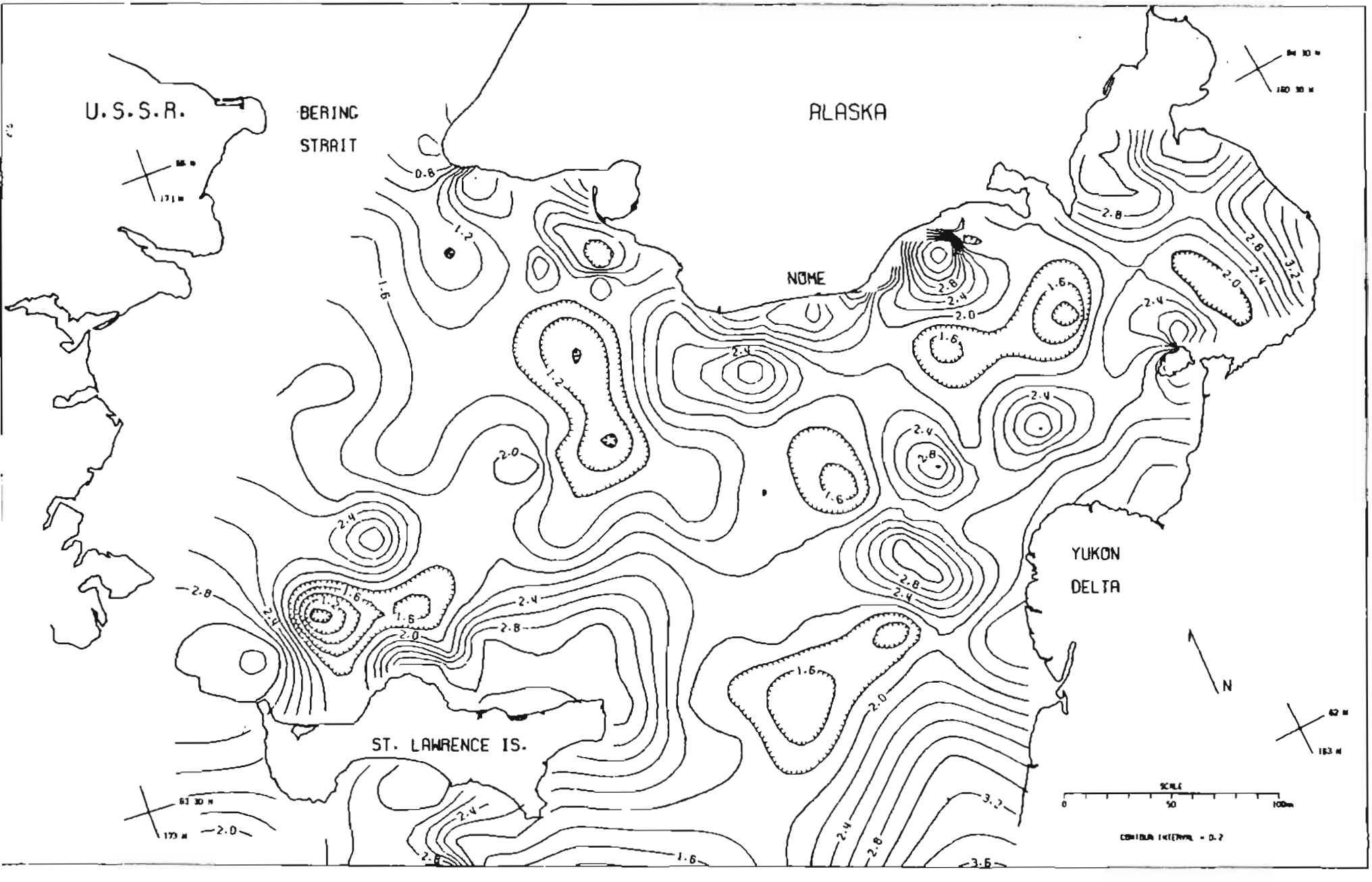

FIG 37 NR % IN BOTTOM SURFACE SEDIMENT OF NORTON BASIN, BERING SEA

NORTON BASIN PERSPECTIVE VIEW

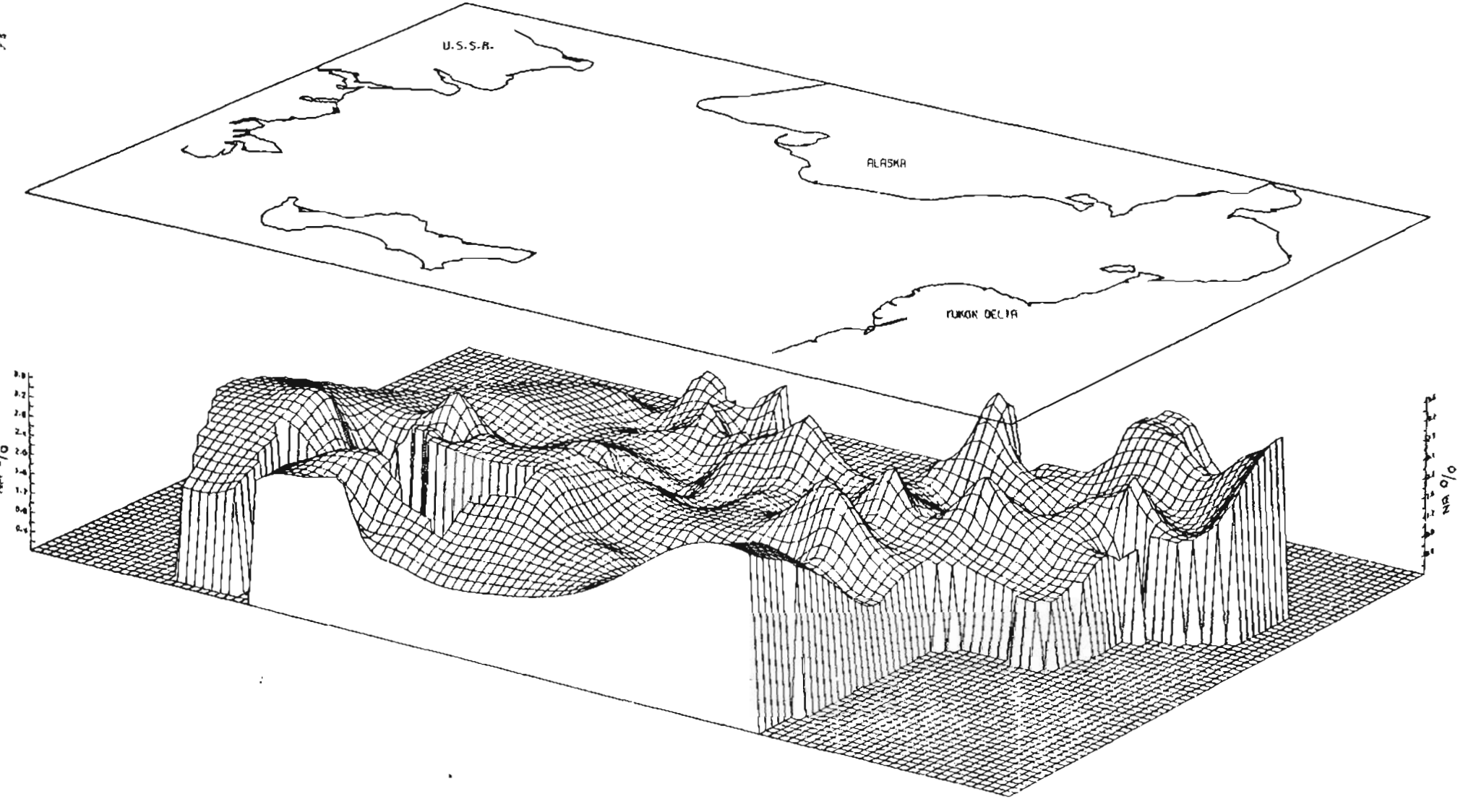

FIG 38 Na % IN BOTTOM SURFACE SEDIMENT OF NORTON BASIN, BERING SEA

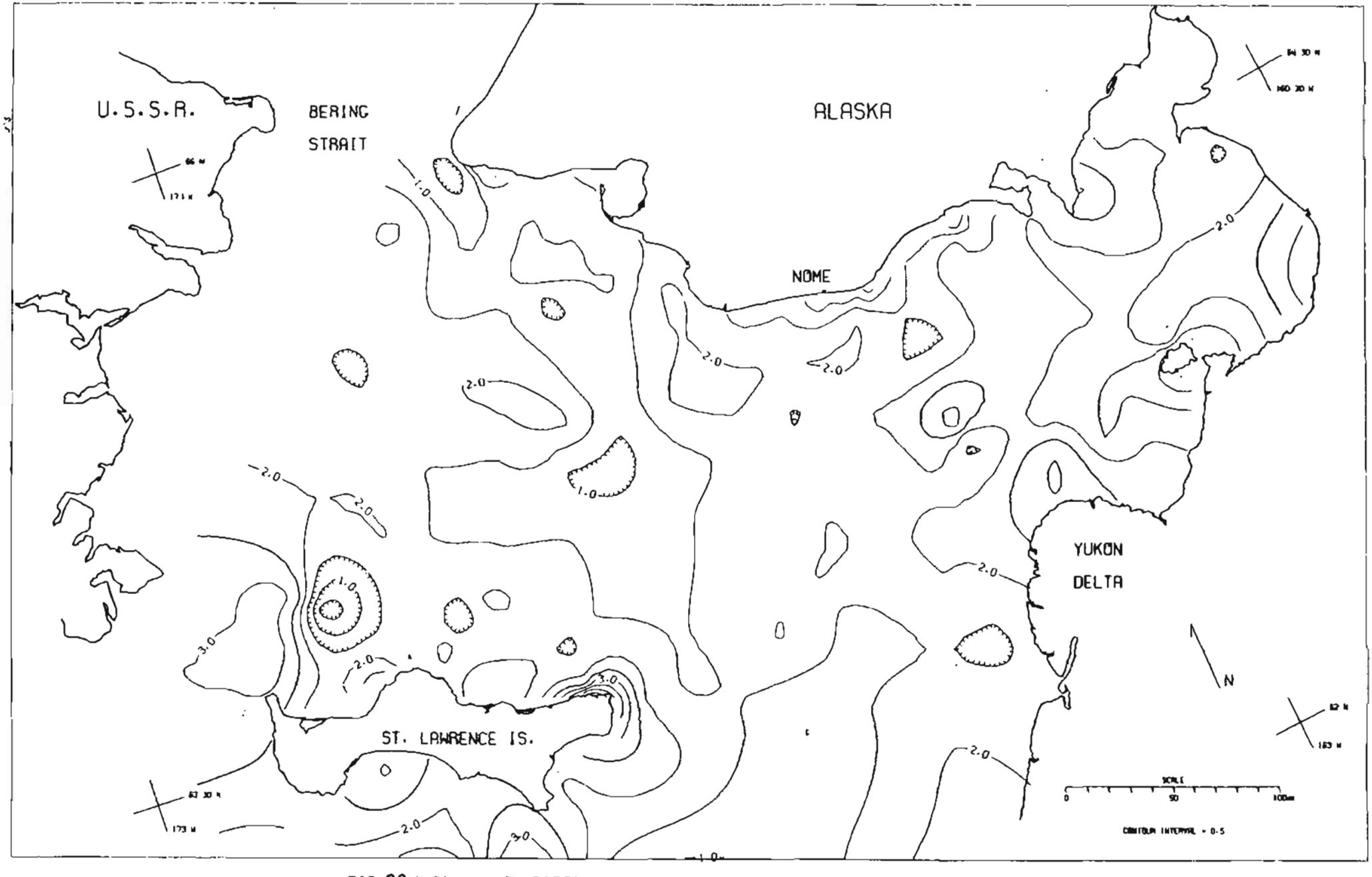

FIG 39 K % IN BOTTOM SURFACE SEDIMENT OF NORTON BASIN, BERING SEA

NORTON BASIN PERSPECTIVE VIEW

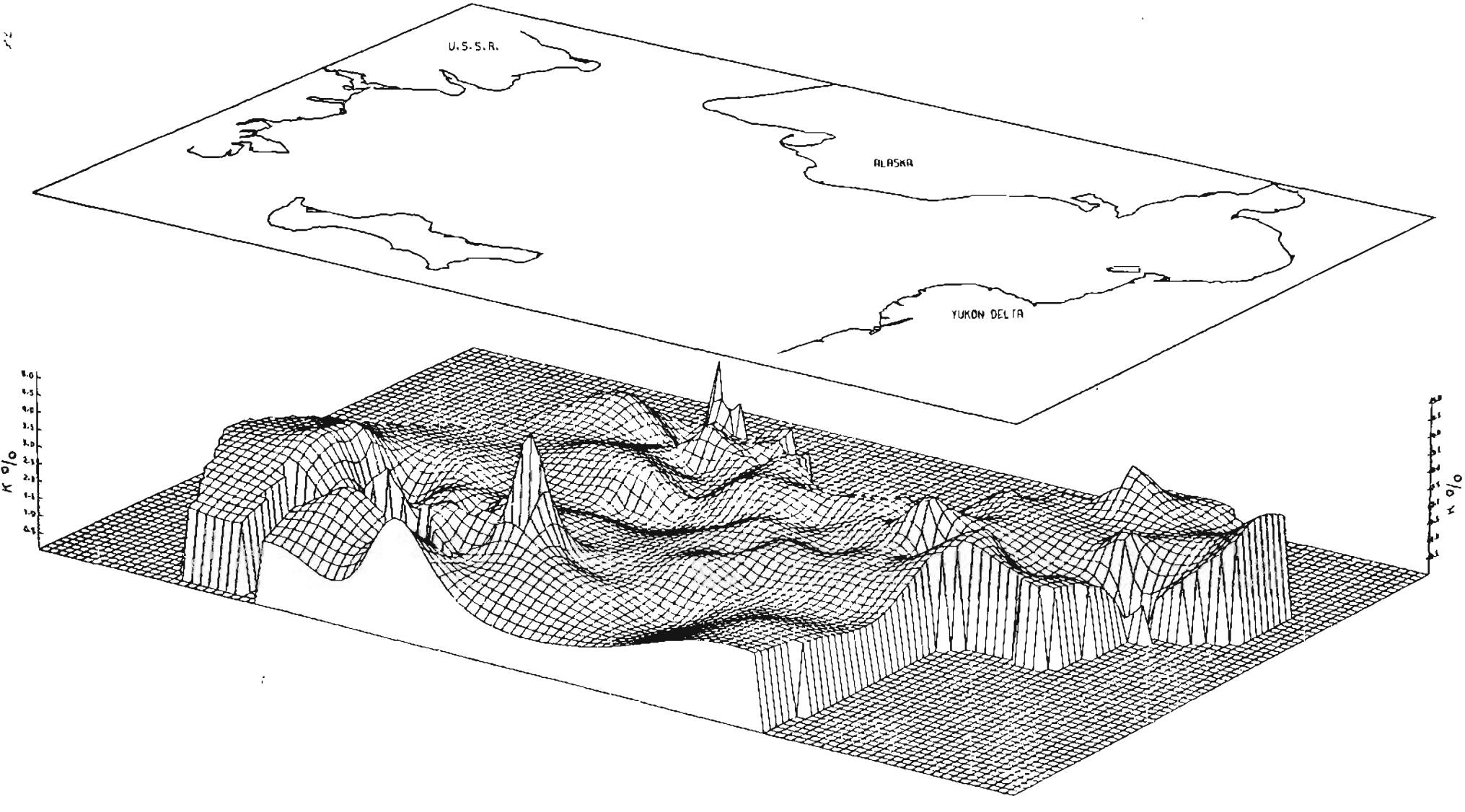

FIG 40 K % IN BOTTOM SURFACE SEDIMENT OF NORTON BASIN, BERING SEA

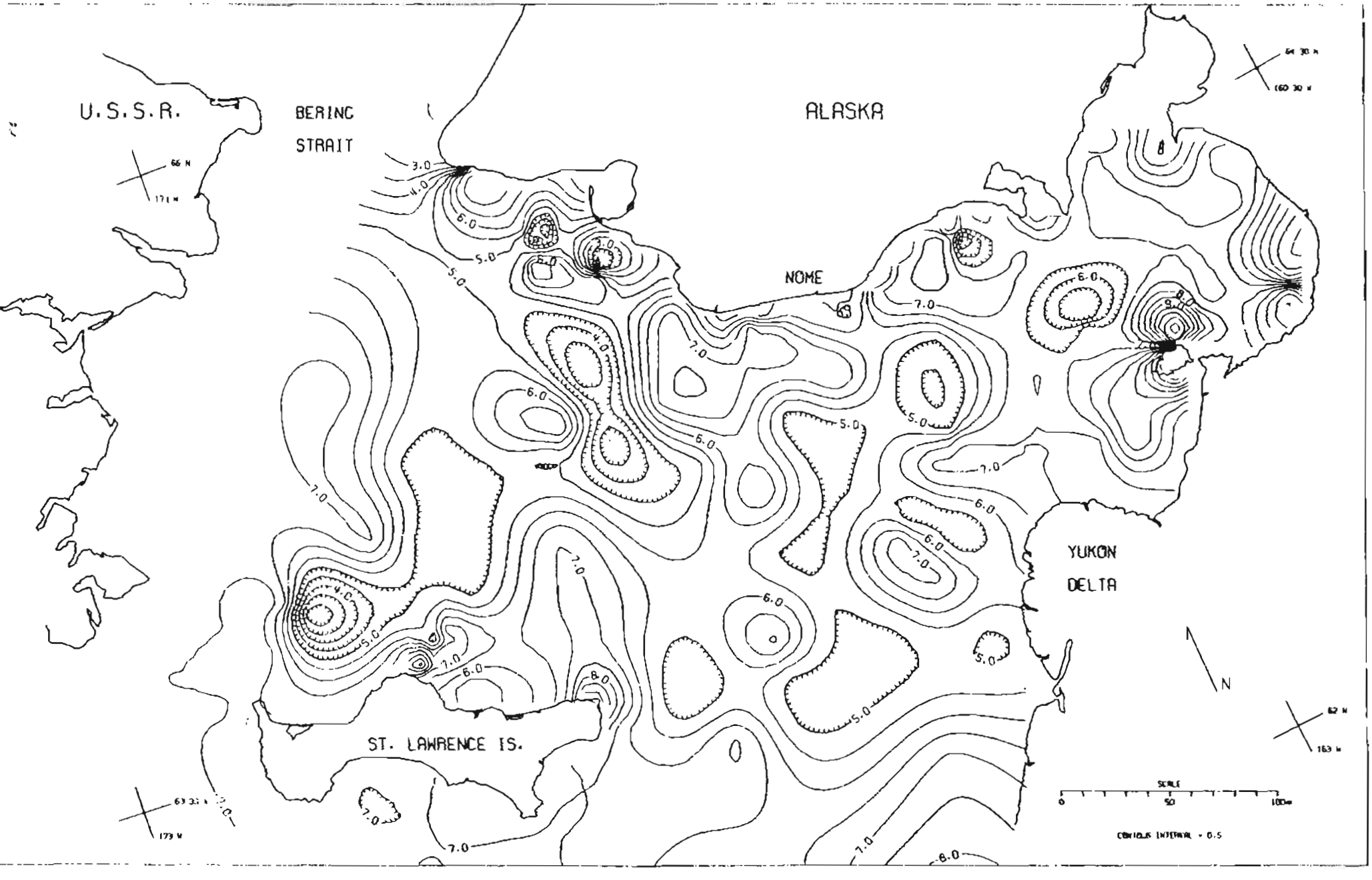

FIG 41 AL % IN BOTTOM SURFACE SEDIMENT OF NORTON BASIN, BERING SEA

NORTON BASIN PERSPECTIVE VIEW

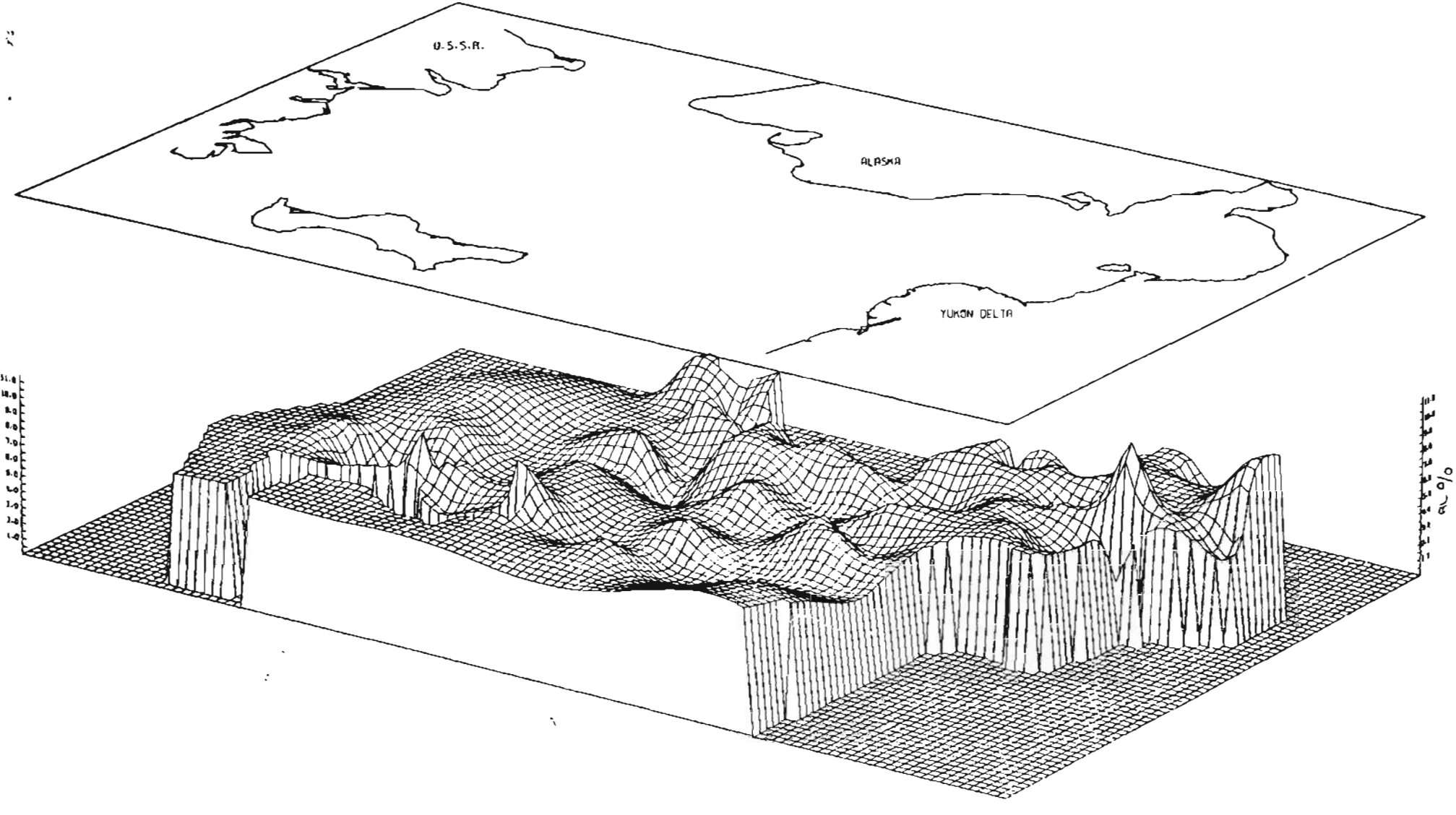

FIG 42 AL% IN BOTTOM SURFACE SEDIMENT OF NORTON BASIN, BERING SEA

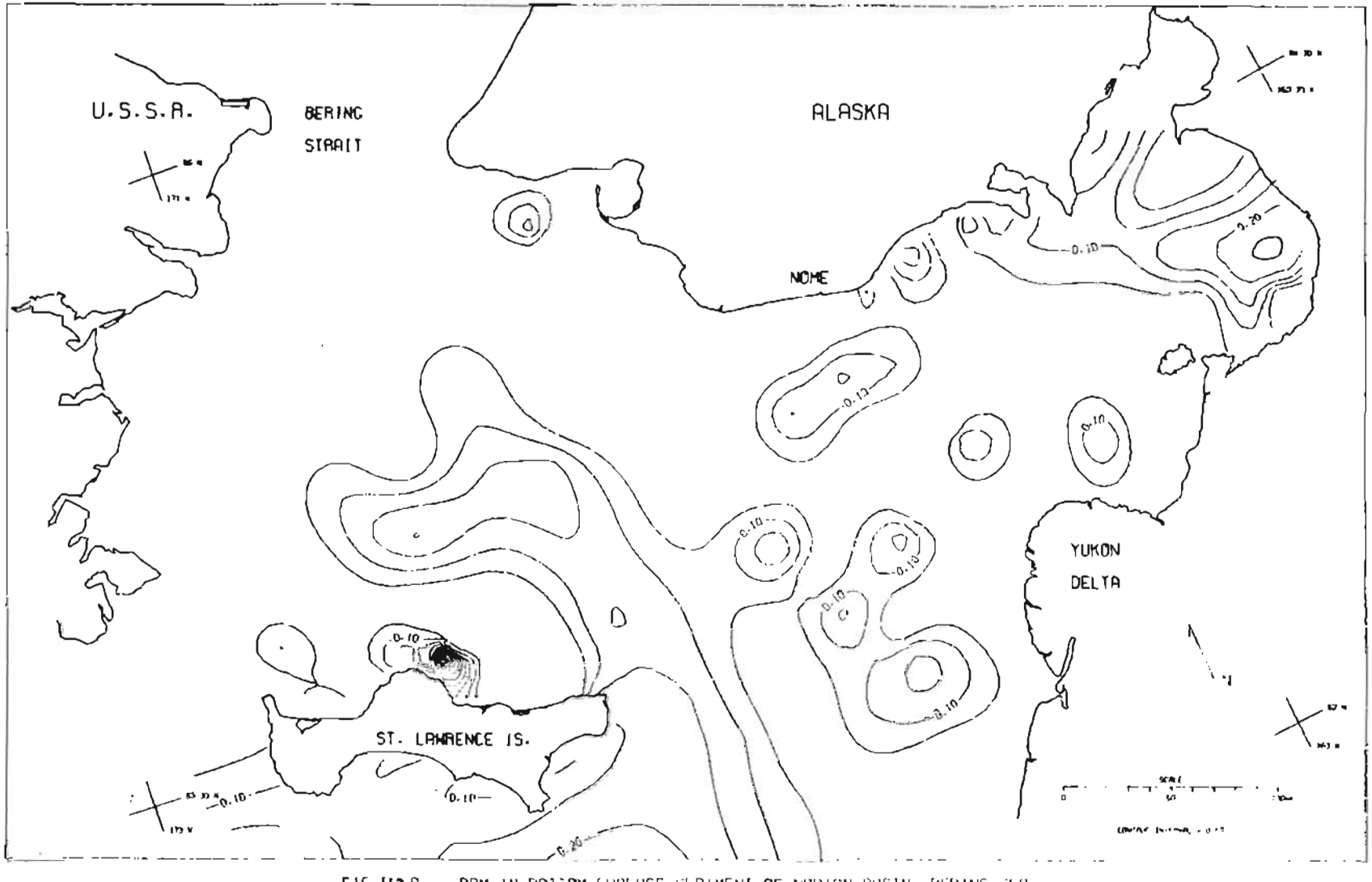

FIG 43 P PPM IN BOTTOM SURFACE SEDIMENT OF NORTON BASIN, BERING SEA

NORTON BASIN PERSPECTIVE VIEW

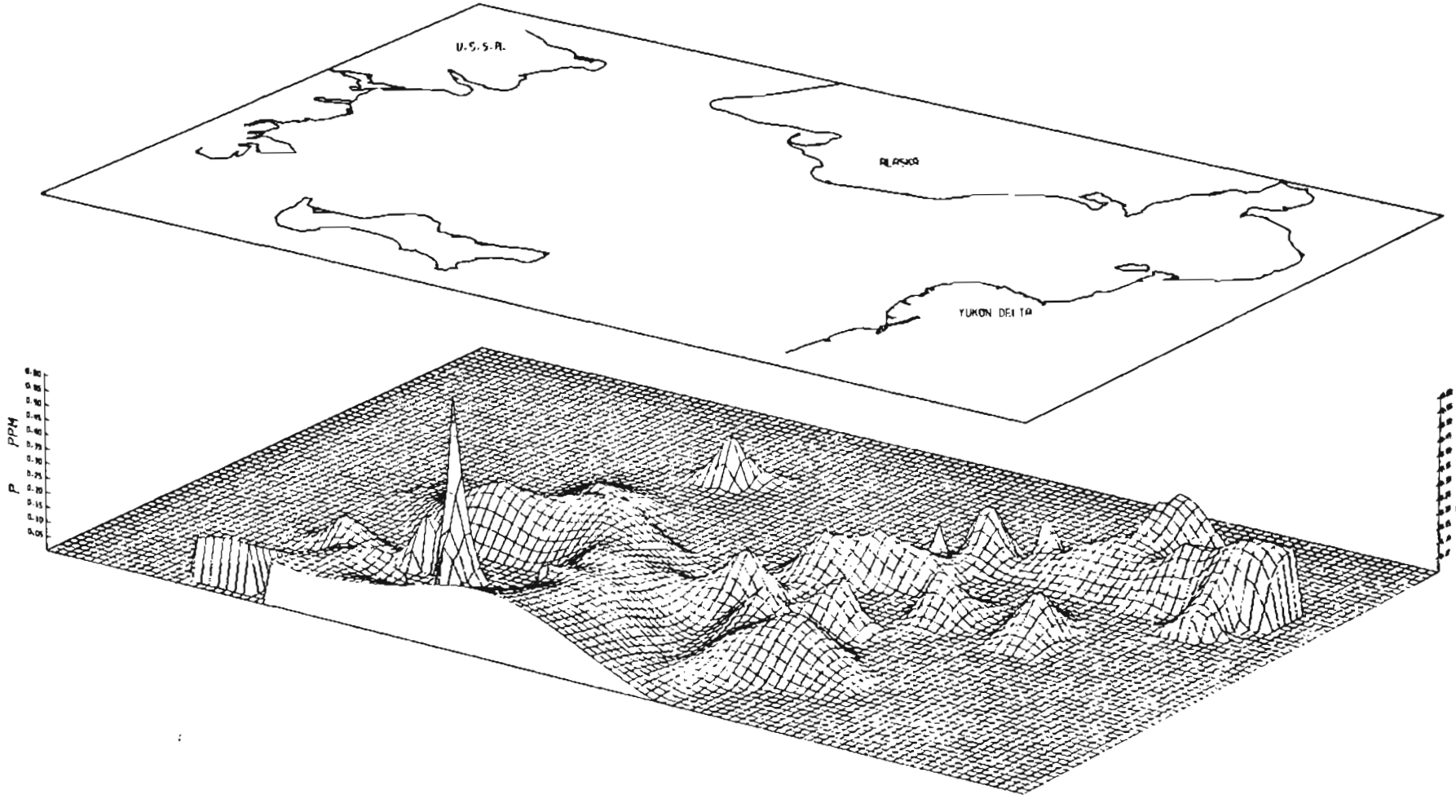

FIG 44 P PPM IN BOTTOM SURFACE SEDIMENT OF NORTON BASIN, BERING SEA

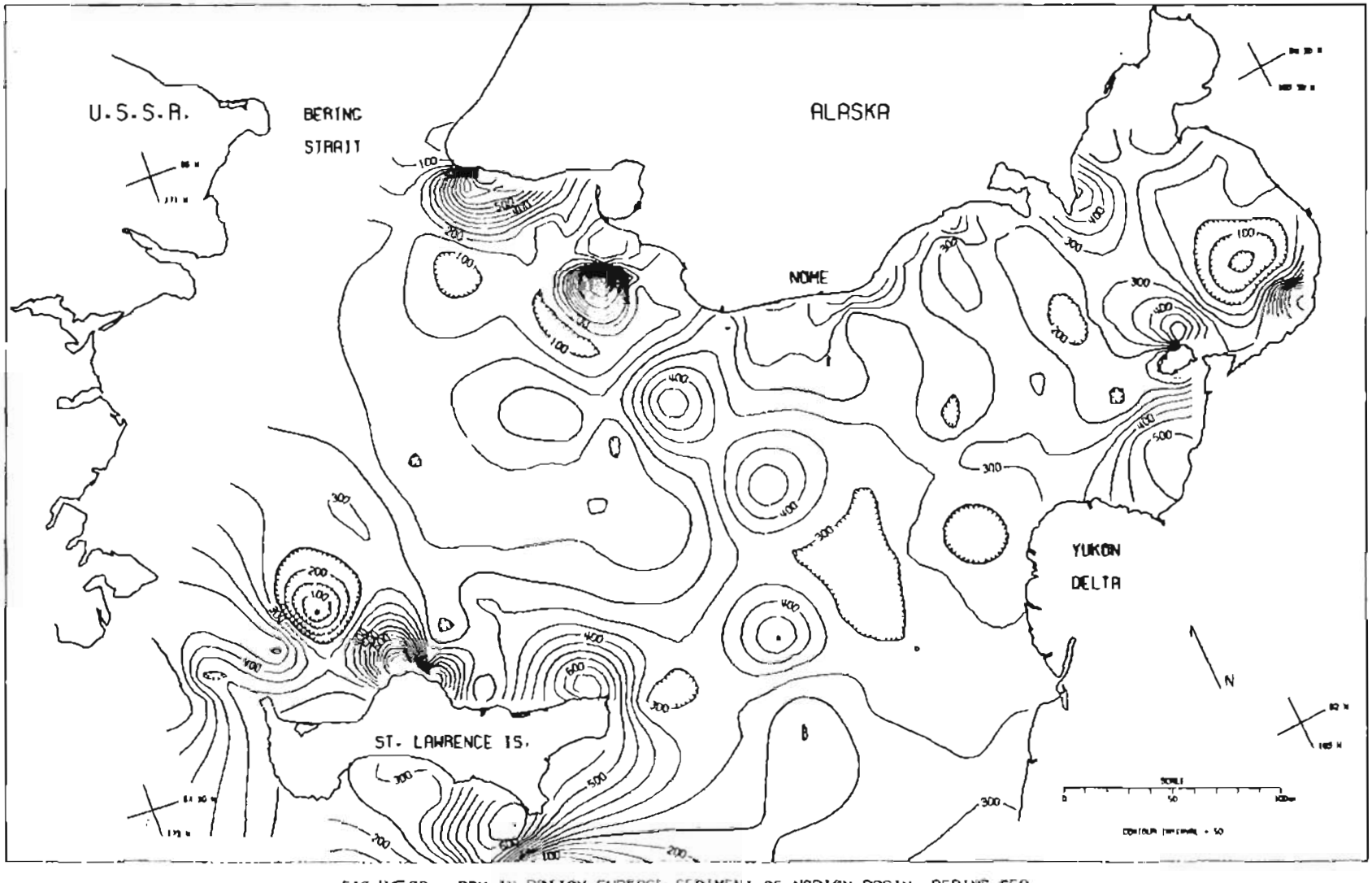

FIG 45 SR PPM IN BOTTOM SURFACE SEDIMENT OF NORTON BASIN, BERING SEA

NORTON BASIN PERSPECTIVE VIEW

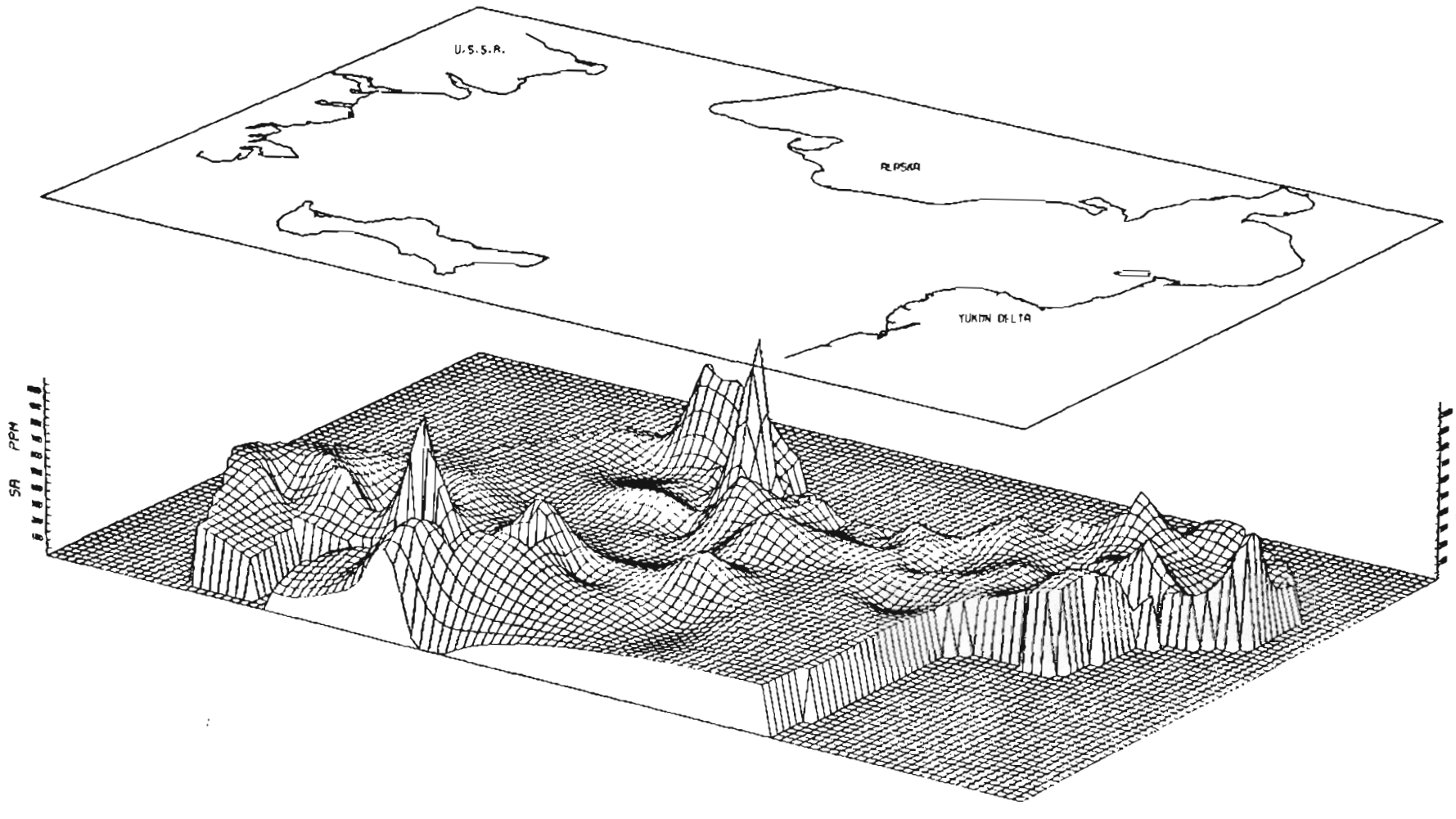

FIG 46 SR PPM IN BOTTOM SURFACE SEDIMENT OF NORTON BASIN, BERING SEA

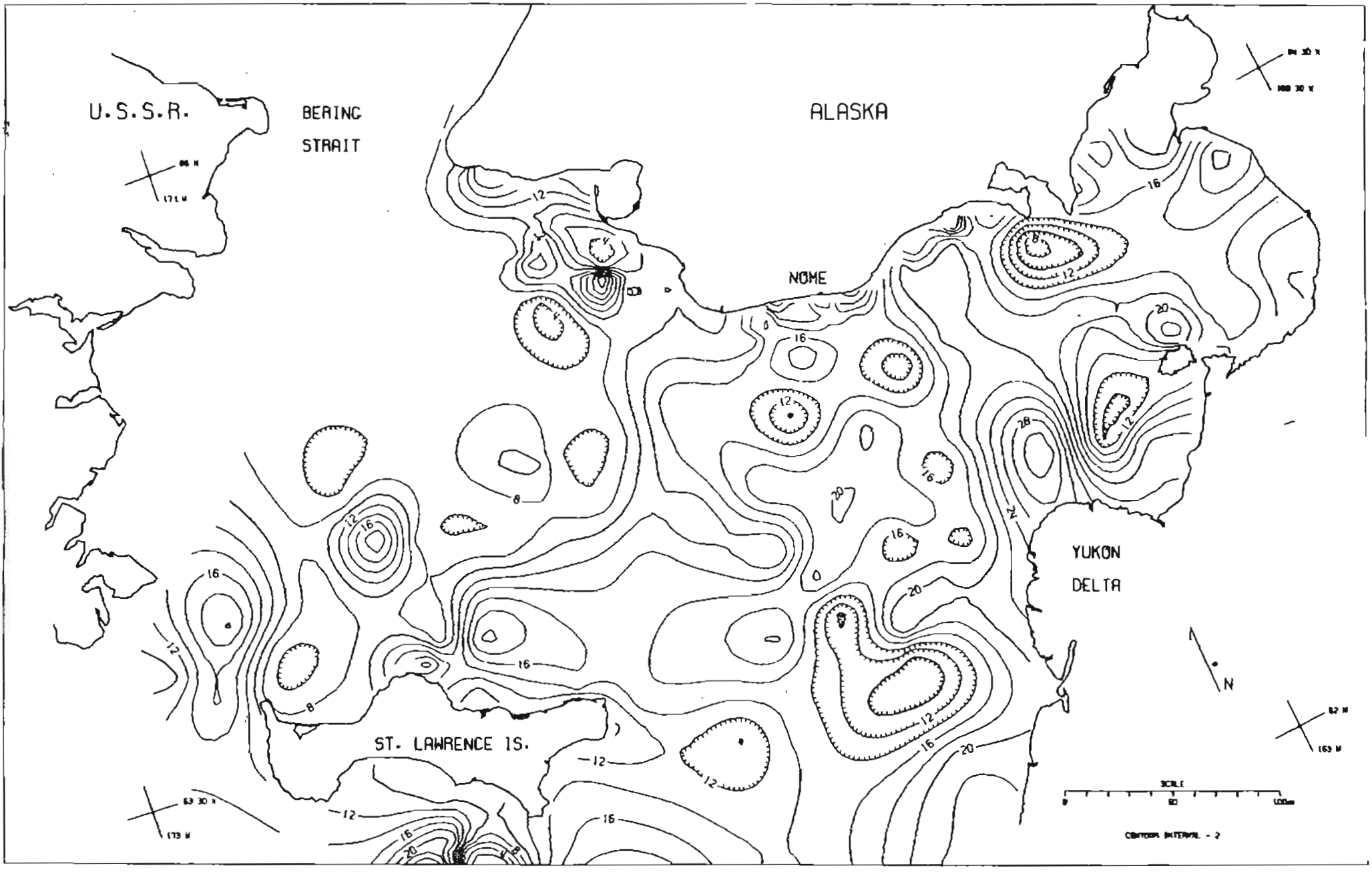

FIG 47 SC PPM IN BOTTOM SURFACE SEDIMENT OF NORTON BASIN, BERING SEA

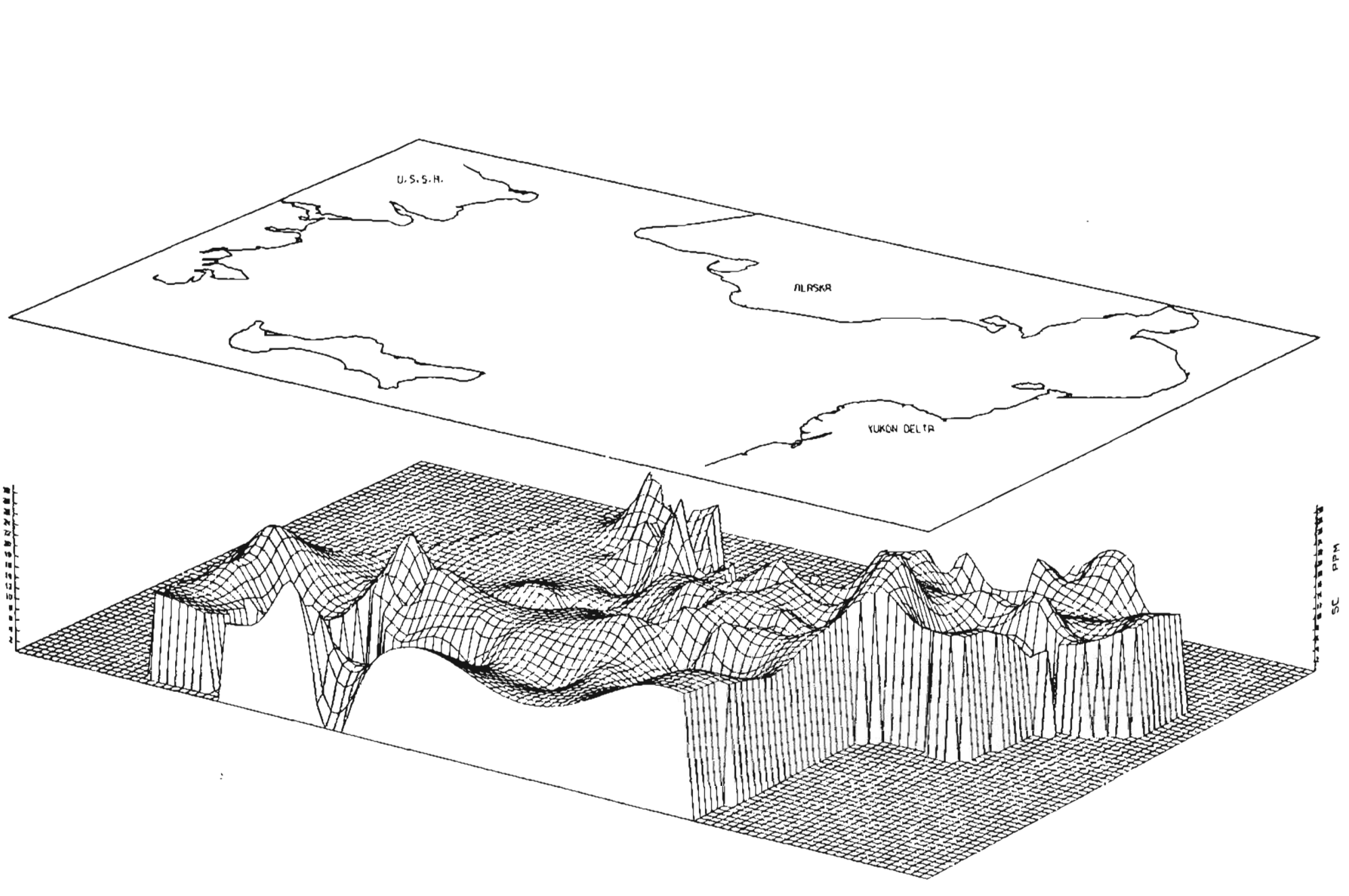

FIG 48 SC PPM IN BOTTOM SURFACE SEDIMENT OF NORTON BASIN, BERING SEA

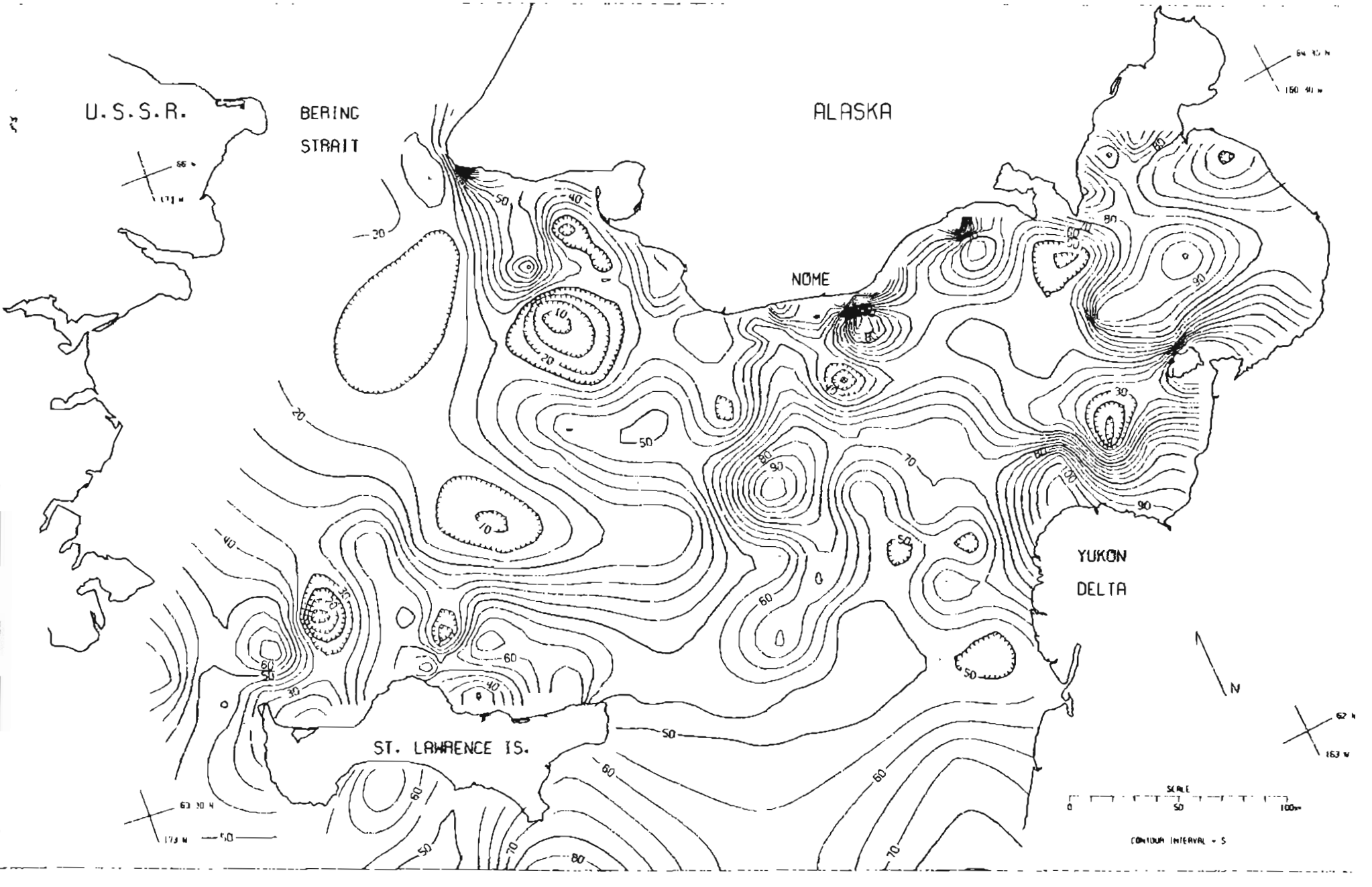

FIG 49 LA PPM IN BOTTOM SURFACE SEDIMENT OF NORTON BASIN, BERING SEA

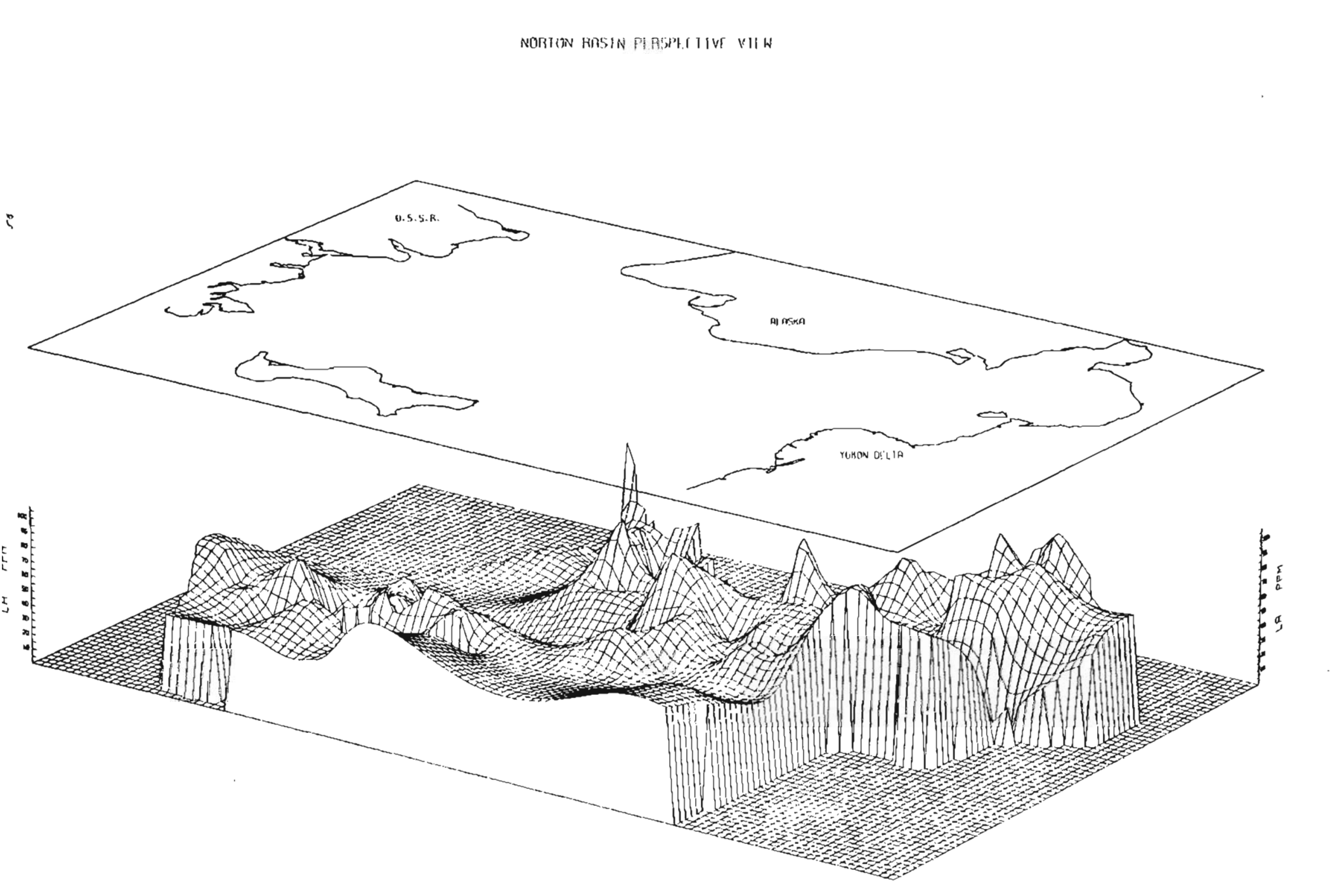

FIG 50 (A) PPM IN BOTTOM SURFACE SEDIMENT OF NORTON BASIN, BERING SEA

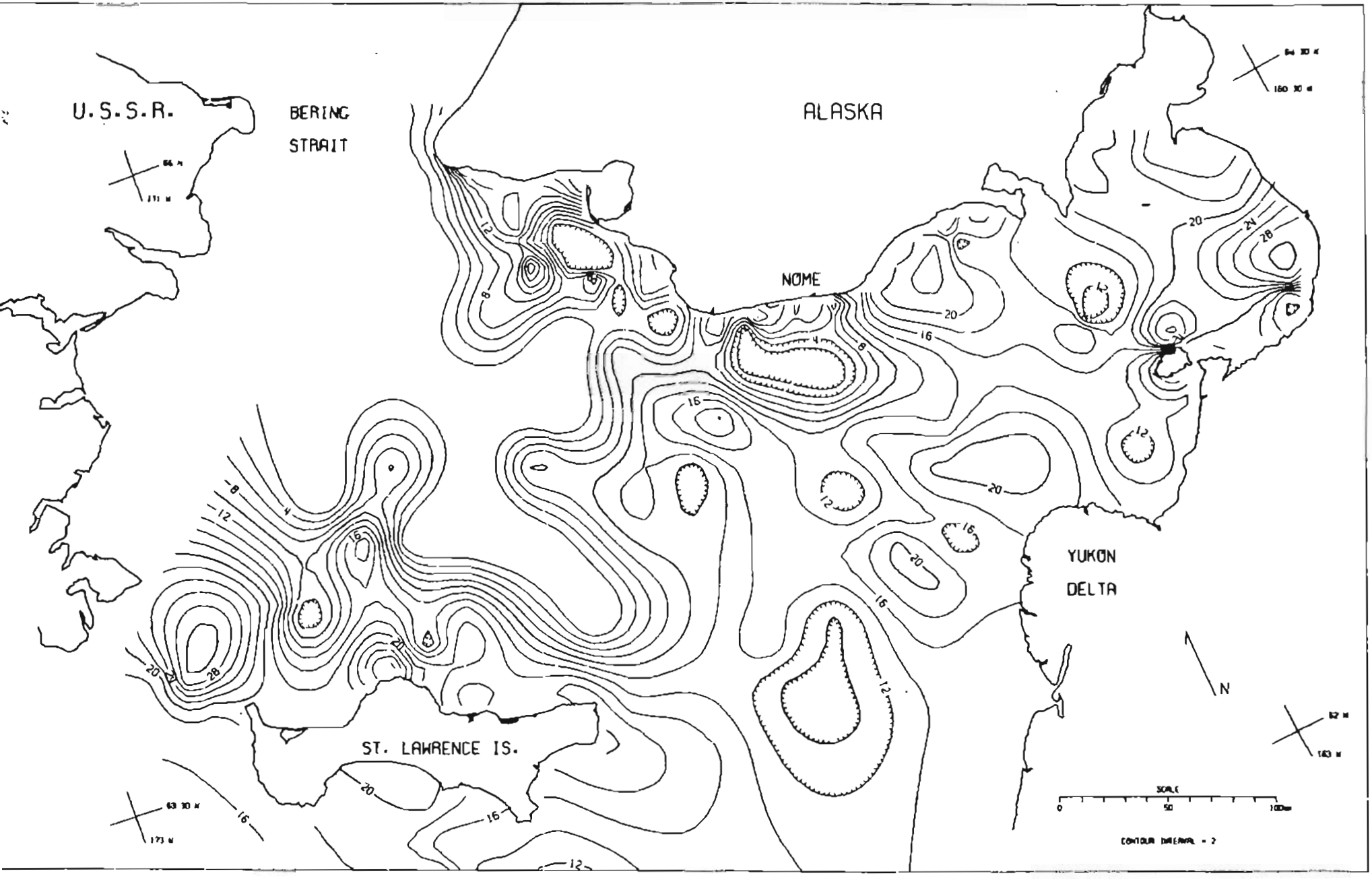

FIG 51 CA PPM IN BOTTOM SURFACE SEDIMENT OF NORTON BASIN, BERING SEA

NORTON BASIN PERSPECTIVE VIEW

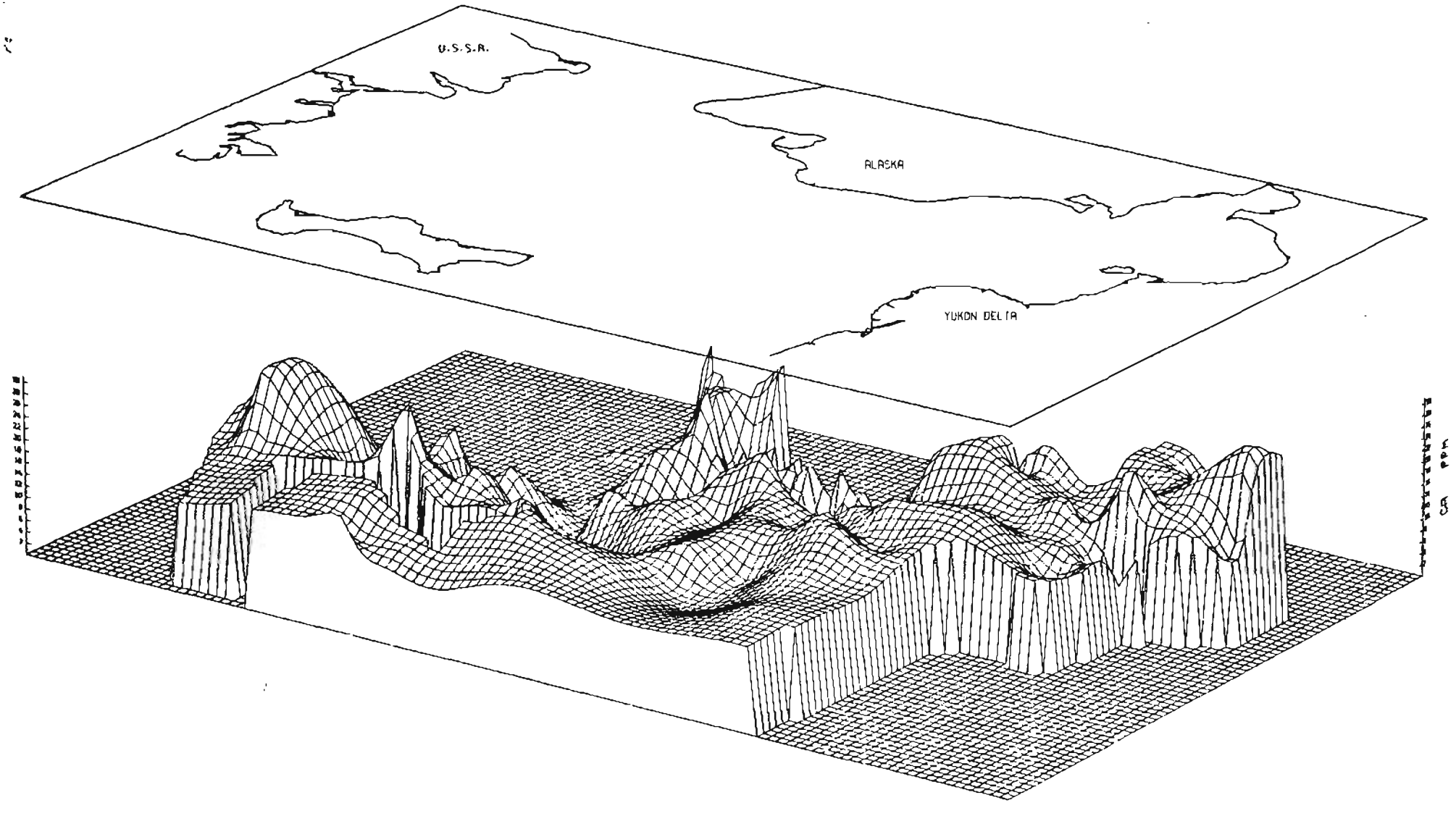

FIG 52 CA PPM IN BOTTOM SURFACE SEDIMENT OF NORTON BASIN, BERING SEA

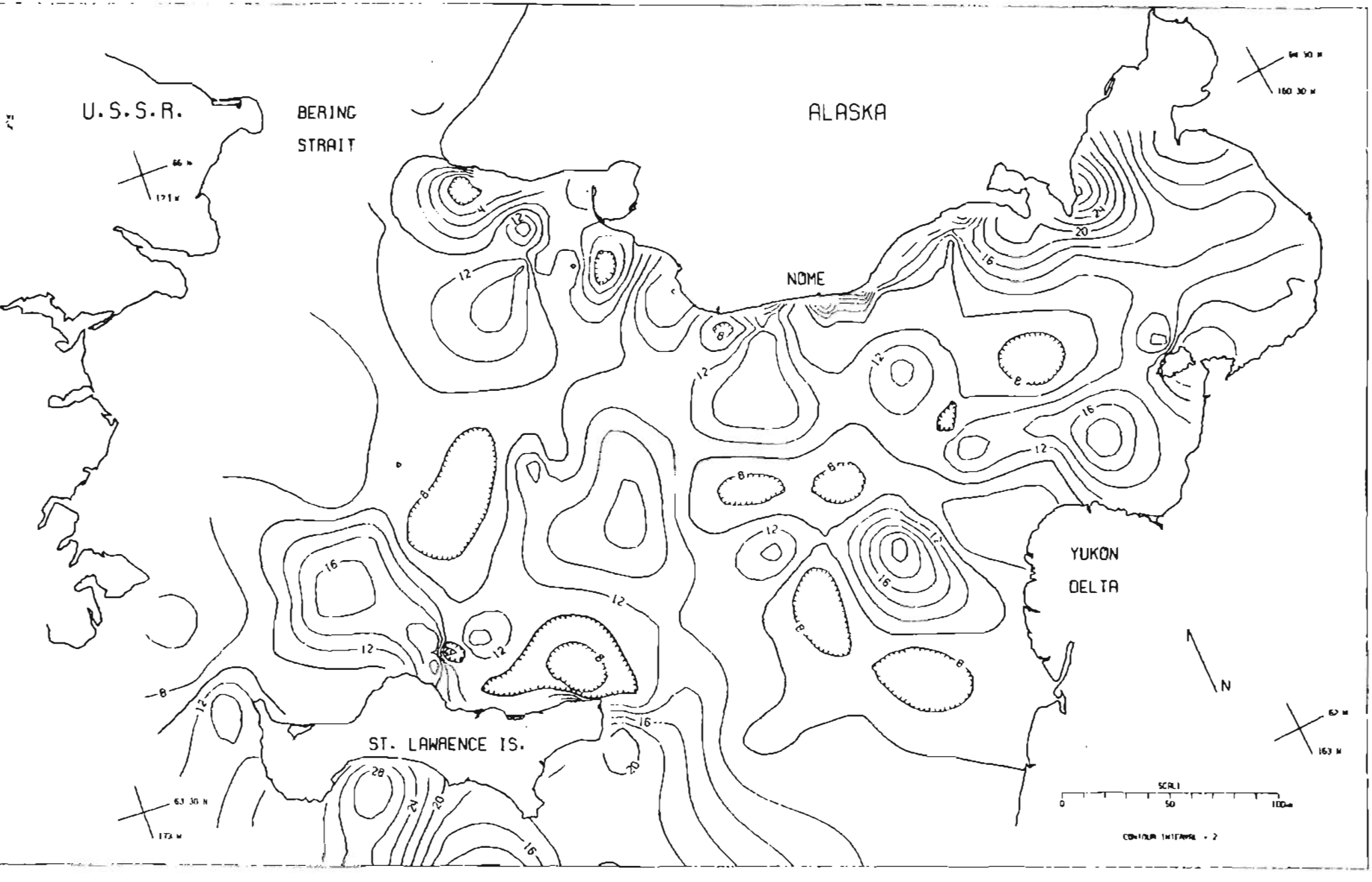

FIG 53 NB PPM IN BOTTOM SURFACE SEDIMENT OF NORTON BASIN, BERING SEA

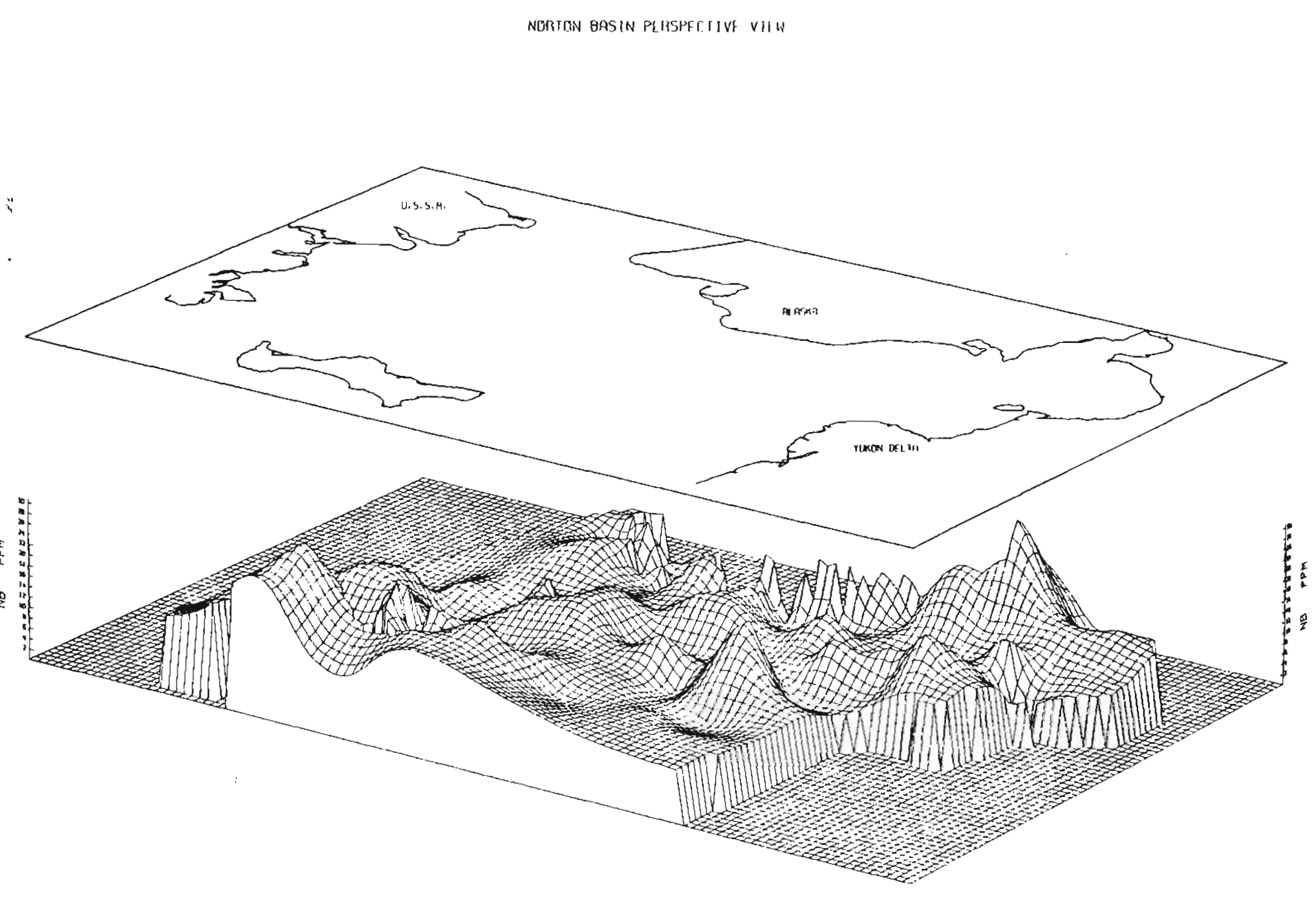

FIG 54 NB PPM IN BOTTOM SURFACE SEDIMENT OF NORTON BASIN, BERING SEA

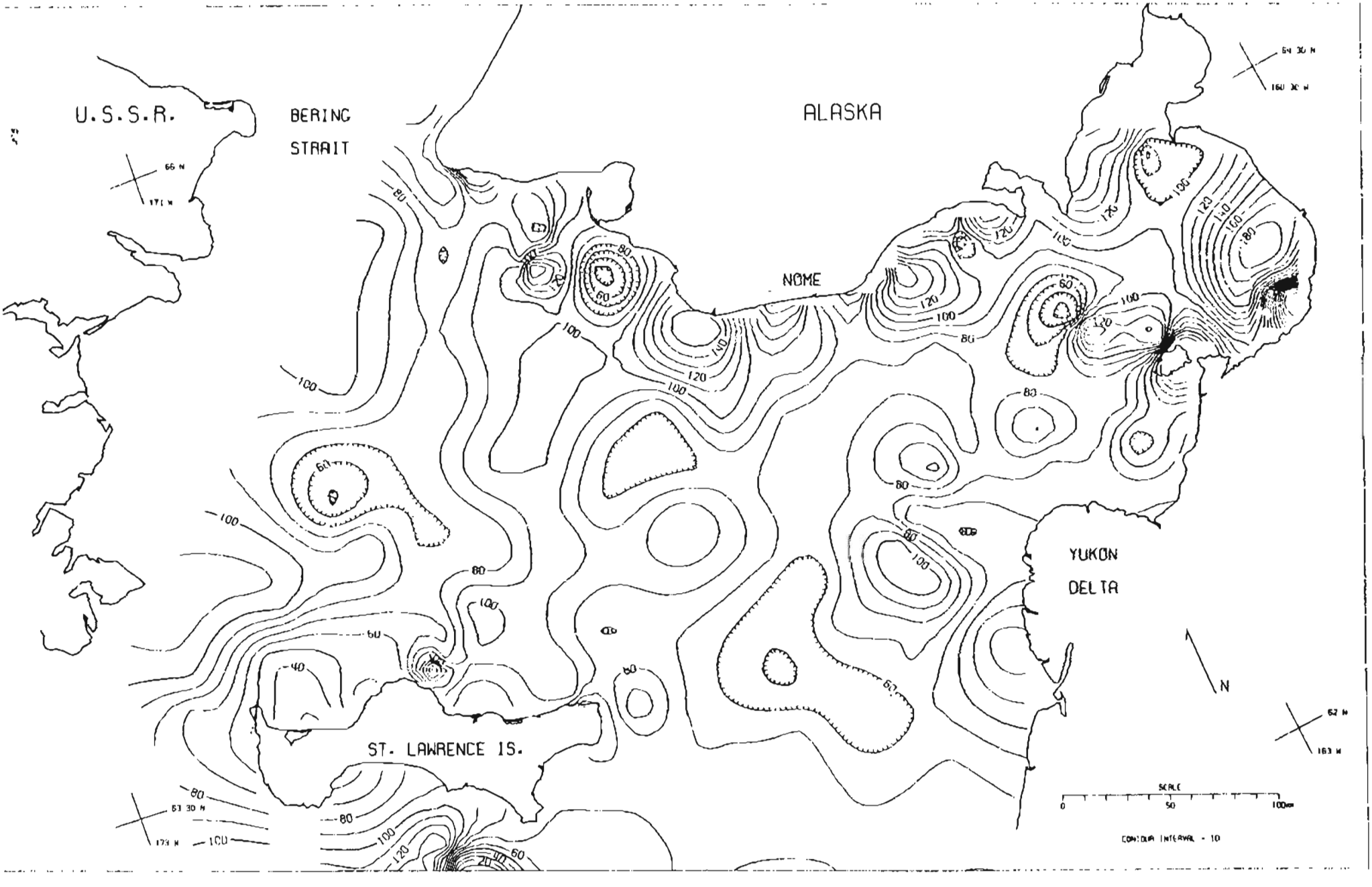

FIG 55 B PPM IN BOTTOM SURFACE SEDIMENT OF NORTON BASIN, BERING SEA

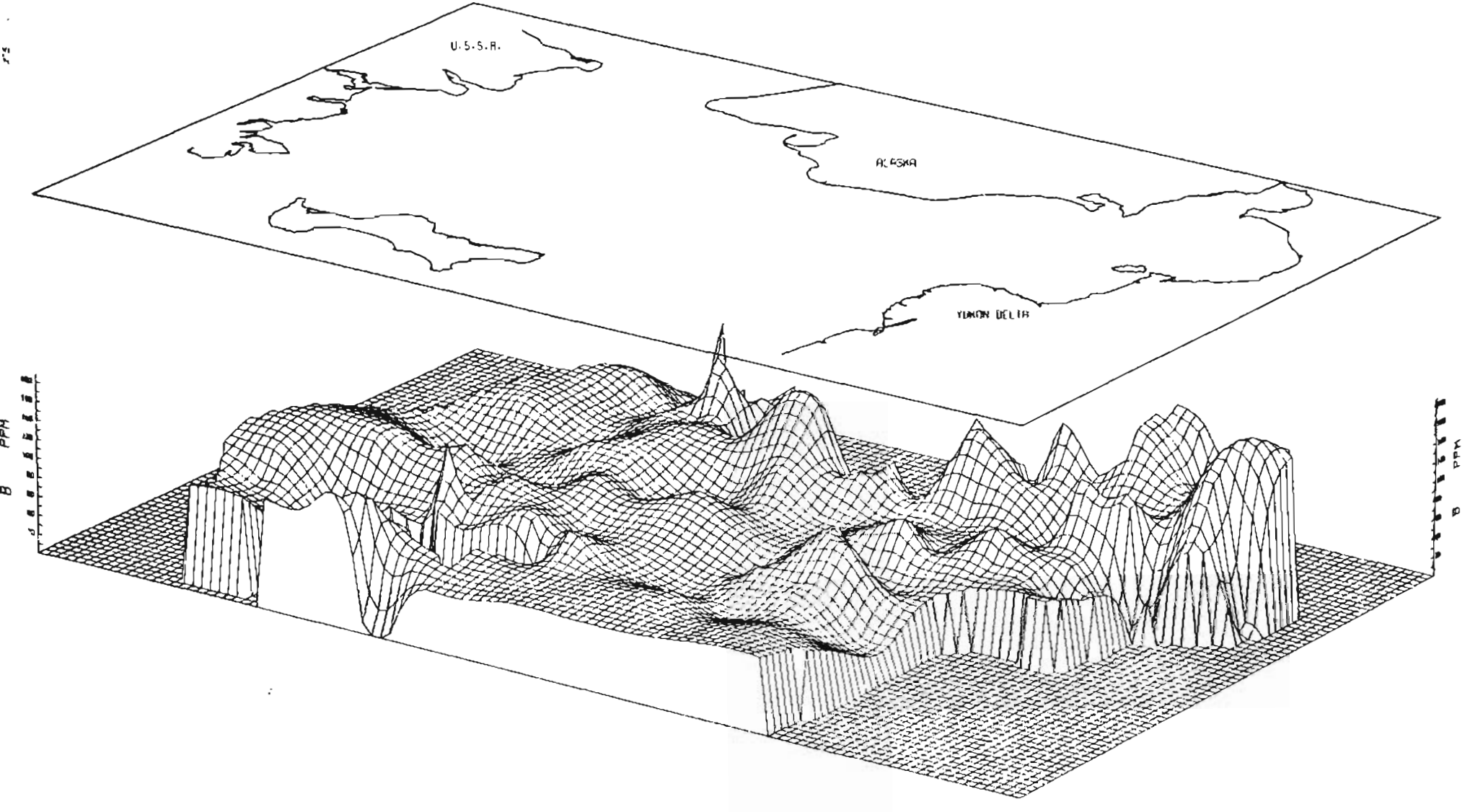

FIG 56 B PPM IN BOTTOM SURFACE SEDIMENT OF NORTON BASIN, BERING SEA

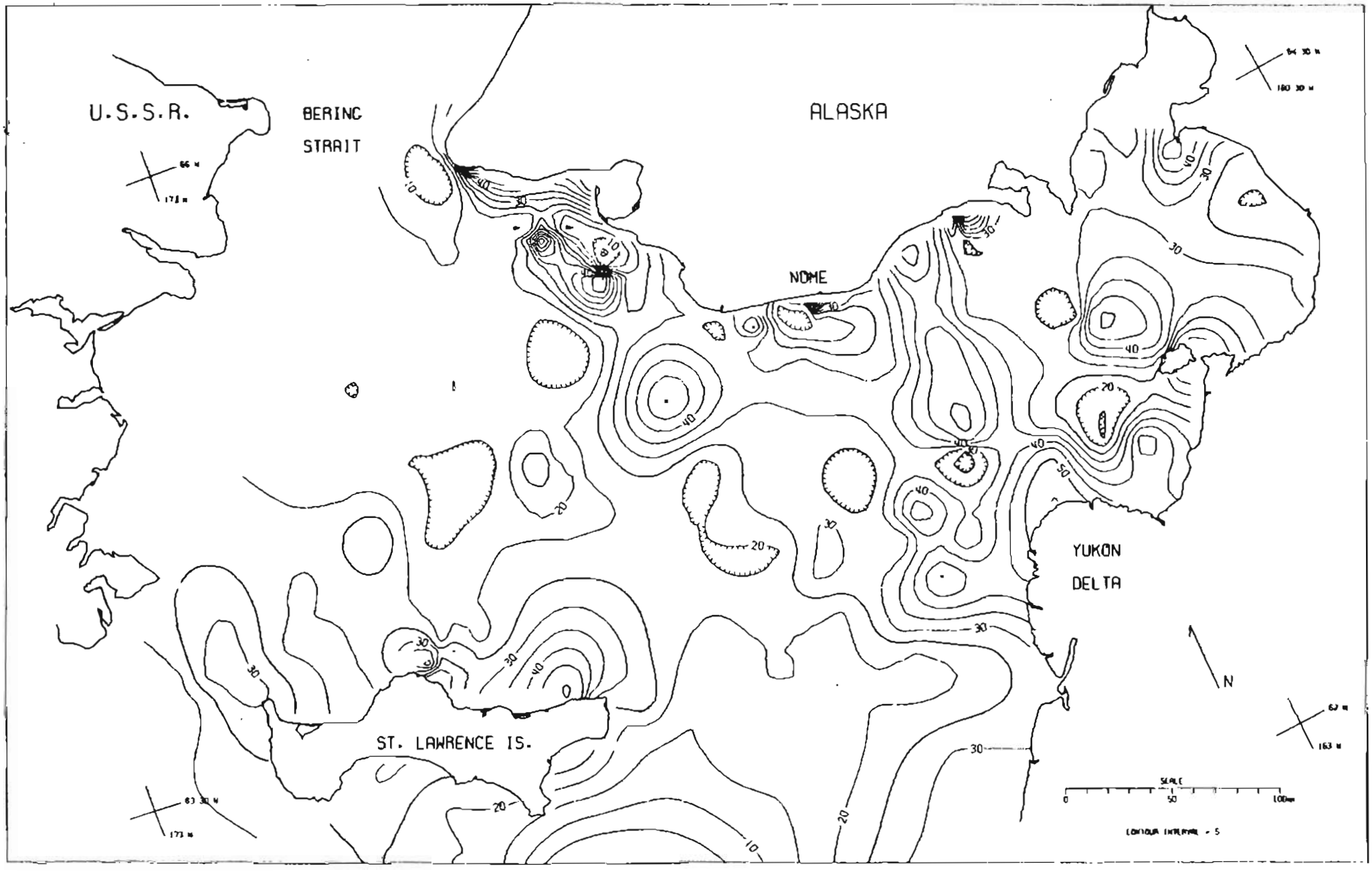

FIG 57Y PPM IN BOTTOM SURFACE SEDIMENT OF NORTON BASIN, BERING SEA

NORTON BASIN PERSPECTIVE VIEW

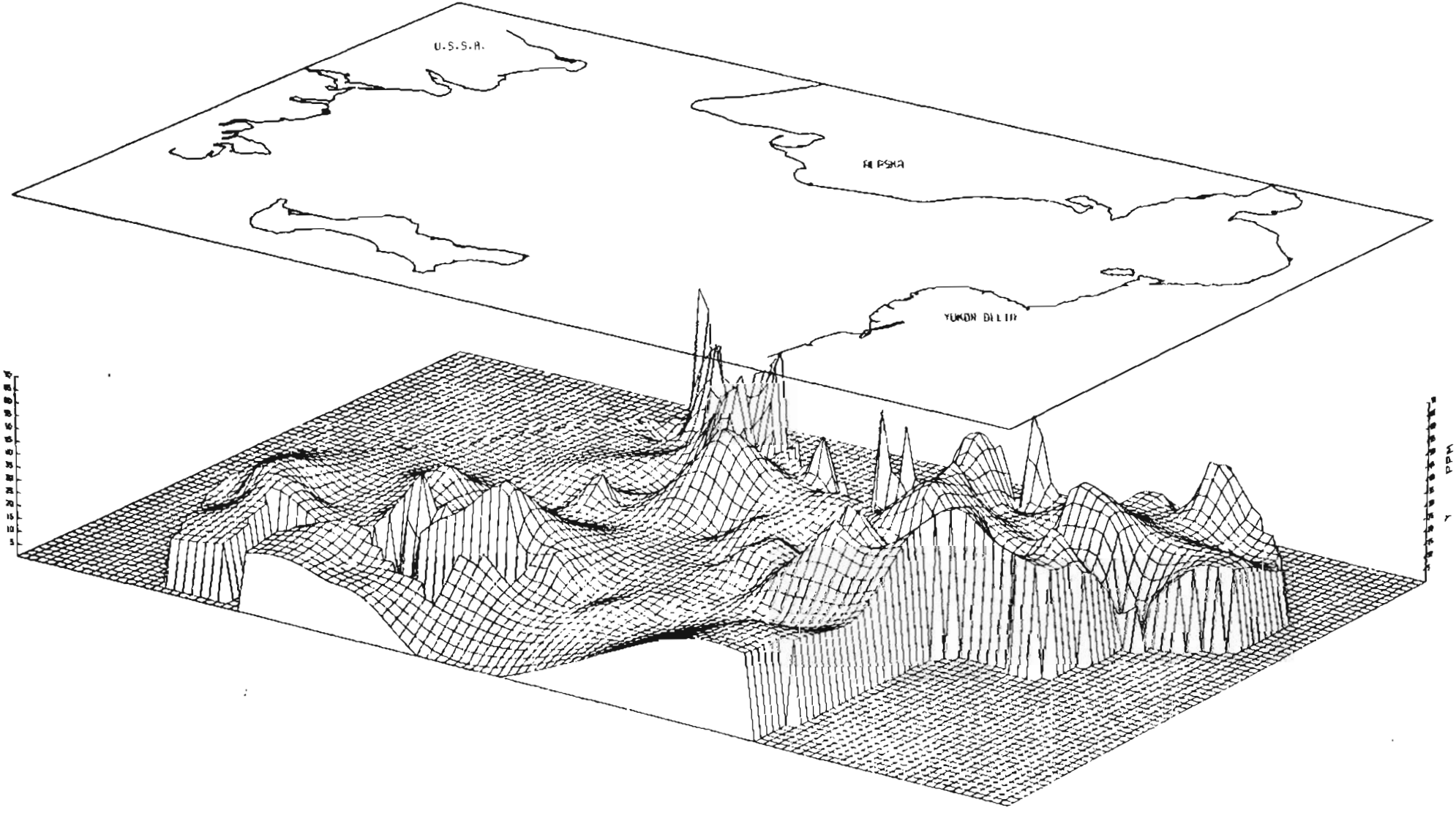

FIG 58 Y PPM IN BOTTOM SURFACE SEDIMENT OF NORTON BASIN, BERING SEA

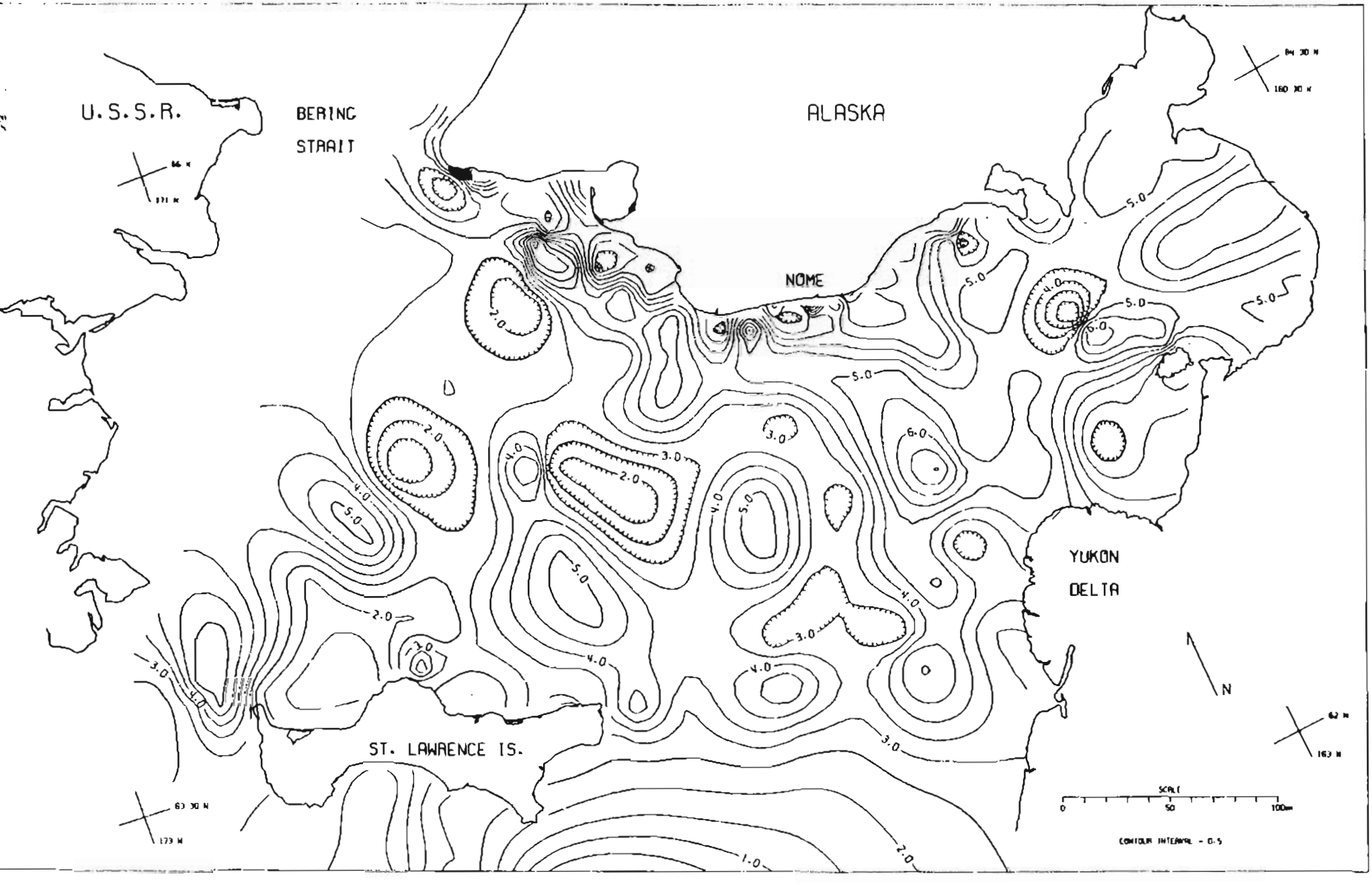

FIG 59 YB PPM IN BOTTOM SURFACE SEDIMENT OF NORTON BASIN, BERING SEA

NORTON BASIN PERSPECTIVE VIEW

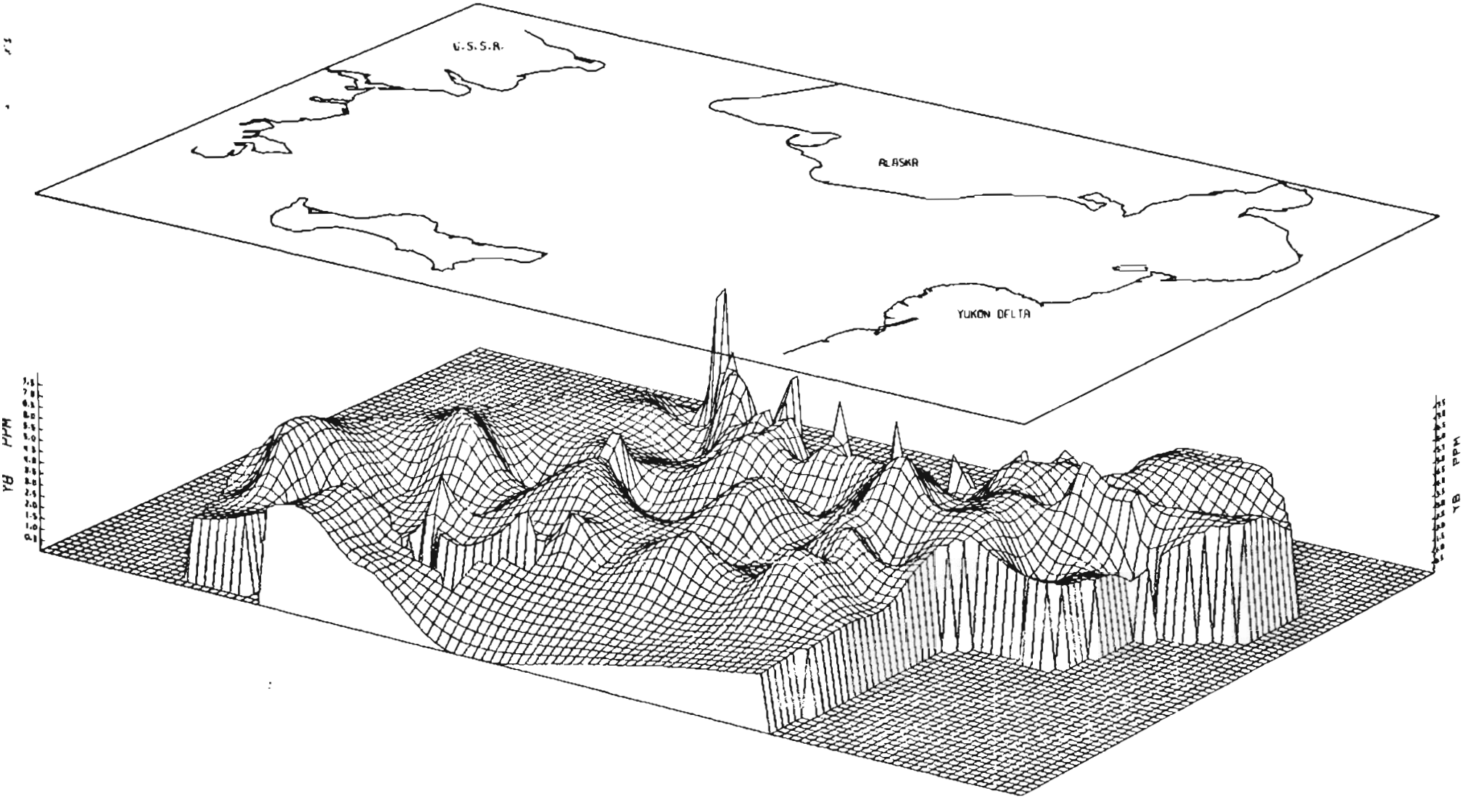

FIG 60 YB PPM IN BOTTOM SURFACE SEDIMENT OF NORTON BASIN, BERING SEA

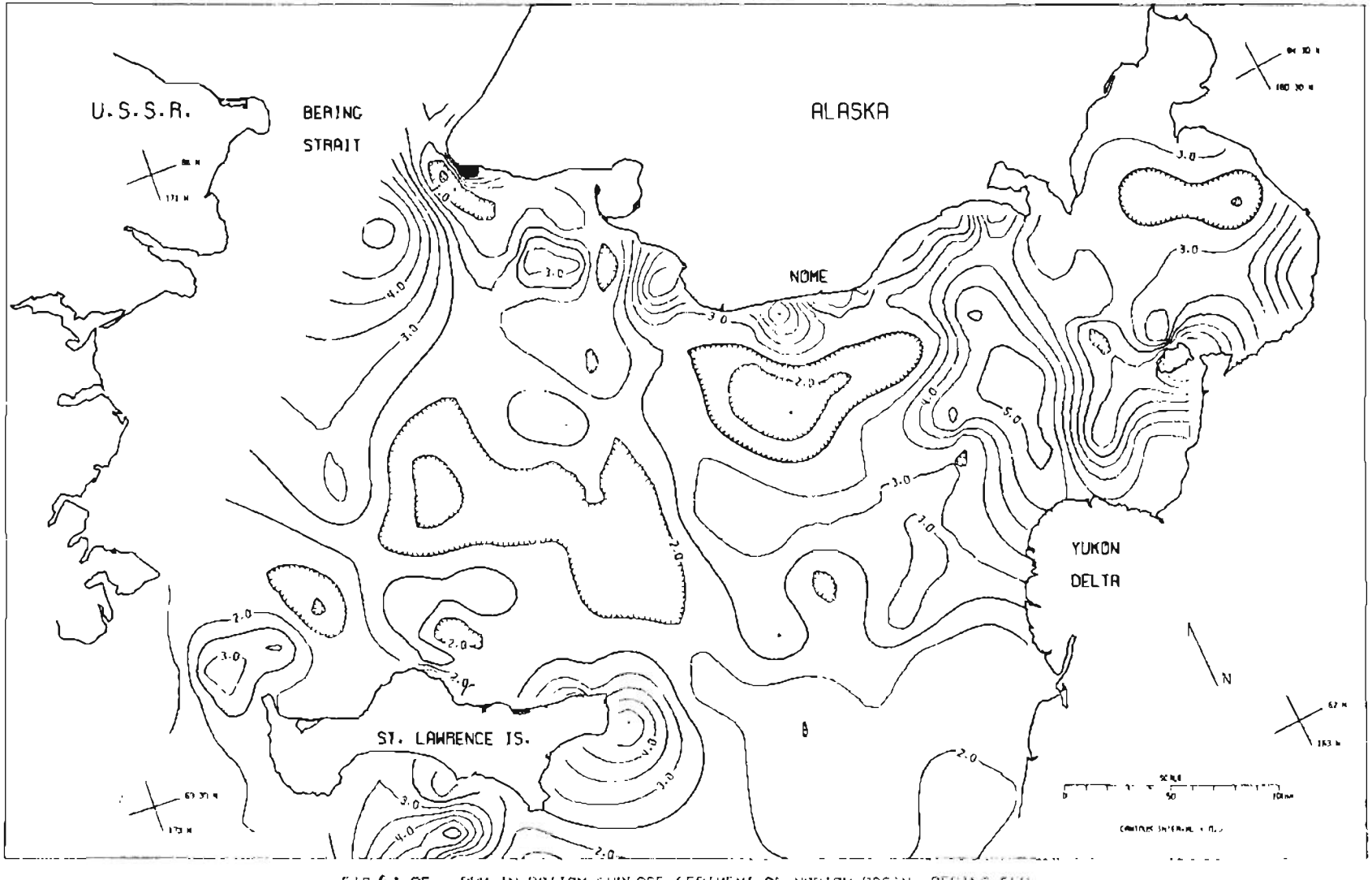

FIG. 61 BE PPM IN BOTTOM SURFACE SEDIMENT OF NORTON BASIN, BERING SEA

NORTON BASIN PERSPECTIVE VIEW

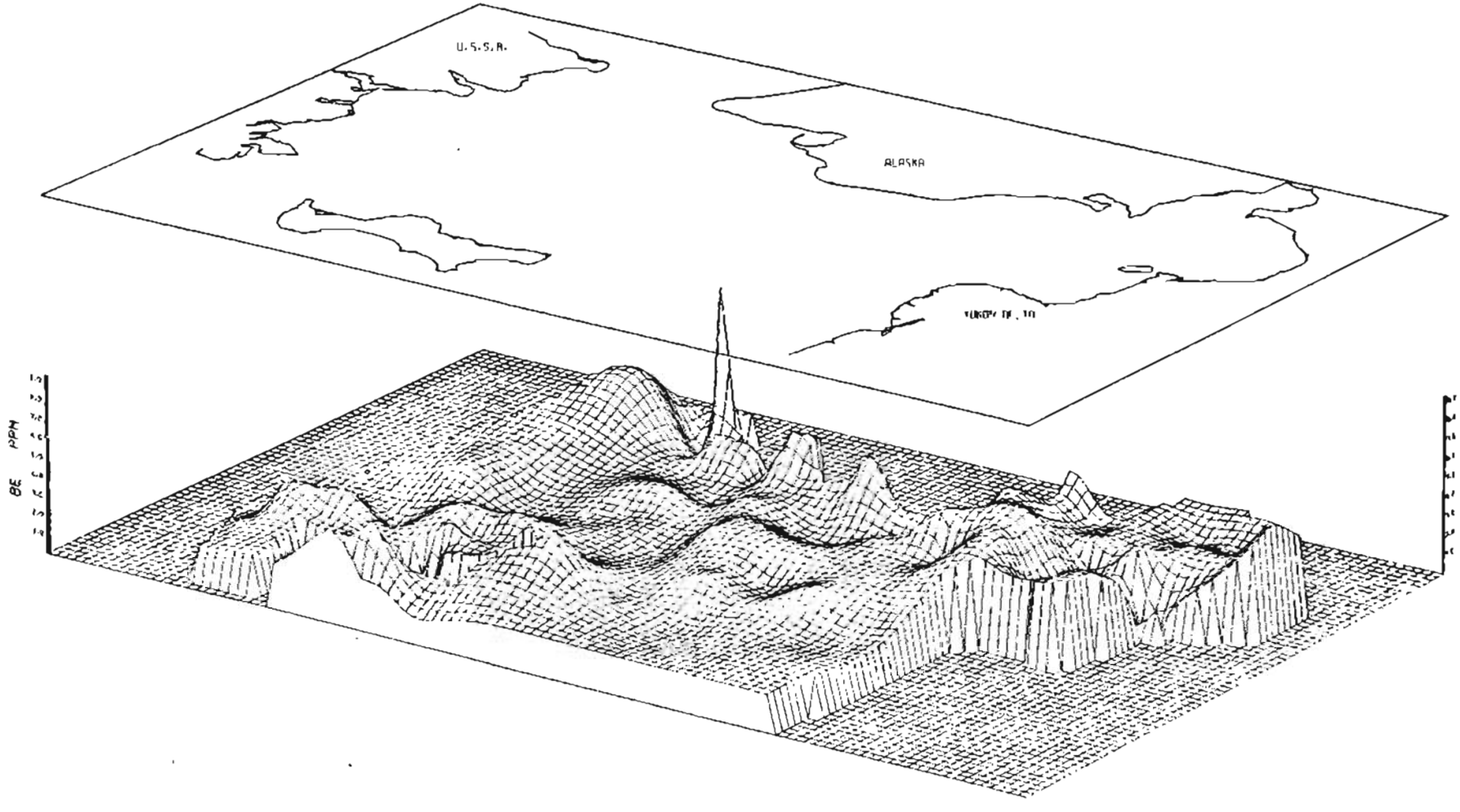

FIG. 62 BE PPM IN BOTTOM SURFICIAL SEDIMENT OF NORTON BASIN, BERING SEA

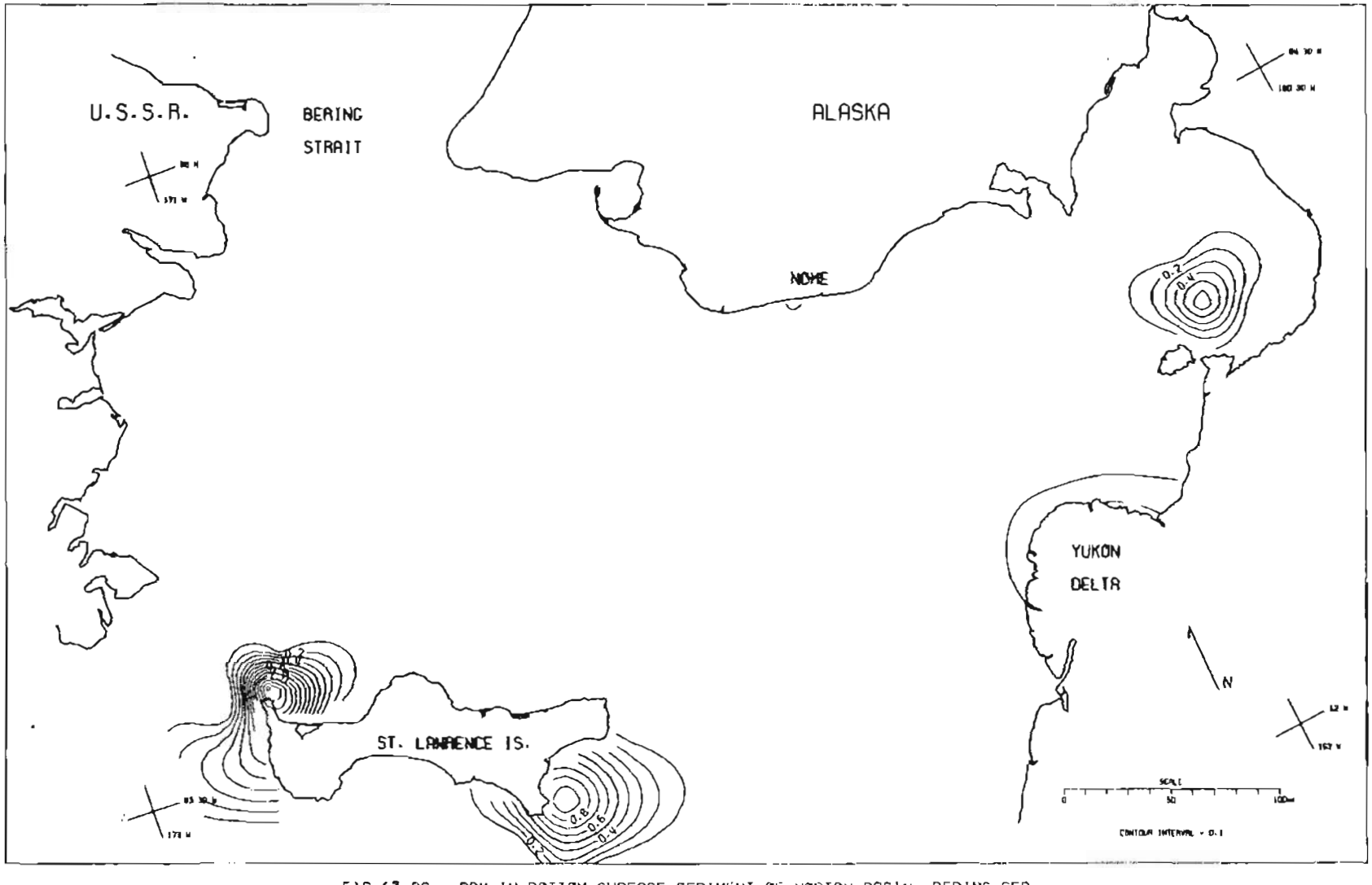

FIG 63 AG PPM IN BOTTOM SURFACE SEDIMENT OF NORTON BASIN, BERING SEA

NORTON BASIN PERSPECTIVE VIEW

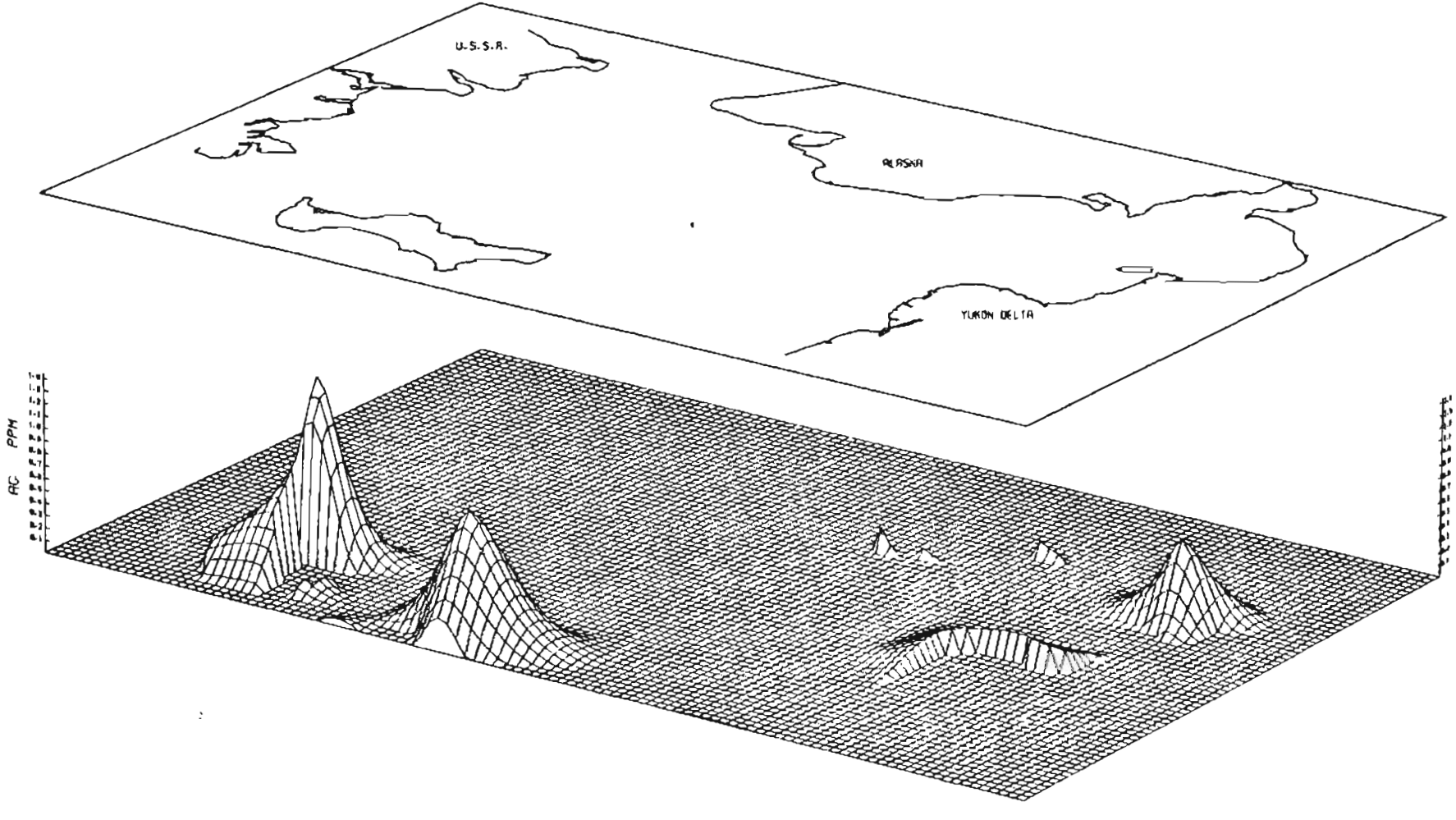

FIG 64 AC PPM IN BOTTOM SURFACE SEDIMENT OF NORTON BASIN, BERING SEA

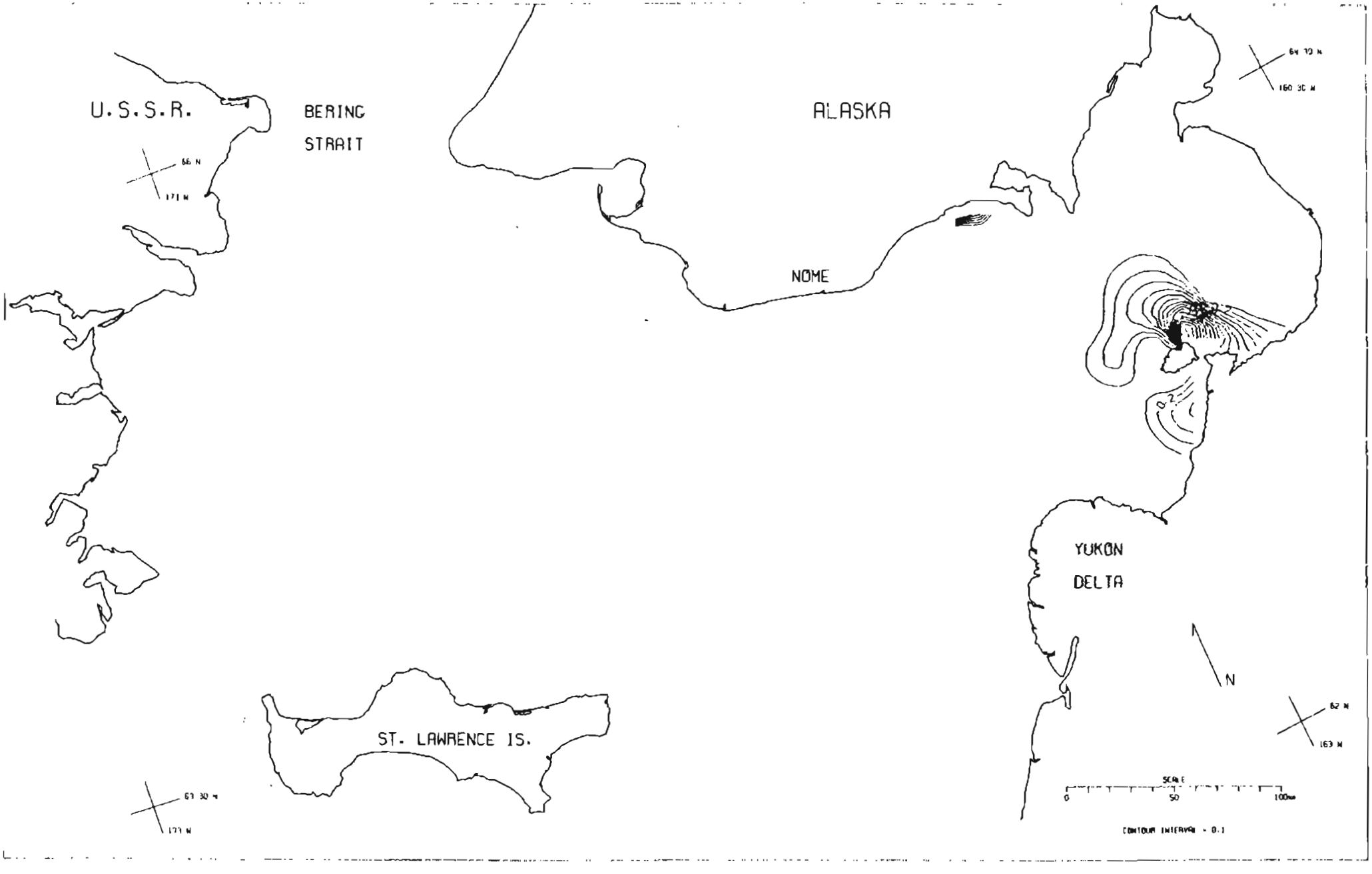

FIG 65 M0 PPM IN BOTTOM SURFACE SEDIMENT OF NORTON BASIN, BERING SEA

NORTON BASIN PERSPECTIVE VIEW

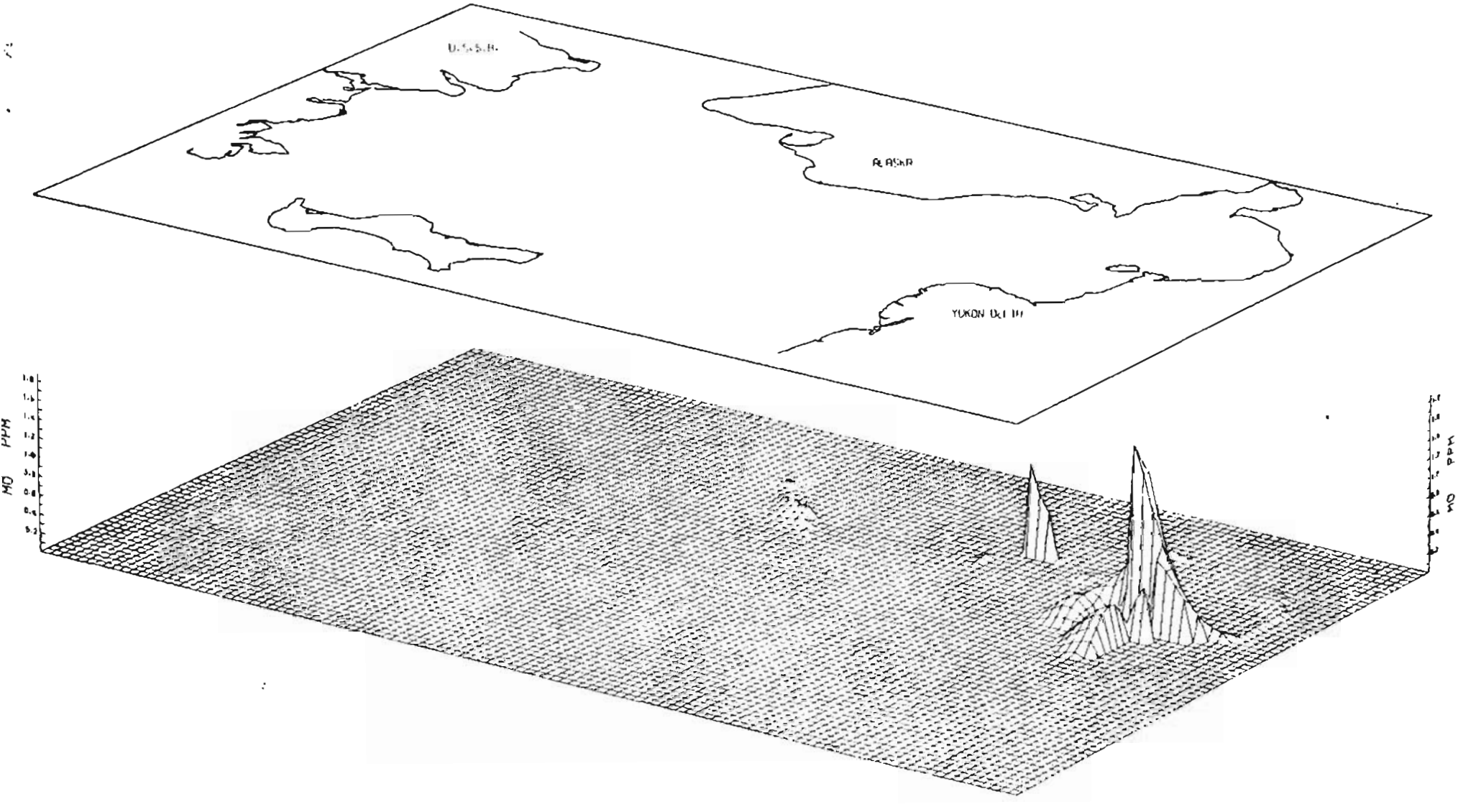

FIG 66 MO PPM IN BOTTOM SURFACE SEDIMENT OF NORTON BASIN, BERING SEA